Technische Universität München

Master Program in

Earth Oriented Space Science and Technology

ESPACE

Master Thesis:

IMPACT OF ALBEDO MODELLING ON GPS ORBITS

Author:

Carlos Javier Rodríguez Solano

Supervisor:

Univ.-Prof. Dr.phil.nat. Urs Hugentobler

November, 2009

Declaration

This thesis is a presentation of my original research work. Wherever contributions of others are involved, every effort is made to indicate this clearly, with due reference to the literature, and acknowledgment of collaborative research and discussions.

Supported by the Programme Alβan, the European Union Programme of High Level Scholarships for Latin America, scholarship No. E07M402085MX.

Munich, 02.11.2009

Carlos Javier Rodríguez Solano

Acknowledgements

For the realization of this thesis I am very thankful with Professor Hugentobler for the great time and support he invested on it, also the long discussions with him have been very enriching. The final results of Chapter 5 are only possible to present here, thanks to the computations performed by Peter Steigenberger.

During the duration of ESPACE I have counted with the support and patience of Professor Rummel and Karin Hedman, I appreciate a lot all the advices they gave me. Furthermore from all the professors and people involved in ESPACE, I learned many new things and got in touch with very exiting areas of science.

Without one of the scholarships of the Programme Alβan living and studying in Munich would have been practically impossible, I am very grateful for this opportunity.

For the support during these two years and for reading the manuscript of the thesis, thank you very much Sarah.

Finalmente por el gran apoyo intelectual y emocional que me han conducido hasta aquí, agradezco a mi padre, madre y hermana.

Gracias

Abstract

Some studies have suggested the importance of modelling the Earth radiation that reaches GPS satellites, an effect that is not currently included by most of the Analysis Centres that contribute to the computation of the IGS (International GNSS Service) Final Orbits. It is also thought that Earth radiation could be partially responsible for the observed bias between SLR (Satellite Laser Ranging) and GPS (Global Positioning System) measurements, known as the GPS – SLR orbit anomaly. Furthermore this bias sets the actual limits for the accuracy that can be achieved in the computation of the GPS orbits.

In this thesis several models of different complexity are developed, in particular models for Earth radiation that reaches the satellites and models of the satellite structure that interact with the radiation coming from the Earth. The complete development of these models is given in the thesis together with deep analysis about the differences of the models. For the interested person, the programs for the computation of the acceleration due to Earth radiation pressure are also provided.

The computed acceleration is also introduced in the computation of GPS orbits. First the perturbing acceleration is used for a very simple study case where a general understanding of the effect of Earth radiation on the orbits can be acquired. Second the perturbing acceleration is introduced in the Bernese GPS Software for the computation of GPS orbits as done by CODE (Center for Orbit Determination in Europe). The effects on the orbits are studied per revolution and per year.

The computed orbits using the Bernese GPS Software are compared with SLR measurements, to have an external validation. Doing that a reduction of the GPS – SLR orbit anomaly is obtained, leading to a potential subcentimeter accuracy of the orbits.

Finally as Earth radiation and satellite models of different complexity were tested, it is possible to give a recommendation of the key factors for an adequate but simple modelling of Earth radiation pressure for GPS satellites.

Table of Content

1 Introduction

1.1 Motivation

One of the most used satellite systems, with important applications for navigation, positioning and geodesy is the GPS. According to Seeber (2003): *"The NAVSTAR GPS (NAVigation System with Time And Ranging Global Positioning System) is a satellite-based radio navigation system providing precise three dimensional position, navigation and time information to suitably equipped users."* To compute a position on the Earth's surface, the positions of at least four satellites are used together with the travelled distance of the signal from the satellite's antenna to the receiver. A good description of how GPS works can be found in Misra and Enge (2001).

In the case of GPS, the better the positions of the satellites are known, the higher the precision that can be achieved on Earth for positioning. One of the GPS users with higher demands is the geodetic community, especially those dealing with the Terrestrial Reference Frame or the motion of the tectonics plates. For these applications the International GNSS Service (IGS), that can be considered as the highest precision international civilian GPS community, provides Final Orbits with accuracy better than $5\,cm$, Dow et al. (2005). These orbits are computed, as explain by Schaer et al. (2009), using direct observations from the satellites to reference stations on Earth, together with force models that include the principal perturbations to the orbit. Such perturbations are in decreasing order of magnitude: low terms of geopotential, attraction of Sun and Moon, solar radiation pressure, solid Earth and ocean tides and finally general relativity.

An independent way to test the accuracy of Final Orbits is by using a different measurement system. This has been done using Satellite Laser Ranging (SLR), since two GPS satellites are equipped with laser retro reflectors. The accuracy of SLR measurements is $5-6\,mm$, so they can be taken as ground truth, see for example Seeber (2003) for an overview of this technique. As more SLR measurements were available, a consistent bias of $4-5\,cm$ became evident, which has been called the GPS – SLR orbit anomaly. Urschl et al. (2008) and Ziebart et al. (2007) have found indications that this bias could be due to the Earth radiation impacting the satellites, an effect that is currently not included in the modelling of Final Orbits.

Consequently there is an increasing interest of the scientific community that uses GPS to know: which is the impact of the Earth radiation on these satellites? Moreover if the effect is not negligible would be desirable to know: which are the key parameters for an adequate but simple modelling of this effect?

1.2 State of the Art

There are many works from different teams of scientist around the world related to the topic of this thesis. These works can be classified into four different main subtopics:

- SLR validation of GPS orbits, computation of orbit residuals between the two systems.
- Models for the Earth radiation reflected and emitted from the Earth.
- Satellite models mainly for solar radiation pressure.
- Effect of Earth radiation pressure on satellites.

Also a very good review of literature of similar topics is done Sibthorpe (2006), so we also refer to it for the more interested reader.

Now concerning the SLR validation of GNSS orbits, Urschl et al. (2008) say that:

"The GPS range residuals show a mean bias of -3 to -4 cm. This bias is already known from previous studies, but its origin still remains unexplained."

In this last work together with Urschl et al. (2005), very interesting results were obtained suggesting that the origin of this bias, also known as GPS – SLR orbit anomaly, could come from the not accurate modelling of radiation pressure, especially the Earth radiation impacting the GPS satellites. Some of these results are presented in Section 1.3 and they can be considered as the main inspiration for the realization of this thesis. Here we just mentioned two publications, however the number of works related to this topic is very large and they started around 1994, when the GPS orbits reached centimetre accuracy.

Some ways of modelling have been proposed by the scientific community to deal with the albedo of the Earth. For example Qiu et al. (2003) calculated the reflected radiation of the Earth through observations taken by telescopes of the Earth radiation reflected by the Moon. Some attempts have been made to give an analytical solution to the Earth radiation reaching artificial satellites, like Borderies and Longaretti (1990).

However we have chosen to model the Earth radiation in a computational way where one assumes some properties of the surface of the Earth (reflectivity and emissivity) and the radiation reaching the satellites is computed in a numerical way. This approach fully coincides with the one of Knocke et al. (1988). Following also a very similar methodology Bandheri and Bak (2005) and Ziebart et al. (2004) calculate the Earth irradiance reaching different satellites by using reflectivity and emissivity data from Earth observing satellite missions like TOMS (Total Ozone Mapping Spectrometer) and CERES (Clouds and Earth's Radiant Energy System).

The last works described for the Earth radiation model all use the assumption that the Earth is a Lambertian sphere, it means all the radiation is reflected or emitted in a diffuse way, and therefore there is no consideration of specular reflection. A more sophisticated model, constructed by Martin and Rubincam (1996), to study the effect of the albedo of the Earth on the LAGEOS I satellite, takes into account data of the phase function provided by the ERBE (Earth Radiation Budget Experiment) mission, this data is a function of the scene type, weather and the relative location of the surface element, satellite and Sun.

Regarding the satellite models, one can find in the literature many works dealing with the interaction of the satellites with solar radiation pressure, which for some satellites is a very considerable perturbation. Therefore these existing models can be extrapolated and applied for the case of Earth radiation interacting with GPS satellites.

Fliegel et al. (1992) and Fliegel and Gallini (1996) have made public the optical properties and dimensions of the different GPS satellites (Block I, Block II and Block IIR), together with the physical description of the effect of radiation on the surface of the satellites. Using the information provided by them it is then possible to construct realistic satellite models to deal with radiation pressure; in particular they constructed the ROCK models for solar radiation pressure that became a standard inside the geodetic community.

Following a similar technique as the one described above, the team leaded by Ziebart, at the University College London, have developed very sophisticated tools for dealing with non-conservative forces acting on different satellites. They do not do simplifications on the satellite structure and can take into account almost every non-conservative force or effect one could think of.

In a different approach where GPS measurements are fitted and use to construct radiation pressure models, we find the empirical models developed by Springer et al. (1999) and Bar-Server and Kuang (2004), which are capable of achieving GPS orbits with centimetre accuracy in the respective programs they use: the Bernese GPS Software and the GIPSY-OASIS Software Package. Furthermore the solar radiation pressure models are often combined in these software packages with the estimation of radiation pressure parameters to improve the performance of the orbit accuracy, see for example Beutler et al. (1994).

The combination of Earth radiation models with satellite models have been already done by some authors, for example for the specific case of spherical satellites (like LAGEOS I). Martin and Rubincam (1996), Knocke et al. (1988) and many others have provided deep studies of the effects of this perturbation on the position of these satellites.

More recently Ziebart et al. (2007) study this perturbation for GPS satellites using a simple box-wing model. The results are promising since a reduction of the GPS – SLR orbit anomaly is observed for few days of GPS orbits. They say that the Earth radiation pressure together with an acceleration due to the thrust of the navigation antennas can reduce the bias by about $21\,mm$. Davis and Trask (2007) also say that possibly the laser retro reflector array (LRA) may be shifted closer to the Earth by around $11\,mm$ for PRN05 and $13\,mm$ for PRN06, which would reduce the bias by 32 and $34\,mm$ for these two satellites (the only ones in the GPS constellation that carry LRA).

Finally it can also be mentioned that in future studies planned by our team, the impact of albedo modelling on geodetic time series will be studied. Also there are plans to participate in an experiment with other teams coordinated by Ziebart to further study the effect of modelling Earth radiation pressure on the GPS – SLR bias. This just tells that the work presented here is on-going work and many questions still remain open or new question are being generated in the present.

1.3 Scientific Questions

Taking into account what has been written in the last pages, the scientific questions we intend to answer in this thesis are the following:

1) Which is the magnitude and behaviour of the acceleration due to Earth radiation pressure acting on GPS satellites?
2) Is this acceleration negligible or it is worth to include it in the current modelling of GPS orbits?
3) Is this perturbation in the orbit capable of producing a radial shift in the orbits and if it does why?
4) Can this perturbation produce a similar pattern as the one observed between SLR measurements and GPS orbits (Figure 1.1)?
5) Which are the key factors for an adequate but simple modelling of the effect of Earth radiation on GPS satellites?
6) Is the GPS – SLR orbit anomaly reduced in a long term by including this acceleration on the computation of real GPS orbits?

Note that Ziebart et al. (2007) have already partially answer the questions 1), 2), 3) and 6), however their study was limited to few days of data and to only one Earth radiation and satellite model. On the other hand in this study we deal with per orbit and per year perturbations, testing at the end the different Earth radiation and satellite models with a complete year of real GPS orbits and SLR measurements. Moreover we test models of different complexity, to acquire a good and deep understanding of the impact of Earth radiation on GPS orbits.

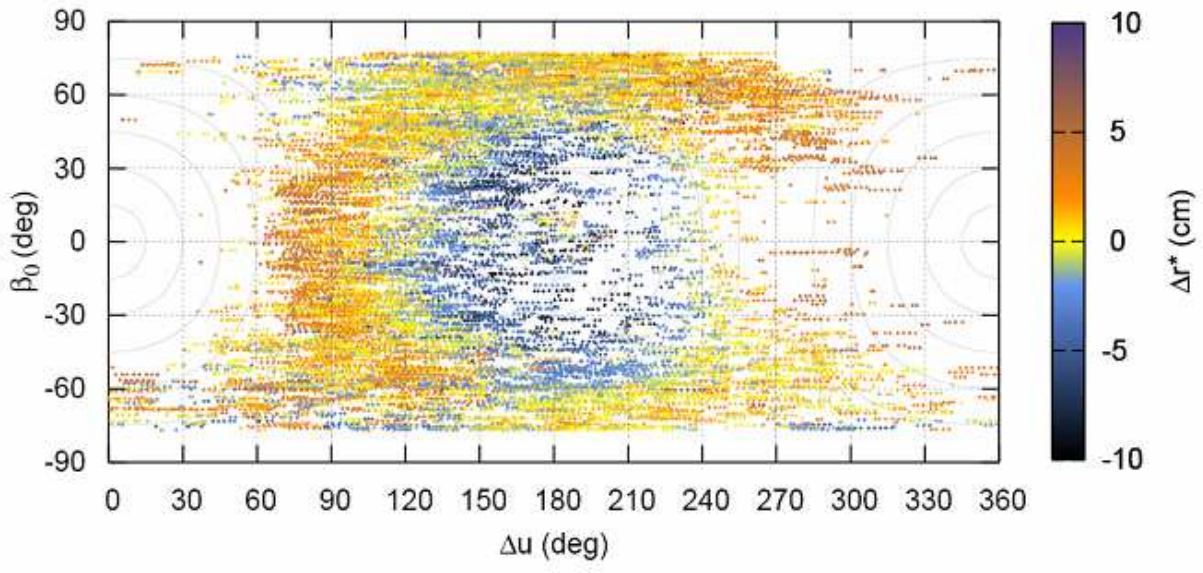

Figure 1.1 Color-coded SLR range residuals in cm minus mean value for the GPS satellites PRN05 and PRN06, derived from CODE final orbits. Source Urschl et al. (2008)

The questions 4) and 5) have not yet been mentioned in the literature so they are accounted to be new contributions, especially for the scientific community that uses GPS data with very high requirements of accuracy. By the other hand for questions 1), 2), 3) and 6) we have intended to go deeper as the previous studies, by testing several models and by using longer test periods.

1.4 Chapter Overview

Chapter 2 and 3 are devoted to the development of the Earth radiation and satellite models, respectively. In both chapters models of different complexity are deeply studied. The combination of these models will lead us to find the answers to the first two scientific questions.

On Chapter 4 we will include the acceleration from relative simple models as perturbation acting on a Kepler orbit. This will give a general understanding of the effect of the acceleration on GPS orbits and will give answers to questions 3) and 4).

Finally the models of different complexity will be included into the Bernese GPS Software (Chapter 5). There we will be able to compute the effect of Earth radiation on real GPS orbits. Using the same software, the comparison with SLR measurements will be done and with this last step questions 5) and 6) are addressed.

Some general recommendations for an adequate but simple modelling of Earth radiation pressure for GPS satellites are given in the Conclusions (Chapter 6). Finally the Appendix provides the Matlab programs of the Earth radiation and satellite models, as well the program to combine both models which computes the acceleration acting on the satellites.

2 Earth Radiation Model

2.1 Introduction

One of the main objectives of this thesis is to study the effect of the Earth radiation on the orbit of GPS satellites. Therefore one of the fundamental quantities to compute is the acceleration due to Earth reflected and emitted radiation for GPS satellites. For this purpose we will construct four different Earth radiation models (ERM):

- ERM-A: analytical Earth radiation model for constant albedo.
- ERM-N: numerical Earth radiation model for constant albedo.
- ERM-LAT: numerical Earth radiation model for latitude dependent albedo.
- ERM-CERES: numerical Earth radiation model with satellite data.

These models will in general give the irradiance of the Earth at a certain satellite altitude and relative positions of satellite, Earth and Sun. The irradiance which units are Watt per square meter combined with the satellite models (Chapter 3) will give the acceleration acting on the satellites due to the Earth radiation. The computation of the irradiance is therefore a key factor in this chapter.

For the computation of the Earth radiation model some general assumptions are made:

- The Earth surface reflects radiation as a Lambertian sphere. Therefore the reflected radiation can be represented by a simple phase function, see for example Qiu et al (2003) and Borderies and Longaretti (1990). This assumption is also used by Ziebart et al (2004) for the specific purpose of computing the irradiance for GPS satellites.
- The total albedo of the Earth is assumed to have a value of 0.3, see for example Kiehl and Trenberth (1997) for a comparison of different values of Earth's albedo.
- There is conservation of energy for the Earth as a whole, which means that all the energy from the Sun that is intercepted by the Earth, must go back to space either as reflected or emitted radiation.
- Since the GPS satellites are at relative large distance from the Earth and therefore receive radiation from around 38% of the Earth's surface, see Eq. (2.26), we assumed in general average values. We use an average radius of the Earth, we consider it to be a sphere and the radiation to be reflected or emitted at its surface.

For more information on the albedo of the Earth and the energy transport on it, we refer to Taylor (2005) and Lindsey (2008).

2.2 Mathematical Model

2.2.1 Lambertian Surface

In order to construct a radiation model of the Earth, assuming that its surface (or atmosphere) behaves like a Lambertian surface, in this section crucial concepts from Astronomy and Radiometry, based on the books of Karttunen et al. (1996)* and Boyd (1983) are intruced. The first book is a guide to construct the reflected irradiance from a flat Lambertian surface, see Eq. (2.8). The second book gives the conventional radiometric quantities, see Table 2.1.

The albedo or more specifically the bond albedo α is the ratio of reflected radiant power Φ_{refl} to incident radiant power Φ_{in}, at all wavelengths and in all directions:

$$\alpha = \frac{\Phi_{refl}}{\Phi_{in}}. \tag{2.1}$$

The radiant power or flux Φ, which unit is Watt, is the rate at which radiant energy is transferred from one region to another by the radiation field, as defined by Boyd (1983). Therefore the reflected radiant power from a surface is simply $\Phi_{refl} = \alpha\Phi_{in}$ and the irradiance at a satellite (or observer) distance d, for radiation that is reflected isotropically, should be

$$E_{refl} = \frac{\Phi_{refl}}{4\pi d^2}. \tag{2.2}$$

Table 2.1 Radiometric quantities and units

Quantity	Symbol	Definition	Unit
Radiant energy	Q	$\int \Phi dt$	J
Radiant energy density	u	dQ/dV	J/m^3
Radiant power or flux	Φ	dQ/dt	W
Radiant exitance	M	$d\Phi/dA$	W/m^2
Irradiance	E	$d\Phi/dA$	W/m^2
Radiance	L	$d^2\Phi/dA_{proj}d\Omega$	$W/m^2 sr$
Radiant intensity	I	$d\Phi/d\Omega$	W/sr

* Some of the symbols used by Karttunen et al. (1996) were changed in order to adjust to the radiometric conventions and to have a consistent notation throughout this Thesis.

However the radiation is in general reflected anisotropically, and the irradiance must be corrected by a factor $C\Psi(\theta)$ depending on the phase angle θ to the surface normal.

$\Psi(\theta)$ is called the phase function, it describes the reflecting properties of a given surface and it can be computed as the radiant intensity at the given angle θ divided by the radiant intensity at normal incidence. For the specific case of a Lambertian surface, the radiant intensity is given by $I(\theta) = I(0)\cos\theta$, so it follows that the phase function is

$$\Psi(\theta) = \begin{cases} \cos\theta & if \quad \theta \in [0, \pi/2] \\ 0 & if \quad \theta \in (\pi/2, \pi] \end{cases} \tag{2.3}$$

and the normalization constant C is such that

$$\frac{C\int_S \Psi(\theta) dS}{4\pi d^2} = 1, \tag{2.4}$$

where the integration is extended over the surface of a sphere of radius d. This implies that all the radiation reflected from the surface is found somewhere on the surface of a sphere.

To compute the normalization constant C for a Lambertian surface, first we solve the integral from (2.4) as

$$\int_S \Psi(\theta) dS = 2\pi d^2 \int_0^{\pi} \Psi(\theta)\sin\theta\, d\theta = 2\pi d^2 \int_0^{\pi/2} \cos\theta \sin\theta\, d\theta = \pi d^2, \tag{2.5}$$

so we get $C = 4$ and the reflected irradiance can be written as

$$E_{refl} = \frac{C\Psi(\theta)}{4\pi d^2} \alpha \Phi_{in} = \frac{\alpha}{\pi d^2} \cos\theta \Phi_{in}. \tag{2.6}$$

The incident radiant power is given by $\Phi_{in} = E_{sun} A$ for a surface A perpendicular to the Sun incident radiation, where $E_{sun} \approx 1367 W/m^2$ is the irradiance from the Sun at the Earth distance also known as solar constant, see Taylor (2005). If the Sun radiation is not perpendicular to the surface, but forms an angle γ (Figure 2.1) with the surface's normal, the incident radiant power is be given by

$$\Phi_{in} = E_{sun} A \cos\gamma. \tag{2.7}$$

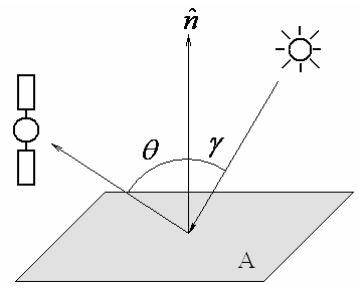

Figure 2.1 Lambertian surface

Finally the reflected irradiance at a satellite distance d, for a given incident angle γ of Sun radiation and for a given angle θ of reflected radiation, is

$$E_{refl} = \frac{\alpha}{\pi d^2} \cos\theta \cos\gamma E_{sun} A \tag{2.8}$$

valid for $\cos\theta \geq 0$ and $\cos\gamma \geq 0$. This result can be integrated over a sphere of radius d and one should get the incident radiant power times the bond albedo:

$$\Phi_{refl} = \int_S E_{refl} dS = \alpha \cos\gamma E_{sun} A = \alpha \Phi_{in}. \tag{2.9}$$

2.2.2 Reflected Radiation

The Earth´s atmosphere reflects part of the radiation coming from the Sun, for simplification we may assume that this radiation is scattered back to space by a sphere covered by a Lambertian surface. In order to account for the amount of radiation scattered back in a specific direction, we solve the problem of a Lambertian sphere.

Analytical Solution

Until now we considered the irradiance for a given surface element. The next step is to construct a sphere formed by many of these surfaces, whereby each surface has a specific orientation to the Sun and to the satellite.

First an approximate solution will be computed where two main assumptions are made. The first one implies that the distance d from the surface elements to the satellite is constant (i.e. the radius of the Earth is negligible respect to the distance d) and the second one that the vector of the satellite direction $\hat{r}$ from a given surface element is also constant. This is interesting since it is possible to obtain an analytical solution, which is not the case when no approximation is used.

For solving the problem first the result obtained in (2.8) for the reflected irradiance in a given direction θ is used. Also three main vectors are defined: a vector in the satellite direction $\hat{r}$, a vector in the Sun direction $\hat{s}$ and a normal vector $\hat{n}$ to the surface element, given by

$$\begin{aligned} \hat{r} &= (1, 0, 0) \\ \hat{s} &= (\cos\psi, \sin\psi, 0) \\ \hat{n} &= (\sin\vartheta\cos\varphi, \sin\vartheta\sin\varphi, \cos\vartheta). \end{aligned} \tag{2.10}$$

The vectors together with the angles ϑ, φ and ψ are shown in Figure 2.2. The first two angles are used to define the position of the surface element on the sphere, while the angle ψ gives the relative orientation of satellite, Earth and Sun.

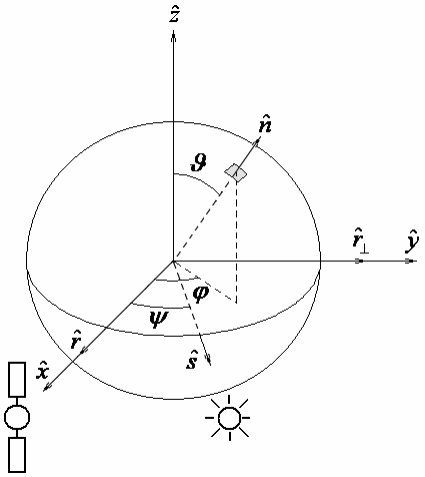

Figure 2.2. Geometry for Lambertian sphere

Coming back to the angles of incident radiation γ and reflected radiation θ, we have

$$\begin{aligned} \cos\theta &= \hat{r}\cdot\hat{n} = \sin\vartheta\cos\varphi \\ \cos\gamma &= \hat{s}\cdot\hat{n} = \sin\vartheta\cos(\psi-\varphi). \end{aligned} \tag{2.11}$$

With the last equations the reflected irradiance for a specific direction, Eq. (2.8), becomes

$$dE_{refl} = \frac{\alpha}{\pi d^2}\sin^2\vartheta\cos\varphi\cos(\psi-\varphi)E_{sun}dA, \tag{2.12}$$

which is then integrated over the illuminated part of the sphere visible to the satellite, using

$$\begin{aligned} dA &= R_E^2\sin\vartheta\, d\vartheta\, d\varphi \\ \vartheta = 0,...,\pi, \qquad \varphi &= \psi-\pi/2,...,\pi/2, \qquad 0\le\psi\le\pi, \end{aligned} \tag{2.13}$$

where R_E is the mean radius of the Earth. The integral of Eq. (2.12) is given by

$$E_{sat}(\psi) = \int dE_{refl} = \int_0^{\pi}\int_{\psi-\pi/2}^{\pi/2}\frac{\alpha}{\pi d^2}\sin^2\vartheta\cos\varphi\cos(\psi-\varphi)E_{sun}R_E^2\sin\vartheta\, d\varphi\, d\vartheta \tag{2.14}$$

which is possible to integrate for ϑ and φ separately:

$$\int_0^{\pi}\sin^3\vartheta\, d\vartheta = \int_0^{\pi}\frac{3\sin\vartheta-\sin 3\vartheta}{4}d\vartheta = \frac{4}{3} \tag{2.15}$$

$$\int_{\psi-\pi/2}^{\pi/2}\cos\varphi\cos(\psi-\varphi)d\varphi = \frac{1}{2}\int_{\psi-\pi/2}^{\pi/2}(\cos(2\varphi-\psi)+\cos\psi)d\varphi = \frac{1}{2}((\pi-\psi)\cos\psi+\sin\psi). \tag{2.16}$$

And combining the results we get

$$E_{sat}(\psi) = \frac{2\alpha}{3\pi^2}\frac{A_E E_{sun}}{d^2}((\pi-\psi)\cos\psi+\sin\psi), \tag{2.17}$$

with $A_E = \pi R_E^2$ being the area intersected by the radiation coming from the Sun and the total incident radiant power intersected by the Earth is $\Phi_{in-total} = \pi R_E^2 E_{sun}$. Qiu et al. (2003) also

obtained that Eq. (2.14) holds for $\psi \le 2\pi/3$ (where the Lambertian assumption holds) in the case of Earth radiation that reaches the Moon.

The quantity $E_{sat}(\psi)$ gives the total irradiance due to the albedo of the Earth as a function only of the angle ψ and a certain distance d. The distance d has been taken until now just as a constant. To determine it correctly we need to consider that the integral of $E_{sat}(\psi)$ over the surface S of the sphere of radius $r_{sat} = R_E + h$, with h the satellite altitude, must be equal to the total reflected radiant power $\Phi_{refl-total}$ of the Earth:

$$\Phi_{refl-total} = \int_S E_{sat}(\psi) dS = \alpha \Phi_{in-total}. \tag{2.18}$$

Using for the computation of the integral

$$dS = 2\pi (R_E + h)^2 \sin\psi \, d\psi, \qquad \psi = 0,...,\pi, \tag{2.19}$$

we rewrite Eq. (2.18) as

$$\Phi_{refl-total} = \int E_{sat}(\psi) dS = \frac{2\alpha}{3\pi^2} \frac{A_E E_{sun}}{d^2} 2\pi (R_E + h)^2 \int_0^\pi ((\pi - \psi)\cos\psi + \sin\psi)\sin\psi \, d\psi \tag{2.20}$$

which can be divided into three integrals:

$$\begin{aligned} &\int_0^\pi \cos\psi \sin\psi \, d\psi = 0 \\ &\int_0^\pi \psi \cos\psi \sin\psi \, d\psi = -\frac{\pi}{4} \\ &\int_0^\pi \sin^2\psi \, d\psi = \frac{\pi}{2} \end{aligned} \tag{2.21}$$

and together we have

$$\Phi_{refl-total} = \frac{4\alpha}{3\pi} \frac{(R_E + h)^2}{d^2} A_E E_{sun} \left(\frac{\pi}{4} + \frac{\pi}{2} \right) = \alpha A_E E_{sun} \frac{(R_E + h)^2}{d^2} \tag{2.22}$$

so it is demonstrated that d must be equal to $R_E + h$ so Eq. (2.18) is satisfied. This can be also simply obtained by considering that as $h >> R_E$ we have $d = h = h + R_E$.

Finally we can write the irradiance vector in the satellite direction $\hat{r}$ due to the total albedo of the Earth α, depending only on the relative position of satellite, Earth and Sun (angle ψ) and on the satellite altitude h, as

$$\vec{E}_{sat}(\psi, h) = \frac{2\alpha}{3\pi^2} \frac{A_E E_{sun}}{(R_E + h)^2} ((\pi - \psi)\cos\psi + \sin\psi)\hat{r} \tag{2.23}$$

which is valid only for $h >> R_E$.

Numerical Solution

In the case that no approximation is used, meaning that the actual direction and distance from the surface element to the satellite is used, the solution is no longer analytical, but it can be computed numerically. Again Eq. (2.8) is used giving the irradiance in the direction of the satellite from a surface element:

$$d\vec{E}_{refl} = \begin{cases} \dfrac{\alpha}{\pi d^2} \cos\theta \cos\gamma \, E_{sun} \, dA\hat{e} & if \quad \cos\theta \geq 0 \quad and \quad \cos\gamma \geq 0 \\ 0 & else \end{cases} \tag{2.24}$$

with $\cos\theta = \hat{e} \cdot \hat{n}$ and $\cos\gamma = \hat{s} \cdot \hat{n}$. The vectors $\hat{n}$ and $\hat{s}$ do not change with respect to the previous section. Additionally the vector $\vec{d} = (R_E + h, 0, 0) - R_E \hat{n}$ and the vector of the satellite direction from a surface element $\hat{e}$, which is computed as $\hat{e} = \vec{d} \big/ \left| \vec{d} \right|$, are defined.

In Figure 2.3 $\hat{r}$ and $\hat{r}_\perp$ are used to indicate the satellite or radial direction $\hat{r}$ and the non-radial direction $\hat{r}_\perp$. In the case of the analytical solution the new defined $\hat{e}$ and $\hat{r}$ were identical. But for the numerical solution we distinguished between the satellite direction $\hat{r}$ and the satellite direction from a surface element $\hat{e}$. In the same figure the angle β is used to indicate the part of the Earth visible by the satellite. In the case of GPS satellites ($h = 20000\ km$) and considering $R_E = 6371\ km$, we have

$$\beta = \cos^{-1}\left(R_E / (R_E + h)\right) \approx 76°. \tag{2.25}$$

With this angle the area of the sphere seen by GPS satellites can be computed. According to Boyd (1983) the area is given by

$$A_{GPS} = 4\pi R_E^2 \sin\beta/2 \tag{2.26}$$

and as the area of the whole Earth is $4\pi R_E^2$, the GPS satellites see around 38% of the total Earth's surface.

Now for the integration of $d\vec{E}_{refl}$ the integration limits of (2.13) can be simply changed due to the condition used in (2.24) to

$$dA = R_E^2 \sin\vartheta \, d\vartheta \, d\varphi \tag{2.27}$$
$$\vartheta = 0, ..., \pi, \qquad \varphi = -\pi/2, ..., \pi/2, \qquad 0 \leq \psi \leq \pi.$$

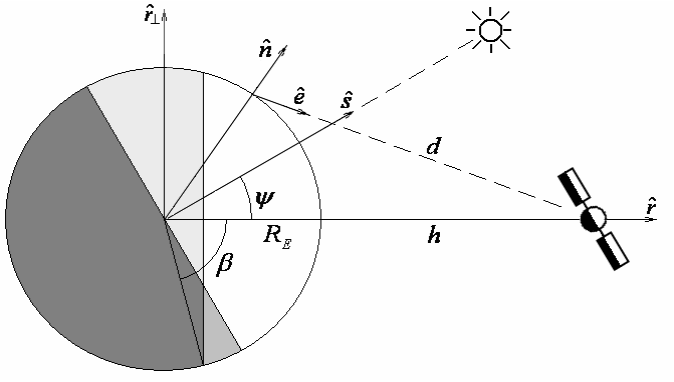

Figure 2.3. View from $\hat{z}$ of Figure 2.2

And the integral of $d\vec{E}_{refl}$ over the illuminated part of the Earth visible to the satellite, which gives the irradiance at the satellite altitude, is given by

$$\begin{aligned} E_{sat}(\psi,h)_{\hat{r}} &= \int d\vec{E}_{refl} \cdot \hat{r} \\ E_{sat}(\psi,h)_{\hat{r}_\perp} &= \int d\vec{E}_{refl} \cdot \hat{r}_\perp . \end{aligned} \tag{2.28}$$

$\vec{E}_{sat}$ has been separated into the radial and the non-radial components. The component perpendicular to the plane satellite – Earth – Sun vanishes as the integral is performed, since the illumination is symmetric in this axis for constant albedo. Note that (2.28) is no longer trivial to solve analytically, but the result can be easily computed in a numerical way. In an analytical approach Borderies and Longaretti (1990) have solved (2.28) just for the special case when the satellite do not see the border of reflected Sun light and emitted infrared radiation, for GPS this means for $\psi < 14°$ or $\psi > 166°$, see Figure 2.3.

Moreover this mathematical model of the albedo of the Earth also coincides with the one used by Bhanderi and Bak (2005), with the only difference that they do not consider a constant albedo of the Earth, but they get the albedo α for each surface element from satellite data. This model will be further explained in 2.3.1 Earth Albedo Toolbox and compared with the model just described here.

Finally one can compute the integral of $\vec{E}_{sat}$ over the surface S of the sphere of radius $r_{sat} = R_E + h$, which gives the radiant power intersected by the Earth times the total albedo of the Earth. This integral is computed using (2.19) and the radial component of the irradiance vector:

$$\Phi_{refl-total} = \int_S E_{sat}(\psi,h)_{\hat{r}}\, dS = \alpha\Phi_{in-total} . \tag{2.29}$$

2.2.3 Emitted Radiation

The radiation power coming from the Sun that is intersected by the Earth can be computed as $A_E E_{sun}$, with $A_E = \pi R_E^2$. A fraction of this radiation is immediately reflected in the visible part of the spectrum, while the other fraction is absorbed and later reemitted as infrared radiation over the total surface of the Earth that has an area of $4\pi R_E^2$, see Taylor (2005). Considering that a fraction α of the incoming radiation is reflected, the equivalent to the solar constant of the Earth at its surface can be written as

$$E_{earth} = \frac{(1-\alpha)}{4} E_{sun} . \tag{2.30}$$

Assuming that the Earth emits this radiation as a Lambertian sphere, one ends up with similar integrals as before, with the difference that now there is no dependency on the angle ψ satellite – Earth - Sun. Therefore we distinguish again between an analytical and a numerical solution.

Analytical Solution

Starting with Eq. (2.6), one can write the irradiance from a surface element at the satellite distance d and direction θ, as

$$dE_{emit} = \frac{(1-\alpha)}{4\pi d^2}\cos\theta\, E_{sun} dA. \tag{2.31}$$

The angle θ is given by (2.11) and the differential of area by (2.27). dE_{emit} is integrated over the part of the sphere visible for the satellite at infinity and we get

$$\begin{aligned} E_{sat}(\psi) &= \int dE_{emit} = \int_0^{\pi}\int_{-\pi/2}^{\pi/2} \frac{(1-\alpha)}{4\pi d^2}\sin\vartheta\cos\varphi\, E_{sun} R_E^2 \sin\vartheta\, d\vartheta\, d\varphi \\ E_{sat}(\psi) &= \frac{(1-\alpha)}{4\pi d^2} A_E E_{sun}. \end{aligned} \tag{2.32}$$

Here $E_{sat}(\psi)$ is used to indicate that the irradiance is in a specific direction, although $E_{sat}(\psi)$ is constant with no dependency on ψ.

The integral over the surface of the sphere of radius $r_{sat} = R_E + h$, can be computed as

$$\begin{aligned} \Phi_{emit-total} &= \int_S E_{sat}(\psi) dS = 2\pi \int_0^{\pi} \frac{(1-\alpha)}{4\pi d^2} A_E E_{sun} (R_E + h)^2 \sin\psi\, d\psi \\ \Phi_{emit-total} &= \frac{(R_E + h)^2}{d^2}(1-\alpha) A_E E_{sun} = (1-\alpha)\Phi_{in-total}, \end{aligned} \tag{2.33}$$

where we see clearly that d must be equal to $R_E + h$, like in the case of the model for reflected radiation.

Finally the irradiance at the satellite altitude h due to the Earth's emitted radiation is expressed as

$$\vec{E}_{sat}(\psi, h) = \frac{(1-\alpha)}{4\pi} \frac{A_E E_{sun}}{(R_E + h)^2} \hat{r} \tag{2.34}$$

which is valid only for $h >> R_E$.

Numerical Solution

If no approximation is used and following the same steps as for the Lambertian sphere, we start with (2.31), the emitted irradiance in the satellite direction from a surface element:

$$d\vec{E}_{emit} = \begin{cases} \dfrac{(1-\alpha)}{4\pi d^2}\cos\theta\, E_{sun} dA\, \hat{e} & if \quad \cos\theta \geq 0 \\ 0 & else \end{cases}. \tag{2.35}$$

The integral of $d\vec{E}_{emit}$ over the part of the sphere visible to the satellite, is now

$$E_{sat}(\psi, h)_{\hat{r}} = \int \vec{E}_{emit} \cdot \hat{r} \tag{2.36}$$

for constant albedo and it should hold that

$$\Phi_{emit-total} = \int_S E_{sat}(\psi)_{\hat{r}}\, dS = (1-\alpha)\Phi_{in-total}. \tag{2.37}$$

2.2.4 Earth Radiation Model

The models for reflected and emitted radiation of the Earth are combined, by simply adding the results of sections 2.2.2 and 2.2.3. This gives two complete models of the Earth's irradiance, an analytical but approximate one (ERM-A) and a model where no approximation is used but has to be computed numerically (ERM-N). The resulting models are presented here together with a summary of the main quantities needed to compute them. Both models depend just on three main parameters that are written in Table 2.2.

The dependency on α is not explicitly written in the albedo models since its value for the Earth is around $\alpha = 0.3$ and instead just $\vec{E}_{sat}(\psi, h)$ was written. However plots are made for different values of α, h and ψ.

Moreover the angle ψ satellite – Earth – Sun can be simply computed as

$$\cos\psi = \frac{\vec{r}_{sat} \cdot \vec{r}_{sun}}{|\vec{r}_{sat}||\vec{r}_{sun}|} \tag{2.38}$$

where $\vec{r}_{sat}$ and $\vec{r}_{sun}$ are the positions of satellite and Sun, both in an Earth centred reference system.

Furthermore it is important to note that the integral of both models over the surface of the sphere of radius $r_{sat} = R_E + h$ is, as expected, the initial incoming radiant power from the Sun:

$$\begin{aligned} \Phi_{out-total} &= \int_S \vec{E}_{sat}(\psi) dS = \alpha\Phi_{in-total} + (1-\alpha)\Phi_{in-total} \\ \Phi_{out-total} &= \Phi_{in-total}. \end{aligned} \tag{2.39}$$

Table 2.2 Earth radiation models parameters

Parameter	Symbol	Unit
Earth's albedo	α	-
Satellite altitude	h	m
Angle satellite – Earth - Sun	ψ	rad

ERM-A: Analytical Earth Radiation Model

$$\vec{E}_{ERM-A}(\psi,h)=\frac{A_E E_{sun}}{(R_E+h)^2}\left[\frac{2\alpha}{3\pi^2}((\pi-\psi)\cos\psi+\sin\psi)+\frac{(1-\alpha)}{4\pi}\right]\hat{r} \tag{2.40}$$

ERM-N: Numerical Earth Radiation Model

$$\begin{aligned} E_{ERM-N}(\psi,h)_{\hat{r}} &= \int d\vec{E}_{refl}\cdot\hat{r}+\int d\vec{E}_{emit}\cdot\hat{r} \\ E_{ERM-N}(\psi,h)_{\hat{r}_\perp} &= \int d\vec{E}_{refl}\cdot\hat{r}_\perp \end{aligned} \tag{2.41}$$

With:

$$d\vec{E}_{refl}=\begin{cases}\dfrac{\alpha}{\pi d^2}\cos\theta\cos\gamma E_{sun}dA\hat{e} & if \quad \cos\theta\geq 0 \quad and \quad \cos\gamma\geq 0 \\ 0 & else\end{cases} \tag{2.42}$$

$$d\vec{E}_{emit}=\begin{cases}\dfrac{(1-\alpha)}{4\pi d^2}\cos\theta E_{sun}dA\hat{e} & if \quad \cos\theta\geq 0 \\ 0 & else\end{cases} \tag{2.43}$$

$$dA=R_E^2\sin\vartheta\, d\vartheta\, d\varphi \tag{2.44}$$

$$\vartheta=0,...,\pi, \qquad \varphi=-\pi/2,...,\pi/2, \qquad 0\leq\psi\leq\pi$$

Table 2.3 Earth radiation models quantities

Quantity	Symbol	Definition	Unit
Solar constant	E_{sun}	1367	W/m^2
Earth's mean radius	R_E	6371×10^3	m
Earth's disc area	A_E	πR_E^2	m^2
Satellite or radial direction vector	$\hat{r}$	$(1,0,0)$	-
Non-radial direction vector	$\hat{r}_\perp$	$(0,1,0)$	-
Sun direction vector	$\hat{s}$	$(\cos\psi,\sin\psi,0)$	-
Normal to surface element vector	$\hat{n}$	$(\sin\vartheta\cos\varphi,\sin\vartheta\sin\varphi,\cos\vartheta)$	-
Surface to satellite distance	d	$\lvert(R_E+h,0,0)-R_E\hat{n}\rvert$	m
Surface to satellite direction vector	$\hat{e}$	$\vec{d}/\lvert\vec{d}\rvert$	-
Radiation incident angle	γ	$\cos^{-1}(\hat{s}\cdot\hat{n})$	rad
Radiation reflection angle	θ	$\cos^{-1}(\hat{e}\cdot\hat{n})$	rad

Plots of Earth Radiation Models

In the following figures the plots of the analytical and numerical Earth radiation models are presented. As independent variable always the angle ψ satellite – Earth – Sun was used. However the results of both models for different values of albedo and satellite altitude were also plotted in order to study the general behaviour of them.

In Figure 2.4 the Earth radiation models are plotted for a GPS satellite altitude of $20000\,km$ and different values of the total albedo of the Earth. Note that always the numerical model has a bigger peak than the analytical one for values close to $\psi = 0°$. Furthermore as the integral (2.39) of both models over ψ should be the same, we see as the analytical model is in general smother than the numerical one and for albedo equal to zero both models are identical. The plots emphasize that the radial component of the models is the most dominant one and the negative sign of the non-radial component just indicates that the irradiance is in the direction $-\hat{r}_{\perp}$.

In Figure 2.5 the Earth radiation models are plotted for a total albedo of $\alpha = 0.3$ and different satellite altitudes. The plots are ordered with increasing altitude and it can be immediately seen that the irradiance decreases with the distance of the satellite to the Earth. One can also note that the difference between the analytical and the numerical model decreases as the satellite altitude increases, something expected since the analytical model was constructed to be valid only for $h >> R_E$. For the case of a satellite in a LEO orbit the difference between both models becomes more important since the approximation made in the analytical model is no longer valid. To know how good the analytical model is compared to the numerical one, we can compute the relative mean difference between both models as

$$\Delta_{ERM} = \frac{\int_S (E_{ERM-A} - E_{ERM-N})dS}{\int_S E_{ERM-N}\,dS} = \frac{\int_0^{\pi} (E_{ERM-A} - E_{ERM-N})\sin\psi\,d\psi}{\int_0^{\pi} E_{ERM-N}\,\sin\psi\,d\psi}, \tag{2.45}$$

where E_{ERM} is the magnitude of the irradiance vector and dS is given by Eq. (2.19).

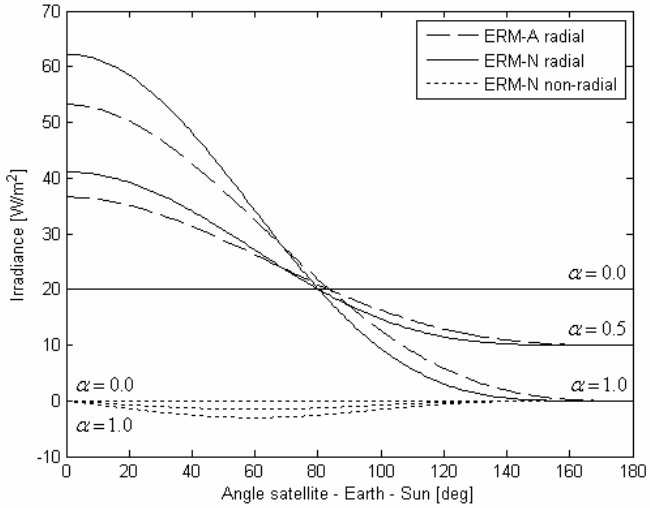

Figure 2.4 Earth radiation models for satellite altitude $h = 20000\,km$ and different albedo values

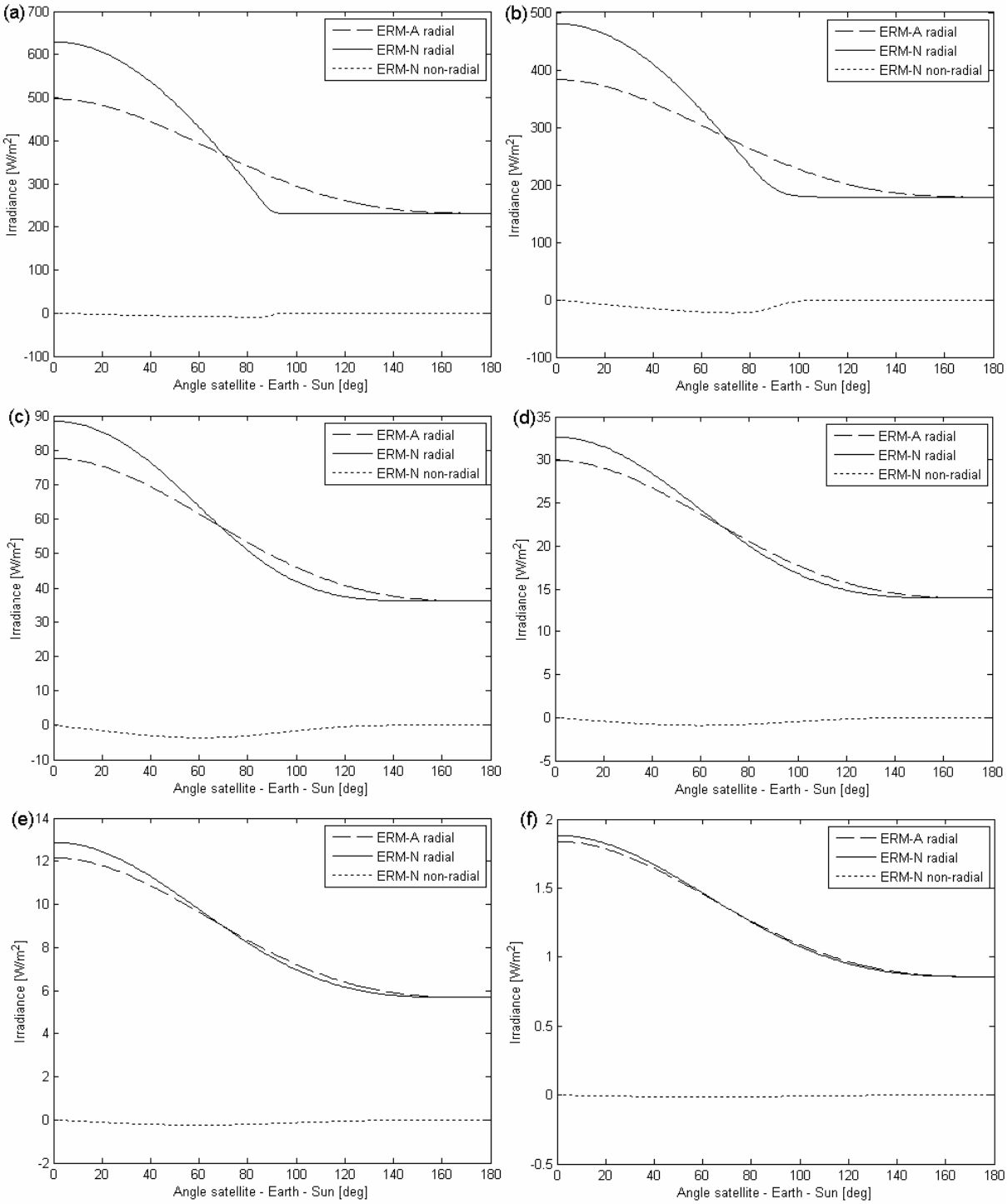

Figure 2.5 Earth radiation models for albedo $\alpha = 0.3$ and different satellite altitudes: (a) $h = 100\,km$, (b) $h = 1000\,km$, (c) $h = 10000\,km$, (d) $h = 20000\,km$, (e) $h = 35000\,km$ and (f) $h = 100000\,km$

Let us now focus just on Figure 2.5(d), where we have the Earth radiation models for albedo equal to 0.3 and a GPS satellite altitude. In this case the relative mean difference between the analytical and the numerical model is $\Delta_{ERM} = 0.002\%$ with total minimum and maximum values of -8.3% and 6.1%, this means the analytical model already provides a reasonable approximation.

Finally note that the irradiances just computed here, can already be used in Chapter 3 for the computation of the acceleration acting on the satellite due to the radiation of the Earth.

2.3 Validation of Earth Radiation Model

In the Earth radiation models of the previous section, the albedo of the Earth was considered to be constant and with a total value of 0.3. Only by using this assumption it was possible to obtain an analytical solution of the Lambertian sphere. But in the numerical model one can change the terms α and $(1-\alpha)$, for reflected and emitted irradiance, by reflectivity and emissivity coefficients dependent on latitude and longitude. Then equations (2.42) and (2.43) can be then written as

$$d\vec{E}_{refl} = \begin{cases} \dfrac{\rho(\varphi,\lambda)}{\pi d^2}\cos\theta\cos\gamma E_{sun} dA\hat{e} & if \quad \cos\theta \geq 0 \quad and \quad \cos\gamma \geq 0 \\ 0 & else \end{cases}$$
$$d\vec{E}_{emit} = \begin{cases} \dfrac{\varepsilon(\varphi,\lambda)}{4\pi d^2}\cos\theta E_{sun} dA\hat{e} & if \quad \cos\theta \geq 0 \\ 0 & else \end{cases} \tag{2.46}$$

where φ and λ are used to indicate latitude and longitude. The reflectivity is given by $\rho(\varphi,\lambda)$ and emissivity by $\varepsilon(\varphi,\lambda)$. Note that in the previous section the albedo α was used as a global value for the Earth, therefore one could assume, that all the energy intercepted at one place of the Earth must be reflected or emitted at the same place, so there is conservation of energy. In reality the conservation of energy is global but not local since there is a big transport of energy on the Earth, for example from the equator to the poles. So it follows that

$$\rho(\varphi,\lambda) \neq 1-\varepsilon(\varphi,\lambda). \tag{2.47}$$

Whether this dependency of the reflectivity and emissivity is important for the irradiance of the Earth that is received by GPS satellites, is a question that will be addressed in the following pages. Some of the reasons to find out the importance of this dependency are:

- The poles reflect more radiation as the equator.
- Land and ocean have different reflectivity and emissivity.
- Clouds have high reflectivity and can be found mainly over certain areas of the Earth.

In order to account for these effects, first the numerical Earth radiation model is compared with the Earth Albedo Toolbox software, see Bhanderi (2007), and second data from satellite measurements is used to construct reflectivity and emissivity as a function of latitude.

The models can be compared as in (2.45) by using the following equation:

$$\Delta_{ERM} = \frac{\int_{-\pi}^{\pi}\int_{-\pi/2}^{\pi/2}(E_{ERM} - E_{REF})\cos\varphi\, d\varphi\, d\lambda}{\int_{-\pi}^{\pi}\int_{-\pi/2}^{\pi/2} E_{REF}\cos\varphi\, d\varphi\, d\lambda}, \tag{2.48}$$

where E_{REF} is the irradiance magnitude from the model used as reference.

2.3.1 Earth Albedo Toolbox

The Earth Albedo Toolbox, developed by Bhanderi (2007), computes the irradiance of the Earth for a given position of satellite, Earth and Sun. It considers just the reflected radiation of the Sun, since the main purpose of the Earth Albedo Toolbox is to be used for Earth and Sun sensors which determine the satellite attitude. To compute the irradiance it uses the mathematical model described by Bhanderi and Bak (2005), which coincides with the numerical Earth radiation model ERM-N.

Therefore by comparing directly the ERM-N model, for reflected radiation and constant albedo with the outcome of the Earth Albedo Toolbox, one can see the difference on the reflected irradiance of the Earth for GPS satellites.

The Earth Albedo Toolbox uses reflectivity data from the TOMS (Total Ozone Mapping Spectrometer) project, see McPeters (2009). With this data one can produce for example maps of mean reflectivity and standard deviation for a complete year, see Figure 2.6.

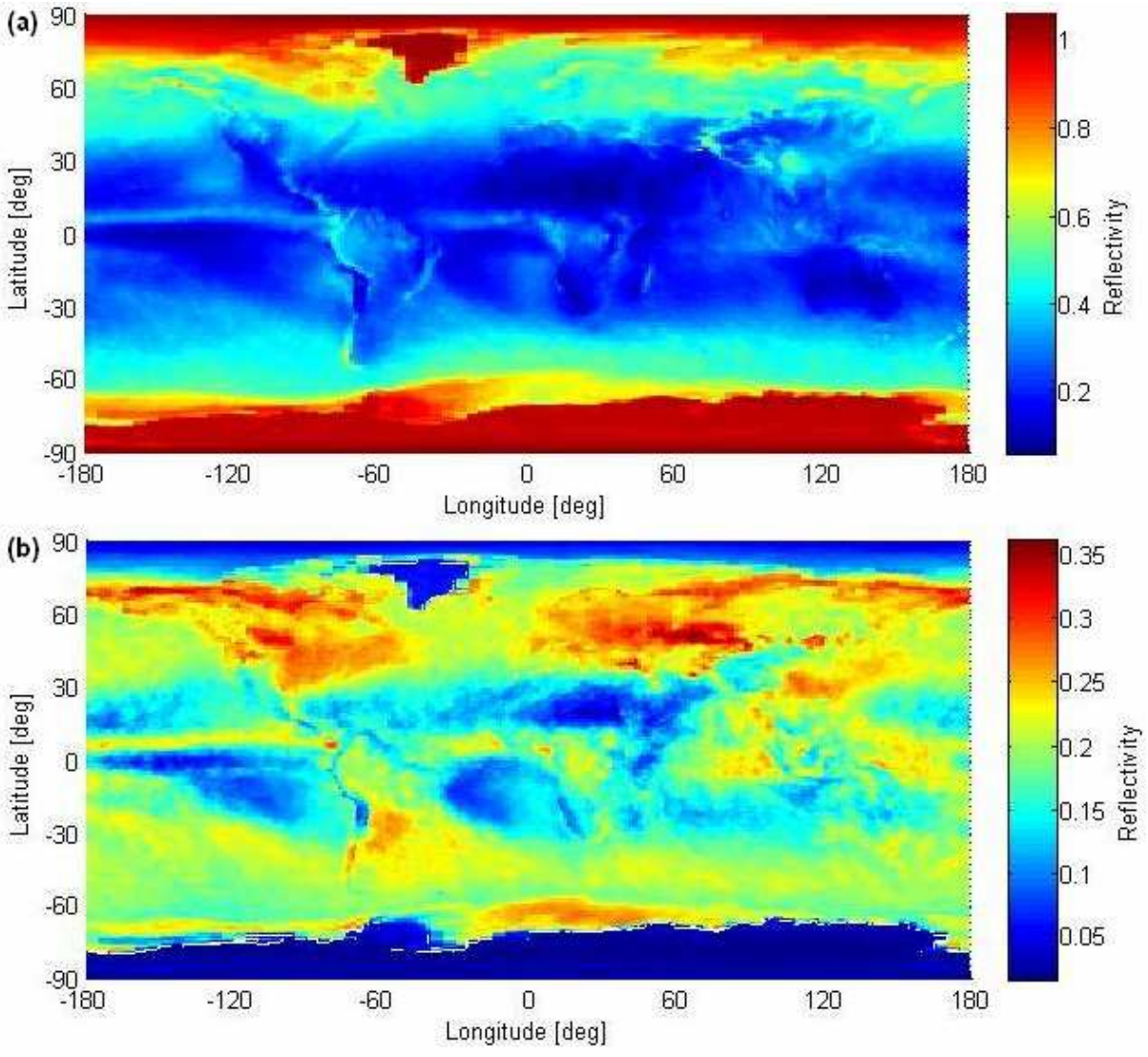

Figure 2.6 TOMS reflectivity data, (a) mean and (b) standard deviation for 2004

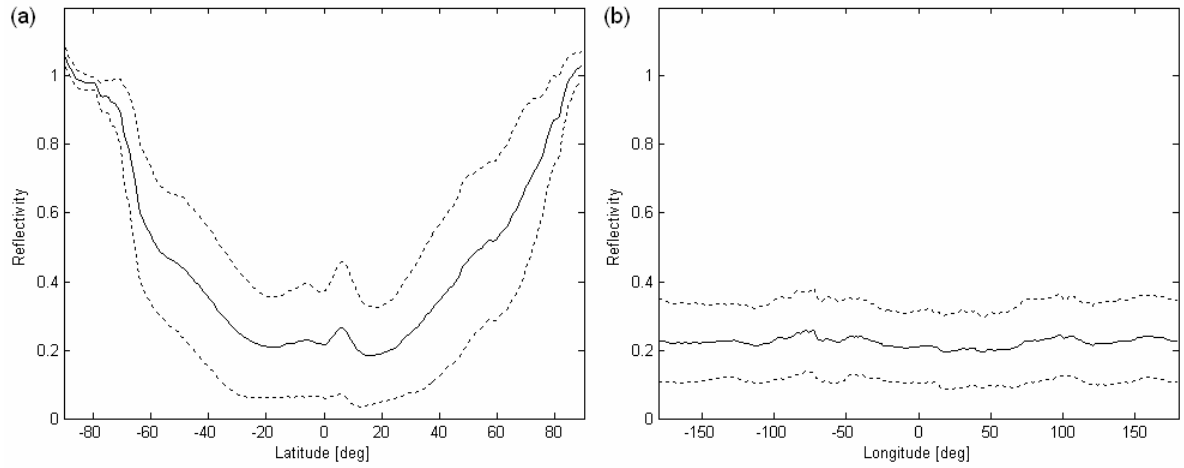

Figure 2.7 Reflectivity (mean ± standard deviation) as a function of (a) latitude and (b) longitude, from TOMS 2004 data

From Figure 2.6(a), one of the first things to note is the big dependency of reflectivity with latitude, therefore in Figure 2.7 the mean reflectivity as a function of latitude and longitude is plotted, using the values of the 2004 annual mean. It can also be seen that land and ocean have different characteristics but the dependency of reflectivity is not as high compared with latitude.

The plot of standard deviation, Figure 2.6(b), shows the temporal variability of reflectivity over one year. The continents in the northern hemisphere for example present high variability, while the area of the desert in Africa or the Poles have low change over one year. Also oceans show less variability than the continents. Probably by plotting monthly averages one could see clear seasonal changes of the reflectivity.

Coming back to Figure 2.7, where the mean reflectivity for latitude and longitude is plotted together with the standard deviation, we see that there is high variability for low and medium latitudes while for the poles there is a low change of reflectivity. Furthermore the dependency with longitude is constant and with a value around 0.22. This does not mean that the total albedo of the Earth has this value. If one computes it using Eq. (2.9) where the irradiance is integrated over the surface of a sphere of radius $R_E + h$, one would find for two different positions of the Sun (Figure 2.8 and Figure 2.9) total albedo values of 0.2841 and 0.3263. This is logical since for the second case the latitude of the Sun is higher and the high values of the reflectivity have as a consequence that the irradiance increases and therefore also the total albedo of the Earth.

To evaluate how the spatial distribution of the reflectivity (Figure 2.6) affects the irradiance received by GPS satellites, we compare the irradiance obtained from the Earth Albedo Toolbox with the one computed using the ERM-N model with constant albedo of 0.3. This is done for all the satellite positions and for two Sun positions, these results are shown in Figure 2.8 and Figure 2.9, where we can see already that the orders of magnitude and the shape of the models are similar. The plots are so smooth since the GPS satellites see a big part of the Earth, Eq. (2.26), and all the reflected irradiance is integrated at the location of the satellite.

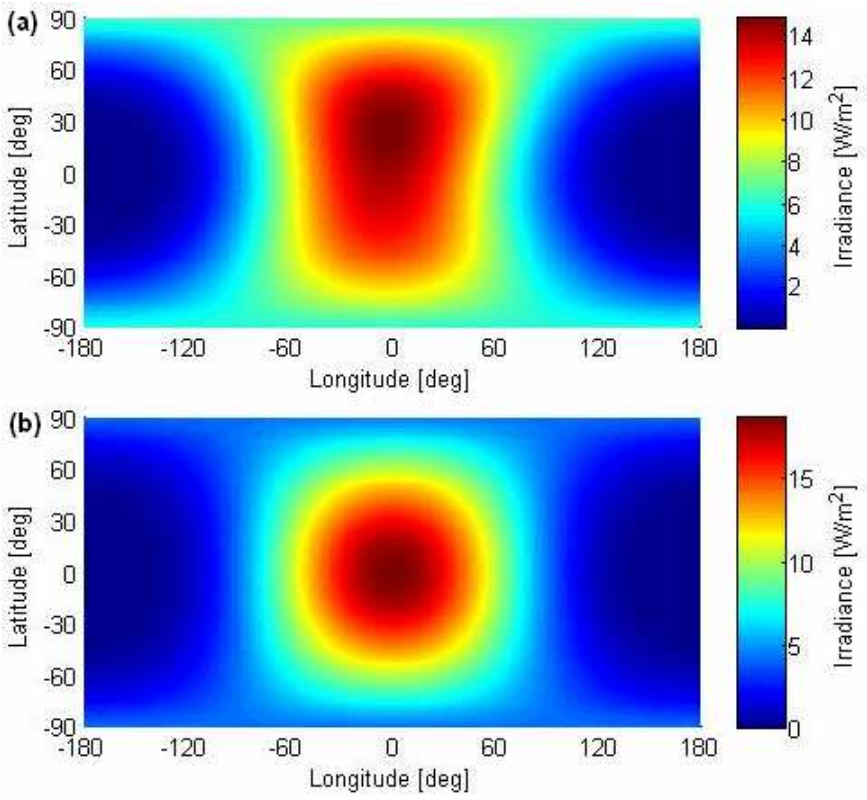

Figure 2.8 Reflected irradiance from (a) Earth Albedo Toolbox and (b) ERM-N at GPS altitude, Sun position $\varphi = 0°, \lambda = 0°$

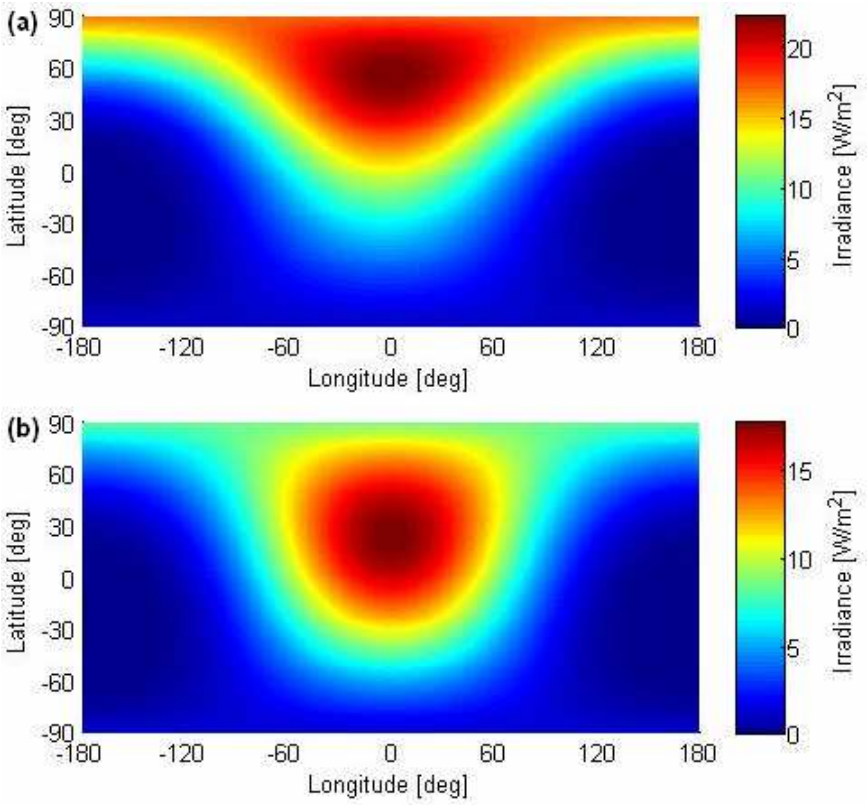

Figure 2.9 Reflected irradiance from (a) Earth Albedo Toolbox and (b) ERM-N at GPS altitude, Sun position $\varphi = 23.5°, \lambda = 0°$

Although the shape and orders of magnitudes of the computed irradiances are similar, the mean differences between both models are 6.2% and -12.4% for the Sun at $\varphi = 0°$ and $\varphi = 23.5°$ respectively. However the maximum and minimum differences are around $\pm 40\%$. These differences are just for the reflected irradiance but still are very large, furthermore we just took into account mean annual data and the changes of reflectivity, Figure 2.7(a), are also not small.

As the differences between the ERM-N and the Earth Albedo Toolbox are large, we will not continue further with the analysis of the errors but we will rather focus into improving our Earth radiation model, for this purpose we will use another set of satellite data which provides both reflectivity and emissivity as a function of latitude and longitude.

2.3.2 Model with Latitude Dependent Albedo

After seeing that the spatial distribution of reflectivity has a considerable impact on the irradiance received by the GPS satellites, we proceed here to improve our Earth Radiation Model. For that purpose we use data from the CERES (Clouds and Earth's Radiant Energy System) project, see Wielicki et al. (1996), to compute the irradiance received by GPS satellites. We use already processed data (level 3) which can be easily transformed in reflectivity and emissivity, this data comes as monthly averages in a grid of $2.5° \times 2.5°$.

CERES together with ERBE (Earth Radiation Budget Experiment) data, see Barkstrom (1984), have been already used by Ziebart et al. (2004), to compute the irradiance received by GPS satellites. The approach followed by them is to use all the available data so almost no error is introduced, while what we do is to fit polynomials over latitude and over time of the year, to have a simplified model that still gives the irradiance at the satellite altitude with a small error.

In the following we will use data mainly from 2007 since this is the year for which we have also used real GPS and SLR measurements. However the approach developed in this study can be used for any year of satellite data.

More specifically, for the person interested in computing similar results, the CERES data used here, see Kusterer (2009), has the following specifications:

- ERBE-like Geographical Averages (ES-4).
- Terra -FM1, Edition 2.
- 2.5 Degree Regional, Monthly (Day) Averages, Total Sky.
- Quantities: Albedo and Longwave Flux.

In general the reflectivity is obtained directly and is called Albedo in the CERES data, but we will continue here using the reflectivity term to avoid confusion with the quantities discussed before in this chapter. The emissivity is computed as $\varepsilon(\varphi, \lambda) = 4E_{LW} / E_{sun}$, see Eq. (2.30), with E_{LW} the Longwave Flux from CERES data and $E_{sun} \approx 1367 W/m^2$ the irradiance from the Sun at the Earth distance.

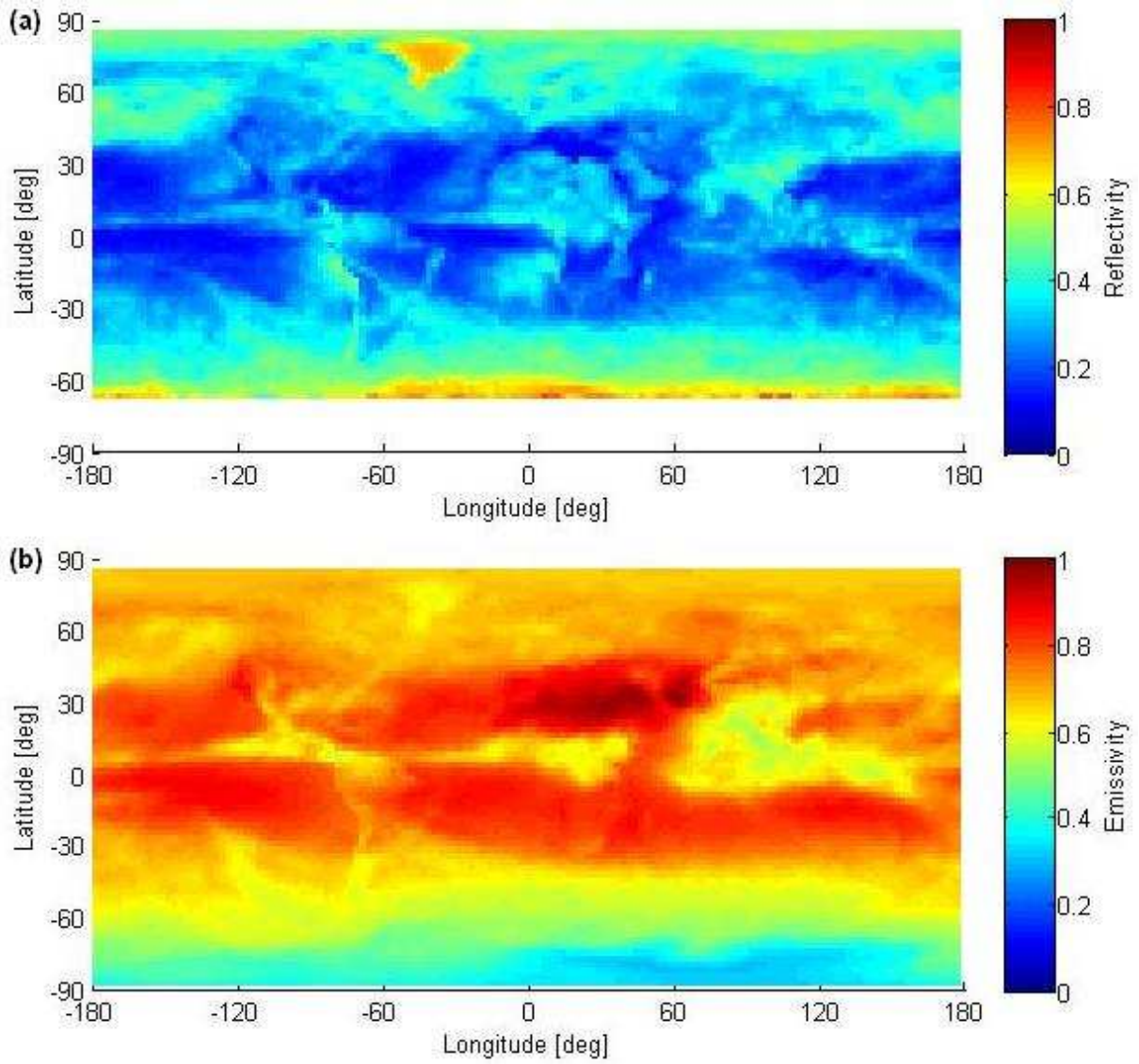

Figure 2.10 CERES data, (a) reflectivity and (b) emissivity for July 2007

As an example we present reflectivity and emissivity data for July 2007 in Figure 2.10. The first thing we can note is the strong dependency with latitude of both quantities, see also Figure 2.6. For the rest of the year the plots are not shown, instead the mean reflectivity and emissivity as a function of latitude for all months are plotted in Figure 2.11.

In these figure we first can appreciate how the reflectivity and emissivity curves are shifting in latitude along the year, where the maximum shift is for the winter and summer months, plotted in blue and red. Also note how the curves are more separated in the northern hemisphere, this is because there is more land than ocean in this hemisphere and the land can change its properties faster than the ocean.

On the right side of Figure 2.11 we have fitted a first order harmonic expansion to reflectivity and emissivity data as a function of latitude:

$$\rho(\lambda) = \rho_{const} + \rho_{\cos}\cos\varphi + \rho_{\sin}\sin\varphi$$
$$\varepsilon(\lambda) = \varepsilon_{const} + \varepsilon_{\cos}\cos\varphi + \varepsilon_{\sin}\sin\varphi. \qquad (2.49)$$

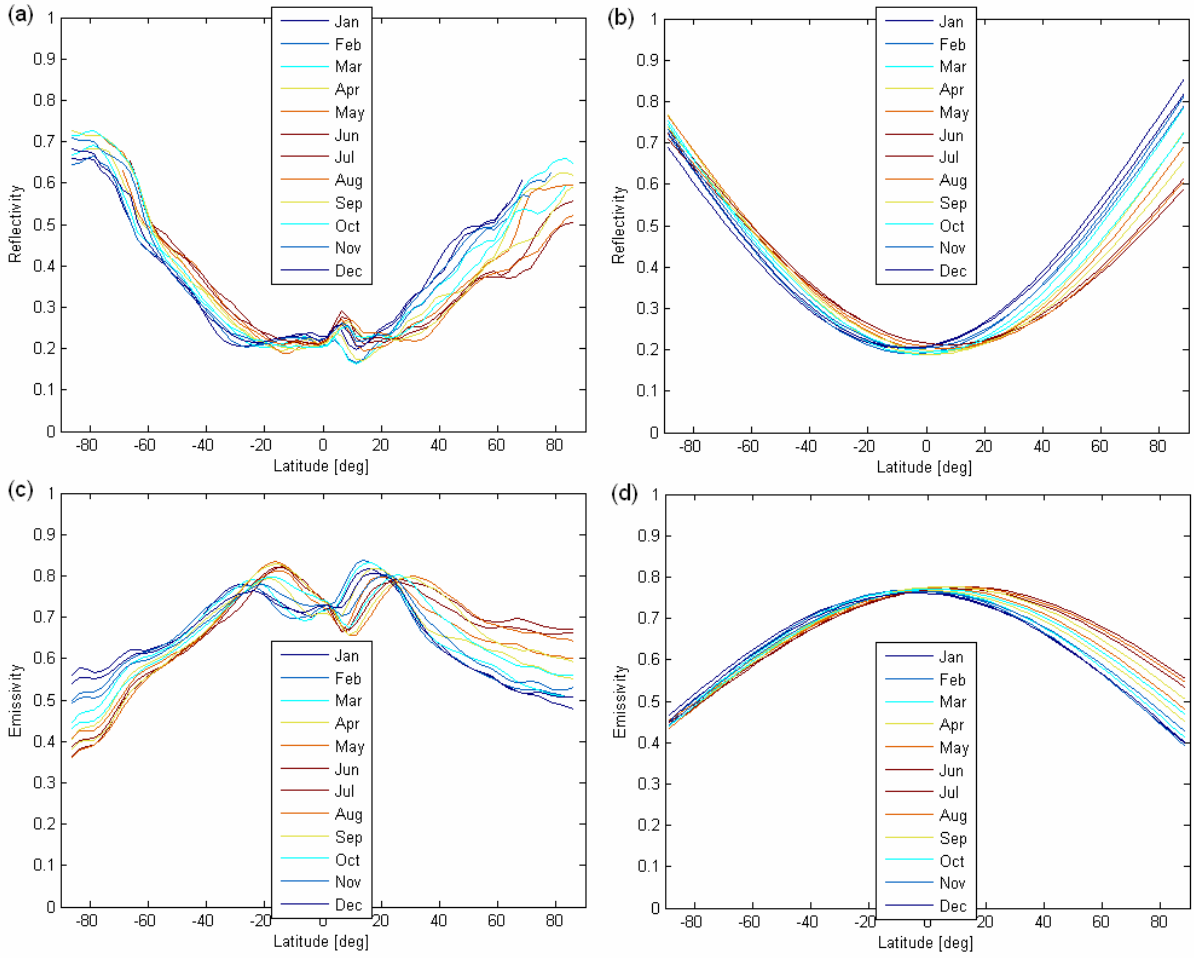

Figure 2.11 Reflectivity as a function of latitude, (a) monthly data, (b) fitted data. Emissivity as a function of latitude, (c) monthly data, (d) fitted data

A least squares adjustment was used together with a weighted of the measurements with $\cos\varphi$, since the area of an sphere decreases in this way with the latitude. These functions were chosen because they are simple and have high correlation coefficients (R) with respect to the data, see Figure 2.12. However note that the change of the curves around $\varphi = 0°$ cannot be modelled with this kind of fit. It must be mentioned that a very similar idea was used by Knocke et al. (1988) where just latitude dependent harmonic functions are fitted by least squares adjustment to seasonally averaged Earth radiation budget data.

In Figure 2.12 the coefficients of Eq. (2.49) are plotted for the 12 months of the year. First let us note that the correlation coefficients (R_{month}) for the reflectivity are above 0.90 while for the emissivity they are above 0.98. That the emissivity is better modelled than the reflectivity is advantageous, since the emitted radiation has a bigger impact in the computation of the irradiance. It should also be mentioned that higher order harmonic expansions have been implemented with some improvement in the correlation coefficients, but almost none in the irradiance that reach GPS satellites. Furthermore we see how these coefficients clearly change over the year, so again we can fit another function in this case over the Day of Year (DOY) and is just a coincidence that a suitable function, for all the coefficients of Eq. (2.49), is of the form

$$Coeff\left(DOY\right) = A + B\cos\left(2\pi DOY/365\right) + C\sin\left(2\pi DOY/365\right) \tag{2.50}$$

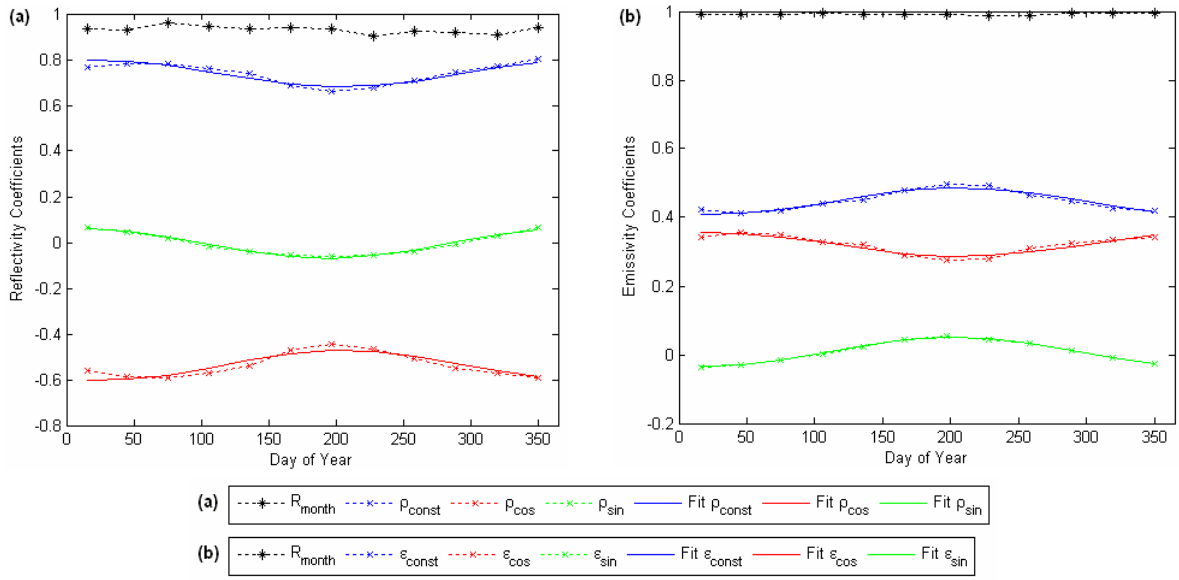

Figure 2.12 Coefficients for Eq. (2.49), for (a) reflectivity and (b) emissivity as a function of the Day of Year (DOY)

These fitted polynomials are plotted with solid lines in the same figures, where we see that although the fit is not perfect, it follows the shape of the coefficients over the year, with mean correlation coefficients of 0.94 for the reflectivity and 0.96 for the emissivity.

We have also done tests with another year of data (2001) and the variation and orders of magnitude of these coefficients are very similar as a function of the Day of Year, so in other words Figure 2.12 is almost the same for different years of CERES data.

This kind of model has then a high potential since we are able to describe the average properties of reflectivity and emissivity of the Earth for a complete year with three numbers (A, B, C) for each of the six coefficients of Eq. (2.49), which leads to a total of just 18 numbers (Table 2.4).

Table 2.4 Annual coefficients for reflectivity and emissivity, for 2007 and 2001

Annual Coefficients:	A_{2007}	B_{2007}	C_{2007}	A_{2001}	B_{2001}	C_{2001}
ρ_{const}	0.7395	0.0557	0.0214	0.7479	0.0577	0.0220
$\rho_{\cos}$	-0.5378	-0.0595	-0.0263	-0.5435	-0.0611	-0.0244
$\rho_{\sin}$	-0.0049	0.0629	0.0114	-0.0040	0.0672	0.0126
ε_{const}	0.4476	-0.0355	-0.0155	0.4462	-0.0321	-0.0068
$\varepsilon_{\cos}$	0.3210	0.0316	0.0146	0.3213	0.0257	0.0034
$\varepsilon_{\sin}$	0.0084	-0.0400	-0.0149	0.0079	-0.0428	-0.0193

2.3.3 Comparison of Models

Approaching the end of this chapter we have already constructed four complete Earth radiation models and now the natural thing to do is to compare them, see Figure 2.13.

In the previous section the question has been posed, whether the simplification of the CERES data is good enough to compute the irradiance from Earth received by GPS satellites. To address this question we proceed as for the Earth Albedo Toolbox. But for the present case a more extensive analysis of the errors is done, taking now into account the reflected and emitted radiation.

The error analysis is as follows: the irradiance for all possible GPS satellite positions ($\varphi = \pm 55°$ since GPS orbit inclination is $55°$) is computed, for

- The first day of each month (worst fit of the data).
- Twelve possible longitudes of the Sun, every 30°.
- Four radiation models ERM-A, ERM-N ERM-LAT and ERM-CERES.

We have called ERM-LAT, the model with reflectivity and emissivity dependent on latitude, while the model that includes all the CERES data, for longitude and latitude, has been called ERM-CERES.

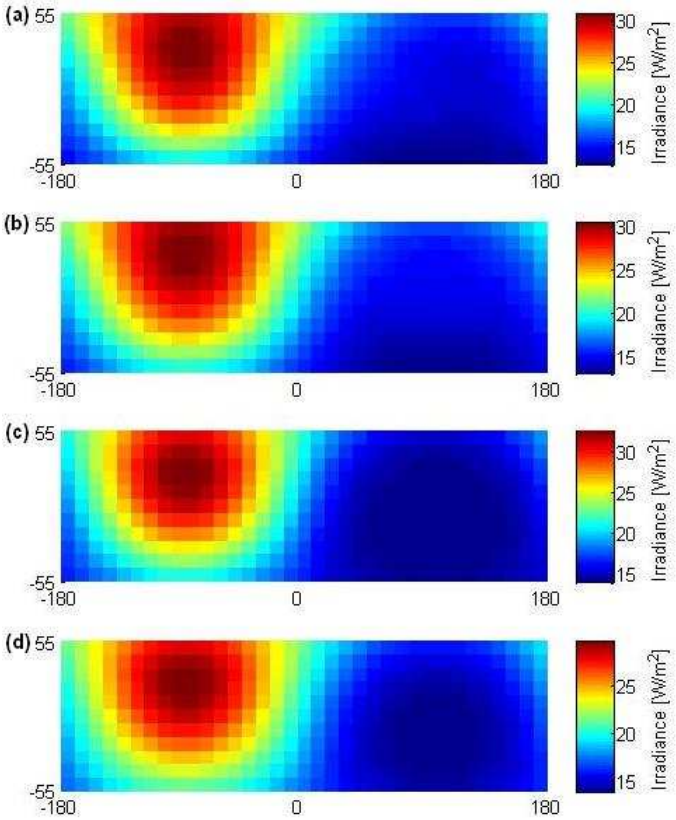

Figure 2.13 Irradiance at GPS altitude for August 2007 and Sun longitude $\lambda = -90°$. (a) ERM-CERES, (b) ERM-LAT, (c) ERM-N and (d) ERM-A

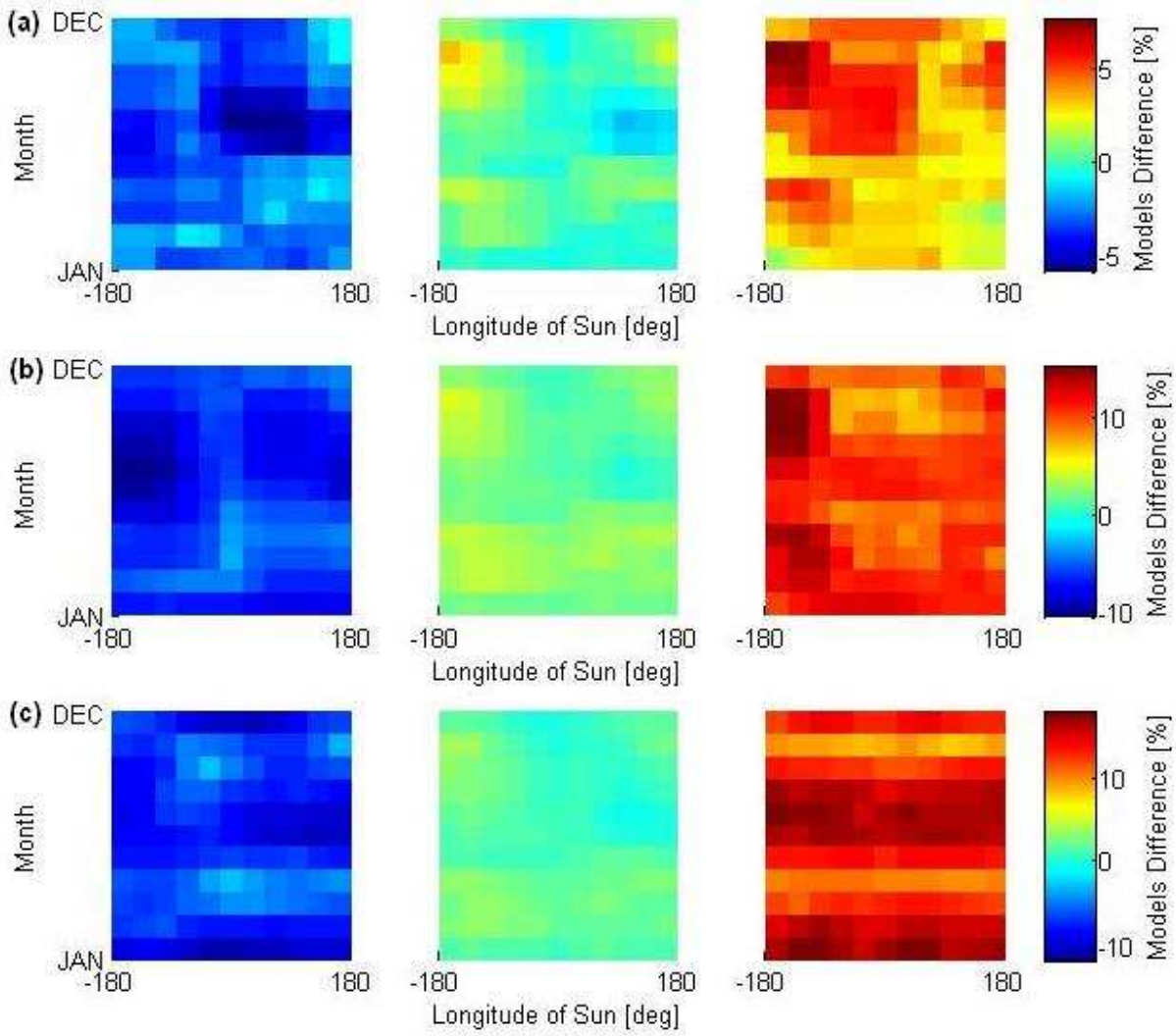

Figure 2.14 Comparison of (a) ERM-LAT, (b) ERM-N, (c) ERM-A with ERM-CERES. Left column: minimum difference, central column: mean difference and right column: maximum difference

From the four computed models (see example of Figure 2.13), we take the differences of the first three with respect to ERM-CERES and compute the mean difference using Eq. (2.48). Also we extract the minimum and maximum of the differences. This is done for each irradiance matrix for all satellite positions for a specific month and longitude of the Sun. The results are shown in Figure 2.14.

Starting with the difference between the analytical model with constant albedo (ERM-A) and the irradiance computed using CERES data (ERM-CERES), we see a clear structure of the error over the months (maximum and minimum plots), related to the latitude of the Sun.

In the case of the numerical model with constant albedo we have differences in the same order of magnitude as for ERM-A. Here we also see some dependency of the error with the time of the year but also with longitude of the Sun. The differences between ERM-A, ERM-N and ERM-LAT were computed in Table 2.5.

The model with reflectivity and emissivity dependent on latitude gives the smallest errors, as expected, from the three models. It is also important to mention that the errors shown in Figure 2.14, do not originate from a bad choice of functions to model the mean of reflectivity and emissivity over the latitude, but simply from the longitude dependency of these

quantities. For ERM-LAT we see a strong dependency of the error with the time of the year as well with the longitude. If this error must be further decreased the answer is to fit a function over latitude and longitude of the CERES reflectivity and emissivity data. For example a spherical harmonics expansion of low degree and order, should decrease more the difference between models.

Finally regarding the ERM-LAT we should recall that the mean maximum and minimum error of this model compared to the ERM-CERES is as low as 3.5% (Table 2.5). This means that for most of the possible position of satellite and Sun, the error remains below this value. This accuracy was achieved by using only 18 numbers to model a whole year of reflectivity and emissivity data. As mentioned before this simplification is possible since the GPS satellites are at far distance from the Earth, such that they receive the irradiance from a major part of the Earth's surface. As consequence the irradiance arriving to the satellites is averaged.

Table 2.5 Summary of Earth radiation models

ERM	Mathematical Model	Reflectivity & Emissivity	Mean Error	Min. Error	Max. Error	Respect to
ERM-CERES	Numerical	CERES data	-	-	-	-
ERM-LAT	Numerical	Lat. dependent	0.1%	-3.2%	3.7%	ERM-CERES
ERM-N	Numerical	Constant	2.1%	-6.7%	10.8%	ERM-CERES
			2.0%	-5.3%	9.0%	ERM-LAT
ERM-A	Analytical	Constant	1.6%	-7.4%	14.0%	ERM-CERES
			1.5%	-6.9%	12.3%	ERM-LAT
			0.0%	-8.3%	6.1%	ERM-N

2.4 Discussion and Outlook

Having compared the different models constructed within this chapter we can identify from Table 2.5 that the analytical and numerical models for constant albedo behave almost the same with respect to the model that includes CERES data. Therefore the more interesting cases to be tested in the following are: ERM-A, ERM-LAT and ERM-CERES, the last one being our reference model.

Regarding the reference model some possible improvements to it have been identified and which are worth to test in future work, but are out of the scope of this Thesis. Specifically the assumption that the Earth behaves approximately as a Lambertian sphere, as seen by GPS satellites, should be proofed. For example oceans at certain angles reflect directly the radiation coming from the Sun acting like a mirror (specular reflection) and not like a perfect diffuse reflector

Borderies and Longaretti (1990) give a small discussion with respect to the specular or diffuse reflection of the Earth, saying that the specular reflection can be more expected from calm seas or lakes, while clouds, snow fields and the continents all tend to produce diffuse reflections and it is estimated that the specular albedo of the Earth is about 10% of the total Earth albedo. With other arguments the conclusion is that the Earth radiation pressure may be calculated to acceptable accuracy using a diffuse reflection model, as it was done in this chapter.

On the other hand to see the effect of not using a diffuse reflection model of the Earth, one could use a similar approach as Martin and Rubincam (1996), who take into account effects of Earth albedo on the LAGEOS I satellite. For this purpose they use data of the phase function provided by the ERBE mission, this data is a function of the scene type, weather and the geometry of the surface element, satellite and Sun. Doing this there is no longer a need of the simplification assumed here of a Lambertian phase function.

Furthermore we took into account seasonal changes of the reflectivity and emissivity, but not faster changes than one month e.g. clouds change fast in time, so it could be interesting to see if there is and effect due to this in the irradiance received by GPS satellites.

The reason why these last improvements were not implemented is because they are considered to be small effects, since the GPS satellites are far enough from the Earth to see a big part of it and therefore they receive an average of irradiance. For example Ziebart et al. (2004) and Qiu et al. (2003) have also considered the Earth to be a Lambertian sphere, for computing the Earth irradiance at GPS distance and at Moon distance, respectively.

As a conclusion we can say that although the constructed models are not perfect, they take into account the major contributors for computing the irradiance received by GPS satellites and further improvements should add details to the models, but should not change the shape or orders of magnitude of them. Therefore we have useful models to get a good understanding of the effect of Earth radiation on GPS satellites.

3 GPS Satellite Model

3.1 Introduction

In this chapter we focus on the construction of simple satellite models exposed to the radiation coming from the Earth. This radiation will then produce acceleration acting on the satellites. First we discuss how the photons interact with the surface of the satellite. Introducing some concepts from the work of Montenbruck and Gill (2000) we have:

"A satellite that is exposed to solar radiation experiences a small force that arises from the absorption or reflection of photons. In contrast to the gravitational perturbations, the acceleration due to solar radiation depends on the satellite's mass and surface area."

In this study we are interested in Earth radiation rather than in Sun radiation, but the concepts are exactly the same. From the last chapter we have the irradiance vector $\vec{E}_{ERM}$ at a given satellite position. Only in this Introduction we will denote the irradiance as Φ, to keep the notation used by Montenbruck and Gill (2000). The irradiance can then be expressed as

$$\Phi = \frac{\Delta E}{A \Delta t} \tag{3.1}$$

which is the energy ΔE that passes through an area A in a time interval Δt. Then from Beutler (2005) we have that quantum mechanics says that each photon of frequency ν and wavelength $\lambda = c/\nu$ (where c is the speed of light in vacuum) carries the energy

$$E = h\nu \tag{3.2}$$

and carries an impulse of

$$p = \frac{E}{c} \tag{3.3}$$

where $h = 6.62 \times 10^{-34}\, Js$ is the Planck's constant. Accordingly, the total impulse of an absorbing body that is illuminated by the Earth changes by

$$\Delta p = \frac{\Delta E}{c} = \frac{\Phi}{c} A \Delta t \tag{3.4}$$

during the time Δt. This means the satellite experiences a force

$$F = \frac{\Delta p}{\Delta t} = \frac{\Phi}{c} A. \tag{3.5}$$

The momentum transferred per time unit onto a unit surface in a radiation field is also called radiation pressure

$$P = \frac{\Phi}{c}. \tag{3.6}$$

With Eq. (3.5) and the developments done in the following section we will be able to compute the force acting on the satellite by knowing the irradiance from the Earth, the area and the optical properties of the surfaces.

Concerning the shape of the satellite, an initial so called “cannon-ball model” is sometimes used as first approximation. One just assumes the satellite to be a sphere with certain average cross section and optical properties. A next step is to consider the satellite as a box-wing, the box representing the bus and the wing the solar panels. Looking at Figure 3.1 we see that a box-wing is already a quite good approximation of the satellite structure, in particular for GPS satellite since all the types of satellites manufactured until now have a similar shape compared to the Block II shown below.

For constructing a satellite model a natural choice of a reference system is body-fixed one. The reference system that one sees in Figure 3.1 is described in Fliegel et al. (1992) as:

“The +Z direction is towards the Earth and therefore along the SV (space vehicle) antennas. The SV is manoeuvred so that the Sun is in the SV plane of symmetry and so that the angle between the Sun and the antennas is always between $0°$ *and* $180°$*. When the angle is less than about* $14°$*, the Sun is eclipsed. The +X is positive towards the half plane that contains the Sun, and +Y completes a right-handed system and points along one of the solar panels center beams. Thus the surface on which the antennas are mounted is called the main body +Z side.”*

This body-fixed reference system is almost the same as the one introduce in the previous chapter, see (Figure 3.3), where the radial direction $\hat{r}$ just points in the -Z direction, while the non-radial direction $\hat{r}_{\perp}$ is the same as +X. Finally the direction vector $\hat{r}_3$ completes the right handed system and is equivalent to –Y.

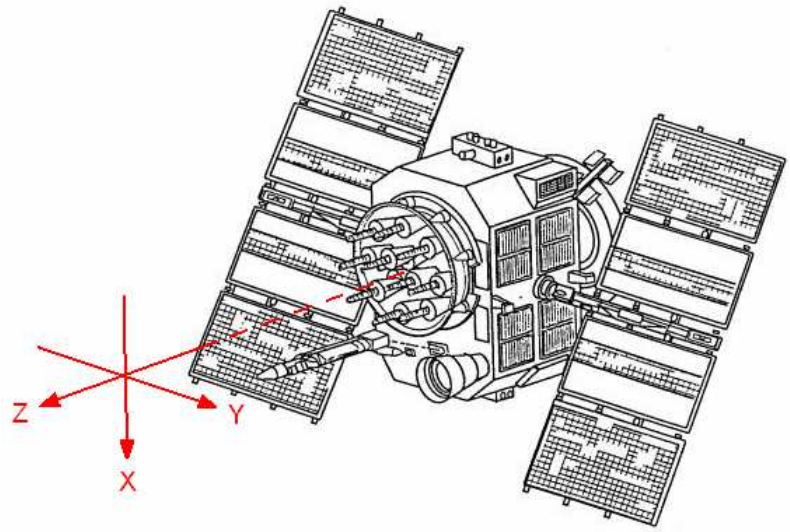

Figure 3.1 Navstar Block II Spacecraft. Source Güller (2009)

3.2 Mathematical Model

In this section we give the mathematical and physical background for the satellite models which receive the radiation coming from the Earth. We will construct here two types of satellite models, a box-wing model where the body of the satellite plus the solar panels are considered and a cannon-ball model where average properties of the satellite are assumed. Furthermore we distinguish for the box-wing model between two solutions:

- An analytical solution that will give explicit formulas for the acceleration acting on the satellites with the main assumption that the radiation from the Earth is just radial, analogous to the Earth radiation analytical model, see (section 3.2).
- A numerical solution where we consider the actual direction of the radiation coming from each surface element of the Earth and reaching each satellite surface, analogous to the Earth radiation numerical model, see (section 3.3).

The basic formulation for the analytical and numerical models is the same and is given in the following.

3.2.1 General Radiation Pressure Model

Based on the general radiation pressure models described by Fliegel et al. (1992) and Hugentobler (2008), we construct a simple box-wing model of GPS satellites as follows:

- Just the face of the satellite pointing to the Earth (+Z side), the solar panels (front and back) and the solar panels masts are taken into account. Smaller elements are not considered since their contribution to the force model should be also small.
- Shadowing effects of satellite components to other components, energy that is absorbed and reradiated as heat and reflection and absorption of radiation between components, are effects that are not considered since they are assumed to be small.
- The angular distribution of sunlight reflected from each surface is approximated as the sum of two beams, one perfectly diffuse (Lambert scattering) and other purely specular, according to Fliegel et al. (1992).
- The attitude of the satellites is assumed to work perfectly and is simply given by the +Z side (where the navigation antennas are located) pointing always to the Earth and the front of the solar panels pointing always to the Sun, see Figure 3.2.

The radiation pressure model, described by Fliegel et al. (1992), is defined by giving each surface of a spacecraft its shape (whether flat or cylindrical), the area, and two optical parameters: the reflectivity (ν), ranging from 0 (black) to 1 (white); and the specularity (μ), ranging from 0 (diffuse) to 1 (specular).

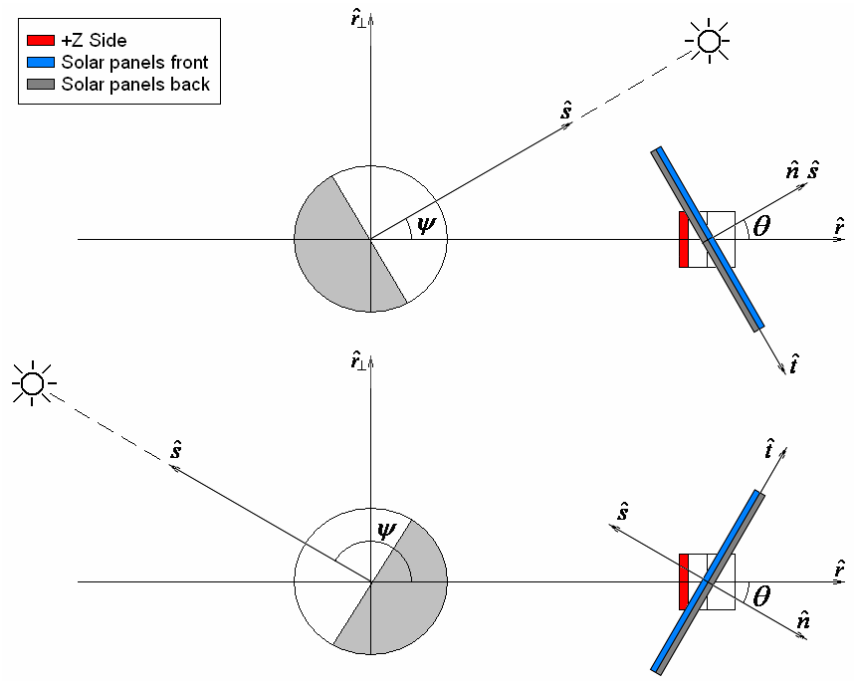

Figure 3.2 Attitude and geometry for box-wing model

With the area of a flat surface indicated by A, the total mass of the satellite M, the angle θ between the incoming Earth radiation and the normal to the surface, the irradiance from the Earth E and the speed of light c, together with incoming Earth radiation plus the specularly and diffusely radiation, it is possible to write three acceleration components for each surface, again according to Fliegel et al. (1992):

- *"The 'normal' component is perpendicular to the surface. It is produced by the normal component of the incoming radiation plus the recoil from the specularly reflected beam."*
- *"The 'shear' component is tangent to the surface and away from the Sun. It is produced by the tangential component of the incoming radiation minus the momentum carried away by the specularly reflected beam."*
- *"The 'diffuse' component is in the same direction as the 'normal' but the effect of this Lambert diffuse reflected radiation perpendicular to the surface is only two-thirds of the so called "normal" (the specularly reflected) component."*

The formulas for these three components are given by

Normal

$$\vec{f}_N = \frac{A}{M}\frac{E}{c}(1+\mu\nu)\cos^2\theta\,\hat{n}, \tag{3.7}$$

Shear

$$\vec{f}_S = \frac{A}{M}\frac{E}{c}(1-\mu\nu)\sin\theta\cos\theta\,\hat{t}, \tag{3.8}$$

Diffuse

$$\vec{f}_D = \frac{A}{M}\frac{E}{c}\frac{2}{3}\nu(1-\mu)\cos\theta\,\hat{n}. \tag{3.9}$$

In the last equations, one cosine factor is produced by the foreshortening by perspective of the area of the surface presented to the Earth; the other sine and cosine factors show the resolution of the force components either normal to the surface or (for the shear acceleration) tangent to it. The directions normal $\vec{n}$ and tangential $\vec{t}$ are illustrated in Figure 3.2.

These equations can be written by another set of optical parameters after Hugentobler (2008), which are the fraction of absorbed photons α, the fraction of reflected photons ρ and the fraction of diffusely scattered photons δ. With these parameters we get:

Absorbed photons

$$\vec{f}_\alpha = \frac{A}{M}\frac{E}{c}\alpha\cos\theta\,\hat{r}, \tag{3.10}$$

Reflected photons

$$\vec{f}_\rho = \frac{A}{M}\frac{E}{c}2\rho\cos^2\theta\,\hat{n}, \tag{3.11}$$

Diffusely scattered photons

$$\vec{f}_\delta = \frac{A}{M}\frac{E}{c}\delta\cos\theta\left(\hat{r}+\frac{2}{3}\hat{n}\right). \tag{3.12}$$

By taking the projection of these last equations onto the normal and tangential directions, the relationship between the two sets of optical parameters and therefore of the equations can be found as

$$\begin{aligned}\alpha &= 1-\nu\\ \rho &= \mu\nu\\ \delta &= \nu(1-\mu)\end{aligned} \tag{3.13}$$

and it can be checked that

$$\alpha+\rho+\delta = 1 \tag{3.14}$$

since each incident photon must fall exactly into one of these three categories.

3.2.2 Box-Wing Analytical Model

A simple analytical box-wing model for GPS satellites can be constructed by adopting the approximation that the radiation coming from the Earth is assumed to be purely radial; this is in general not true but still a good approximation. As the irradiance is just radial, the acceleration can be decomposed into two components, a radial component and a non-radial

component. Furthermore the acceleration can be described just as function of the angle ψ satellite – Earth – Sun.

Let us now write the equations (3.7) to (3.9) in terms of the angle ψ for the radial $\hat{r}$ and non-radial $\hat{r}_\perp$ directions shown in Figure 3.2, where we can also distinguish two cases of the relative position of satellite, Earth and Sun. In the first one for $0 \le \psi < \pi/2$, the radiation of the Earth is received in the back side of the solar panels and we have $\theta = \psi$. For the second case ($\pi/2 \le \psi < \pi$) the radiation is received in the front side of the solar panels and it should hold that $\theta = \pi - \psi$.

From Figure 3.2 we also see that the bus (+Z side) is always perpendicular to the Earth and for the solar panels masts the same can be considered, while for the solar panels the relative position to the Earth is varying during one revolution. Therefore we split the equations in two parts:

Bus and solar panels masts

$$f_{\hat{r}} = \frac{A}{M}\frac{E}{c}\left((1+\mu\nu)+\frac{2}{3}\nu(1-\mu)\right), \tag{3.15}$$

Solar panels

$$f_{\hat{r}} = f_N \cos\theta + f_D \cos\theta + f_S \sin\theta \tag{3.16}$$

$$f_{\hat{r}_\perp} = f_N \sin\theta + f_D \sin\theta - f_S \cos\theta, \tag{3.17}$$

with

$$\theta = \begin{cases} \psi & if \quad 0 \le \psi < \pi/2 \\ \pi - \psi & if \quad \pi/2 \le \psi < \pi. \end{cases} \tag{3.18}$$

Introducing the respective acceleration components in equations (3.16) and (3.17), together with the considerations that (3.17) should be negative for $\pi/2 \le \psi < \pi$ and the implication of (3.18) for the trigonometric functions, one can find after rearranging some terms the following:

Solar panels

$$f_{\hat{r}} = \frac{A}{M}\frac{E}{c}|\cos\psi|\left(1+\frac{2}{3}\nu(1-\mu)|\cos\psi| + \mu\nu\cos 2\psi\right) \tag{3.19}$$

$$f_{\hat{r}_\perp} = \frac{A}{M}\frac{E}{c}\cos\psi\left(\frac{2}{3}\nu(1-\mu)\sin\psi + \mu\nu|\sin 2\psi|\right). \tag{3.20}$$

Also note that using the other set of optical parameters, defined in (3.13), the last equations have even a simpler form:

$$f_{\hat{r}} = \frac{E}{Mc}\left[A_{bus}C_{bus} + A_{sol}|\cos\psi|\left(1+\frac{2}{3}\delta_{sol}|\cos\psi| + \rho_{sol}\cos 2\psi\right)\right] \tag{3.21}$$

$$f_{\hat{r}_\perp} = \frac{E}{Mc}A_{sol}\cos\psi\left(\frac{2}{3}\delta_{sol}\sin\psi + \rho_{sol}|\sin 2\psi|\right), \tag{3.22}$$

where we have also introduced (3.15) and made the distinction between the satellite bus area A_{bus} and the solar panels area A_{sol} .These last formulas together with the irradiance E computed with the Earth radiation models from the last chapter, give the acceleration acting on GPS satellites due to the emitted and reflected radiation of the Earth and depend just on the characteristics of the satellite and the angle ψ satellite – Earth - Sun.

3.2.3 Box-Wing Numerical Model

The radiation coming from the Earth is in general not only radial, in fact the radiation can deviate from the radial direction around $14°$, see Eq. (2.25), where the angle β indicates the part of the Earth visible by the satellite, so one computes $90° - \beta = 14°$. Using the radiation coming from the full disc of the Earth one can not get simple formulas, like (3.21) and (3.22), just depending on the angle satellite – Earth – Sun, therefore the solution is computed in a numerical way.

A procedure how to compute the satellite acceleration on a box-wing model will be given here, where we use the same body-fixed reference system used for the analytical model, with the radial direction $\hat{r}$, the non-radial $\hat{r}_\perp$ and a direction $\hat{r}_3$ which is orthogonal to the previous ones and completes the right handed system. The procedure is describe for the back side of the solar panels, it means for $0 \le \psi < \pi/2$, however the procedure is general and works in the same way for the front side of the solar panels as well for the satellite bus, with just small differences between them.

Let us start by considering an irradiance vector in the body-fixed reference system and the normal to the surface vector in the same reference system (Figure 3.3), given by

$$\vec{E} = \left(E_{\hat{r}}, E_{\hat{r}_\perp}, E_{\hat{r}_3}\right) \qquad (3.23)$$
$$\hat{n} = (\cos\psi, \sin\psi, 0).$$

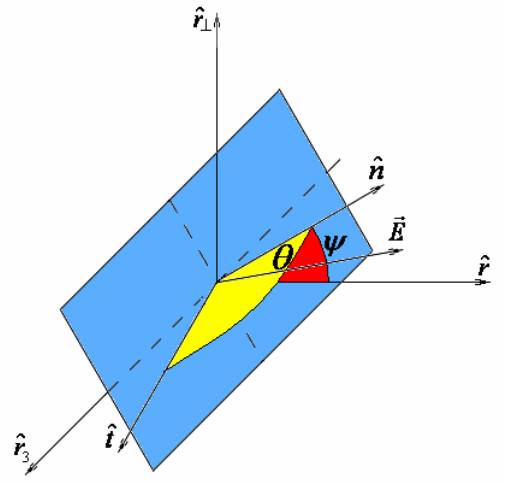

Figure 3.3 Solar panel geometry for the numerical box-wing model

With these two vectors we can define an auxiliary vector $\hat{a}$ perpendicular $\vec{E}$ and $\hat{n}$, then we can also define the tangent direction vector $\hat{t}$, both vectors are given by

$$\hat{a} = \left(\vec{E} \times \hat{n}\right) \Big/ \left|\vec{E}\right| \qquad (3.24)$$
$$\hat{t} = \hat{n} \times \hat{a}.$$

Now the normal and tangent vectors in equations (3.7) to (3.9) are completely defined. The angle between the incoming Earth radiation and the normal to the surface is

$$\cos\theta = \left(\vec{E} \cdot \hat{n}\right) \Big/ \left|\vec{E}\right|. \qquad (3.25)$$

Note that the tangent direction vector must be tangential to the surface of the solar panels, however the pointing direction of it is different to what it was considered in the analytical case. Furthermore it can be seen from Figure 3.3 that $\vec{E}$, $\hat{n}$ and $\hat{t}$ are in the same plane. With the previous definition one can compute the acceleration acting on the solar panels surface by applying equations (3.7) to (3.9), and summing up the accelerations acting on the body-fixed reference system from the irradiance vectors coming from different places of the Earth.

Although it is not possible to give analytical formulas as (3.21) and (3.22), the implementation of the irradiance from the full disc of the Earth is not much more complicated as just considering irradiance in the radial radiation. One just has to take care if the irradiance is reaching the front or the back of the solar panels, specially when $76° < \psi < 104°$, it means when the solar panels are close to parallel with the radial direction and can be illuminated from both sides simultaneously. For the more interested reader we refer to the program code provided in the Appendix.

Finally for the satellite bus, the computation is simpler since $\psi = 0°$ and it does not change its orientation with respect to the Earth. Also note how important the angle ψ is, that alone can completely define the attitude of the satellite.

3.2.4 Cannon-Ball Model

From equations (3.21) and (3.22) we can construct a very simple cannon-ball model by just averaging the magnitude of the acceleration over the angle ψ and using an albedo of 0.3 for the irradiance computation. Doing that we simply have

$$f_{\vec{r}} = \frac{A}{M}\frac{E}{c}C_{ball} \qquad (3.26)$$

where C_{ball} is a constant which is determined numerically and gives the average dimensions and optical properties of the GPS satellites. This type of model has no variation but the one of the irradiance from the Earth, so the acceleration has the same shape of the irradiance but multiplied by a scaling factor.

The data needed as an input for the box-wing and cannon-ball models proposed here is given in the following section, while the plots of the accelerations are shown in section 3.4.

3.3 Dimensions, Optical Parameters and Masses

We present in this section the data used to for the satellite models, based mostly on the publications of Fliegel et al. (1992) and Fliegel and Galini (1996), who got the dimensions and optical parameters of the components directly from the manufactures of the GPS satellites, Rockwell International for Block I and Block II and Lockheed Martin for Block IIR. Regarding the Block IIA satellites, it is reported that their properties are very similar to Block II. We just present here part of the data, the one that is necessary to construct the box-wing model for the radiation coming from the Earth.

Table 3.1 Main dimensions and optical parameters (visible and infrared) for GPS satellites

GPS satellite	Area [m^2]	Specularity μ_{VIS}	Reflectivity ν_{VIS}	Specularity μ_{IR}	Reflectivity ν_{IR}
Block I (Mass $500\,kg$)					
+ Z side	1.510	0.75	0.86	0.50	0.20
Solar panel masts	0.470	0.85	0.85	0.50	0.20
Solar panels front	5.583	0.85	0.23	0.50	0.20
Solar panels back	5.583	0.5	0.11	0.50	0.20
Block II (Mass $885\,kg$)					
+ Z side	2.881	0.20	0.56	0.50	0.20
Solar panel masts	0.985	0.41	0.52	0.50	0.20
Solar panels front	10.866	0.85	0.23	0.50	0.20
Solar panels back	10.866	0.5	0.11	0.50	0.20
Block IIR (Mass $1100\,kg$)					
+ Z side	3.750	0	0.06	0.50	0.20
Solar panel masts	0.320	0.85	0.85	0.50	0.20
Solar panels front	13.600	0.85	0.28	0.50	0.20
Solar panels back	13.600	0.5	0.11	0.50	0.20
TEST (Mass $1000\,kg$)					
+ Z side	5.000	0	0.13	0	0.13
Solar panel masts	0	-	-	-	-
Solar panels front	15.000	0.50	0.20	0.50	0.20
Solar panels back	15.000	0.50	0.20	0.50	0.20

Table 3.2 Parameters for GPS satellites (cannon-ball)

GPS satellite	$A/M\ [m^2/kg]$	C_{ball}
Block I	0.01513	0.8876
Block II	0.01667	0.8551
Block IIR	0.01606	0.8134
TEST	0.02000	0.8174

For the back of the solar panels (Block models) the reflectivity was computed as $\nu = 1 - \varepsilon$, with ε the emissivity the value reported for this surface. The specularity is then calculated from (3.13) and (3.14) assuming that the fraction of reflected and scattered photons is the same, so in general the back of the solar panels absorb most of the radiation.

The data given in Table 3.1 was calculated for the visible part of the spectrum, but we also need the same data for the infrared part or even better specularity and reflectivity as a function of the wavelength. However this data is not available directly for the GPS satellites. Consequently a big assumption we made in the case of TEST models is that the coefficients given for the visible region of the spectrum are also valid for the infrared one, this simple TEST model uses realistic optical properties that were assumed before having access to the more accurate data, it is presented because it was initially used for some of the simulations done in the later chapters.

For the Block I, II and IIR we did further investigations to find specularity and reflectivity for the infrared, however this is not simple since currently there are many types of materials used for the construction of space vehicles and some of the materials are designed to help to the thermal control of the satellite, see for example Pisacane and Moore (1994), consequently the materials have different properties for visible and infrared radiation. Looking at the emissivity values reported by Henninger (1984), one finds the emissivity of the GPS solar panels in the infrared to be $\varepsilon = 0.80$ which is equal to the fraction of absorbed photons, as before it is assumed that the fraction of reflected and scattered photons is the same. Doing that one gets $\nu_{IR} = 0.20$ and $\mu_{IR} = 0.50$, and for the rest of the satellite structure the same values are assumed, further studies if possible should try to improve this.

If one wishes to enhance the performance of the model, one could estimate radiation pressure parameters, during the orbit computation, by the fitting of real GPS observations using polynomials of the type (3.21) and (3.22) . See for example Springer et al. (1999) for a solar radiation pressure model of GPS satellites using this technique. Then if we assume that the only quantities that are not well known are the optical properties of the surfaces, we have just three parameters to estimate:

- C_{bus} : mean of optical properties of the satellite bus, valid interval $[1, 2.66]$
- δ_{sol} : diffusely scattered photons from solar panel, valid interval $[0,1]$
- ρ_{sol} : reflected photons from solar panel, valid interval $[0,1]$

Moreover it should hold that $\delta_{sol} + \rho_{sol} \leq 1$ and they give mean optical properties of front and back solar panels, for the visible and infrared radiation. To separate the front and back of solar panels, then simply five parameters instead of three must be estimated.

3.4 Acceleration acting on GPS Satellites

3.4.1 Acceleration due to Earth Radiation

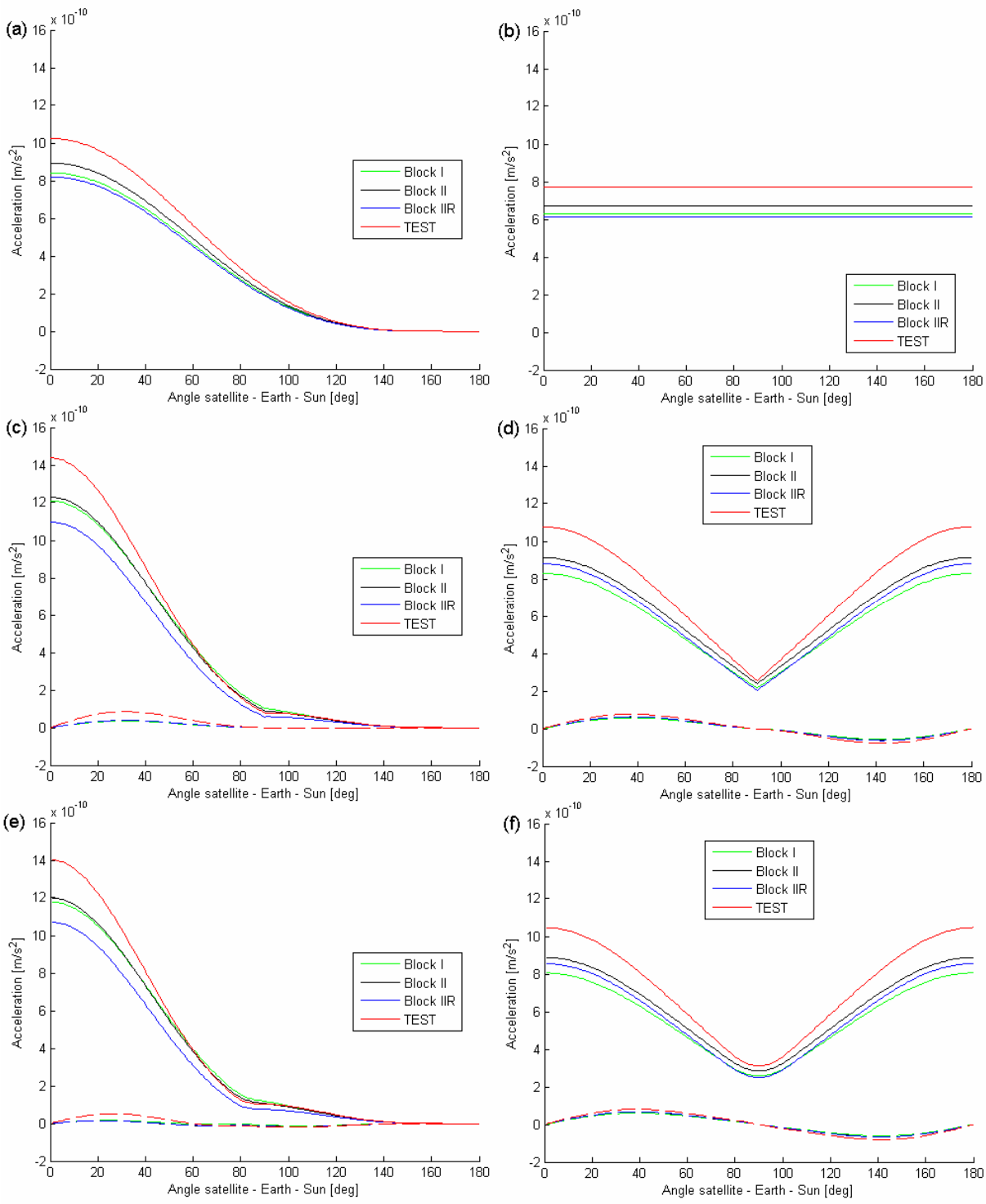

Figure 3.4 Acceleration on GPS satellites due to reflected visible radiation (left) and emitted infrared radiation (right) from the Earth. (a)(b) Cannon-ball model, (c)(d) box-wing analytical model, (e)(f) box-wing numerical model. Solid line -> radial acceleration, dashed line -> non-radial acceleration

The acceleration acting on GPS satellites due to Earth radiation can be now computed and the results are shown in Figure 3.4 using the numerical Earth radiation model for constant albedo of 0.3. Since in the previous section we have separated the surface properties for the visible and for the infrared, the same is done here for the accelerations.

Moreover the accelerations for the satellite types Block I, Block II, Block IIR and TEST are plotted. Block I satellites do not form part of the constellation any longer, however we can see that the acceleration is similar to the other two types of satellites, this means that all satellites have a similar area to mass ratio A/M .

In Figure 3.4 also we have plotted separately the different satellite models: cannon-ball, box-wing analytical and box-wing numerical. Note that the acceleration of the cannon-ball simply follows the curve of the Earth radiation model Figure 2.5(d), while for the box-wing models there is a more interesting behaviour of the acceleration.

Regarding the components of the acceleration for the box-wing models, we see that the radial has its minimum at $\psi = 90°$, which is expected since at this point the least radiation of the Earth is intersected by the satellites . The maximum of the radial component as expected is at $\psi = 0°$ and $\psi = 180°$.

In the case of the non-radial component we see a maximum and a minimum around $\psi = 35°$ and $\psi = 145°$. Looking at Figure 3.2 is obvious that for $0 \le \psi < \pi/2$ the non-radial component should be positive, while for $\pi/2 \le \psi < \pi$ negative. Note that this last component can be around 15% of the radial component for some ψ angles; moreover this non-radial acceleration will influence directly the along-track and cross-track directions, giving non negligible effect in these directions.

In the case of the box-wing numerical model, the main difference compared to the analytical one is for $76° < \psi < 104°$, which was expected since the discontinuity of the acceleration of the analytical model for $\psi = 90°$ should vanish, something closer to what happens in reality when the satellite receives radiation from the full disc of the Earth and not from a source point of radiation.

3.4.2 Acceleration due to Antenna Thrust

The thrust produced by the navigation antennas give a constant radial acceleration and as a consequence a potential shift of the acceleration in this direction. According to Ziebart et al. (2004), we have the following:

"GPS satellites emit between 70 *and* 80 *watts of power along the antenna bore sight in the process of transmitting the L1 and L2 carrier waves. Now, the force, in newtons, due to the absorption of photons from an incident radiation flux (*E*) is given by* $F = E/c$ *where* E *is measured in watts per metre squared and* c *is the speed of light in vacuum, expressed in metres per second. Hence, by Newton's third law when a signal of power (*W*) is emitted there is an equal and opposite reactive force acting along the negative direction of the antenna bore sight."*

The resulting acceleration in then given by:

$$f_{\hat{r}} = \frac{W}{Mc}. \tag{3.27}$$

Considering an emitted power of 80 watts by the antenna, the acceleration for the different satellite types is:

Block I: $5.3\times10^{-10}\ m/s^2$ Block IIR: $2.4\times10^{-10}\ m/s^2$

Block II: $3.0\times10^{-10}\ m/s^2$ TEST: $2.7\times10^{-10}\ m/s^2$

Adding the accelerations due to the visible and infrared radiation, together with antenna thrust, gives the total acceleration acting on GPS which is plotted in Figure 3.5(a) for the case of the numerical box-wing model.

3.4.3 Acceleration due to Sun Radiation

For comparison the acceleration due to Sun radiation acting on GPS satellites is plotted, as described by Fliegel et al. (1992) and Fliegel and Galini (1996), in Figure 3.5(b). There the acceleration is plotted as a function of the angle of the Sun in the body-fixed reference system, in other words the angle in the plane ZX in Figure 3.1. Note that the Sun must remain in this plane since the Y-axis points along one of the solar panels centre beams, thus is always perpendicular to the direction of incident Sun radiation.

The change of acceleration that one sees is only due to rotation of the satellite bus, since the solar panels remain always perpendicular to the Sun and they just give the constant shift of the curves. This variation of the acceleration is around $6.9\times10^{-9}\ m/s^2$ for Block II and $8.3\times10^{-9}\ m/s^2$ for Block IIR, while the change of acceleration on this satellites due to Earth radiation can reach up to $1.5\times10^{-9}\ m/s^2$.

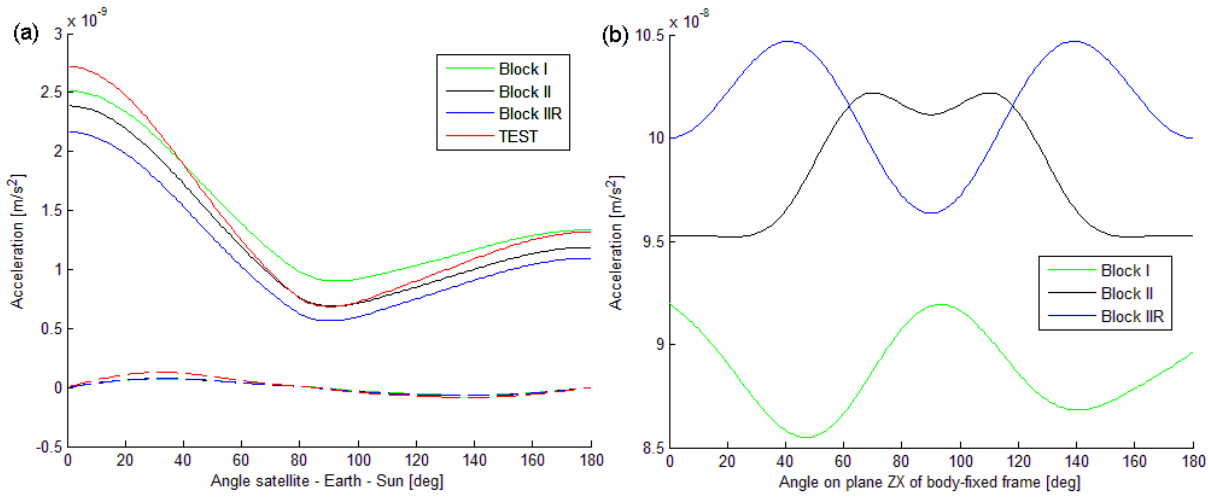

Figure 3.5 Acceleration on GPS satellites due to (a) Earth radiation plus antenna thrust and (b) Sun radiation

3.5 Discussion and Outlook

3.5.1 Magnitude of the Acceleration

Although the acceleration on GPS satellites due to Earth radiation is on average just 2% of the solar radiation pressure, when we look at the change of acceleration due to Earth radiation it can reach maximum values of 21% (Block II) and 18% (Block IIR) of the variation of acceleration due to Sun radiation. This means that potentially there is a mismodelling of this amount by no considering the Earth radiation on the radiation pressure models of GPS satellites. This potential mismodelling alone justifies the effort of including the Earth radiation as a perturbing acceleration in the modelling of GPS satellites orbits.

An interesting effect on the GPS satellites of the same order of magnitude ($1.0\times10^{-9}\ m/s^2$) as the effect of Earth radiation, is the Y-bias which is an acceleration acting on the Y-axis (Figure 3.1) probably because a small misalignment of the solar panels to the Sun, see for example Springer et al. (1999). However the acceleration due to Earth radiation can not explain the Y-bias, since the first one is constrained in the plane ZX of Figure 3.1 or the plane radial non-radial of Figure 3.2, so the component in the Y-axis is very small or zero.

Another effect that is also interesting are the eclipses, since the acceleration due to Earth radiation is greatest precisely during eclipse season, when the satellite, Earth and Sun are aligned, because at some point of the orbit the angle ψ reaches small values and as a consequence the acceleration acting on the satellites is bigger, see Figure 2.5(d).

These last two effects, the Y-bias and the eclipse season, are not further studied during this thesis since outreaches the objectives of it. The last two paragraphs just try to highlight the importance of modelling Earth radiation for GPS satellites and give the opinion of the author on potentially interesting research topics.

Finally regarding still the order of magnitude of the acceleration here computed ($1.5\times10^{-9}\ m/s^2$), one can notice that it is bigger than effects of thermal re-emission on GPS satellites. For example Duha et al. (2006) have computed this acceleration and it is in the order of $100\times10^{-12}\ m/s^2$, it means around 6.7% of the one due to Earth radiation, this again confirms the importance of including the Earth radiation in the computation of GPS orbits.

3.5.2 Other Radiation Pressure Models

A simple model for the albedo radiation pressure was proposed by Beutler et al. (1994), which is similar to the model described in this chapter, but with the satellite model and the Earth radiation model written together. More specifically for the radiation coming from the Earth, their model is as the numerical Earth radiation model for constant albedo, considering just the reflected radiation but no emitted radiation.

For the satellite model they also use a box-wing model similar to our numerical box-wing model. However by analysing the formulas provided by them it seems that not all the optical properties of the satellite surfaces were considered, it means the fraction of photons that are: absorbed, reflected or diffusely scattered, see equations (3.10) to (3.12).

Moreover Beutler et al. (1994) using the simple model for albedo radiation pressure estimated radiation pressure parameters. However the estimated parameters did not seem to improve further the orbit or the albedo acceleration was already absorbed by the parameters used by the solar radiation pressure model, which at this point were around 9 parameters.

Also an interesting solar radiation pressure model, where parameters are estimated from several years of GPS measurements, was made by Bar-Server and Kuang (2004). They find coefficients that better fit the GPS orbits of no eclipsing satellites and the number of estimated coefficients is around 12, doing that it is reported a considerable improvement of the orbits.

The article of Bar-Server and Kuang (2004) provides an interesting comparison of two types of current approaches to deal with the solar radiation pressure for GPS satellites:

"The 'ground –model' approach is based on pre-launch models and measurements of the spacecraft optical and thermal properties. The 'empirical' approach uses the observed orbital motion of the spacecraft to infer the solar radiation forces (and other forces) acting on the spacecraft."

Taking into account that the model developed by Bar-Server and Kuang (2004) is an 'empirical' one, they finish the article with a comparison between both approaches:

"The 'ground-based' design process is carried out by modelling the spacecraft as a collection of components, each with its own shape, size, optical and thermal characteristics. Given the nominal mission profile and orbital geometry, the process employs various ray tracing, finite element and finite difference techniques to simulate the effects of impinging photons on the spacecraft, and derive the solar radiation model."

This process is described as complicated but the result is usually fairly good if the spacecraft in-orbit behaviour does not deviate from the nominal. For example Ziebart et al. (2003, 2004, 2005) have developed very interesting tools to take into account complex satellite structures, where in principle small details can be included and they consider other effects as heat flow inside the spacecraft, shadowing of different elements and reflection effects between elements. The results they got are very promising and their satellite models seem to take into account almost everything that one could think of, when dealing with non-conservative forces acting on satellites.

However there are some deficiencies of the 'ground-based' models as pointed out by Bar-Server and Kuang (2004):

"The in-orbit satellite behaviour may deviate from the nominal. Misorientation, bending and flexing of structures are quite common. For example, the non-nominal Y bias force can be attributed to solar array misalignment and to a yaw bias. Also, actual aging effects may deviate significantly from the model. The actual accuracy of the model can only be roughly estimated …"

While for the ‘empirical’ model some advantages are seen:

“It reflects the actual in-orbit behaviour. It is more accurate and it directly accounts for the combined radiation pressure of all spacecraft components. It provides a tool for learning about actual in-orbit behaviour of satellites and for flagging and monitoring problem satellites.”

And by the other hand the author of this thesis also sees some disadvantages of the ‘empirical’ models. For example in most of the cases the polynomials used to find the radiation pressure parameters are based on trial and error and are proposed just on the basis of which fits best the data, therefore they are not based on clear physical models of satellite structure, optical properties or irradiance coming from the Sun or the Earth. As a consequence of the polynomials that are used, from the estimated coefficients one cannot easily extract physical properties of the satellite, for example optical properties or the attitude of the spacecraft.

In this chapter we have developed a satellite model for radiation coming from the Earth and we have not intended to do a similar one for the radiation coming from the Sun. However the differences between both models are small, being for the GPS satellites the relative orientation the main one. As mentioned before for the case of Sun radiation, the solar panels are always perpendicular to it and what is changing the acceleration is the rotation of the satellite bus around the Y-axis, as the satellite is orbiting the Earth. While for the case of radiation coming from the Earth the orientation of the satellite bus remains fixed but the solar panels are rotating.

Also our box-wing model falls evidently into the category of ‘ground-based’ models just discussed above. However we have also discussed the possibility of estimating radiation pressure parameters using for example equations (3.21) and (3.22). In this case the estimated coefficients have a clear physical meaning of the satellite optical properties and the corresponding polynomials are derive just using the satellite structure and attitude. But a problem that one can almost immediately identify is that if one estimates radiation parameters (as proposed here) for the acceleration due to Earth radiation, combined with a purely empirical solar radiation pressure model, probably the coefficients will be either absorbed by the solar empirical model or will not give a clear physical meaning.

3.5.3 Further Improvement

The main error that is considered to be still remaining in the box-wing satellite models, is the lack of information of the surface properties in the infrared, if more information is available a natural step is to incorporate this properties into the model. To overcome this problem another possibility is to estimate radiation pressure parameters.

Considering the arguments previously exposed, the author thinks that the best way to estimate radiation pressure parameters would be with a ‘semi-empirical’ model whose polynomials are found from ‘ground-based’ models. In this case one knows with enough accuracy the irradiance from Earth and Sun and the satellite structure, remaining as parameters to estimate optical properties and attitude. These parameters could be also

constrained to some of the a priori knowledge that we have about them. This is exactly what has been proposed here for the Earth radiation, estimating a minimum of three parameters.

As a simple exercise let us think of a solar radiation pressure model, where we considered the structure to be a simple box-wing model, how many parameters do we need then to estimate? Let us consider that for each surface we need 2 optical parameters. Then for the bus we can consider we have 3 different types of surfaces, +Z side, -Z side and other sides (±Y and ±X), note that the ±Y sides are poorly illuminated by the Sun. Then with the solar panels we have a total of 8 parameters to be estimated. We could also consider a small misalignment of the satellite attitude for example in the Y-axis, so we need one extra parameter. In total one could estimate around 9 parameters which in principle would give information on some physical properties of the satellite.

Now considering the Earth radiation pressure model, one could use some of the parameters estimated from the solar pressure model or do an estimation using both models, as we propose the parameters to be the optical properties of the surfaces, they are the same for both Earth and Sun radiation models.

Finally it can be said that although the box-wing satellite models constructed here have not reached perfection and some improvements can be clearly seen. The more detailed or elaborate modelling is not expected to change the behaviour of the acceleration or its orders of magnitude.

4 Perturbation on Kepler Orbit

4.1 Introduction

4.1.1 Numerical Integration

After the development and computation of the Earth radiation and the GPS satellite models, we can use the acceleration resulting from the combination of both models to study the effect of it on a simple Kepler orbit. The only forces that are considered are the gravitational attraction of the Earth (as a uniform perfect sphere) and the computed acceleration due to Earth radiation. In other words in the equation of motion of the two body problem, we introduce a perturbing acceleration:

$$\ddot{\vec{r}} = -GM_{\oplus}\frac{\vec{r}}{r^3} + \vec{f}_E . \tag{4.1}$$

Where $\vec{r}$ is the satellite position vector from the geocenter given in an inertial reference system, $GM_{\oplus} = 398.6005\times10^{12}\ m^3/s^2$ is the product of the gravitational constant G and the mass of the Earth $M_{\oplus}$ (assuming the mass of the satellite to be negligible compared to the mass of the Earth) and the perturbing acceleration vector due to the Earth's radiation is denoted by the symbol $\vec{f}_E$.

To solve equation (4.1) we use one of the numerical integration tools provided in the Matlab Software, for example ODE45 has enough accuracy for the study of our problem. Furthermore we make use of the method of Cowell for the orbit integration, see Gruber (2008). The basic idea is that the equation of motion is integrated stepwise using rectangular coordinates and is rewritten in two first order differential equations:

$$\dot{\vec{r}} = \vec{v}, \qquad \dot{\vec{v}} = -GM_{\oplus}\frac{\vec{r}}{r^3} + f_E , \tag{4.2}$$

with $\vec{v}$ the satellite velocity vector.

It must be clarified that the orbit integration process is a complex issue with many works devoted just to it, see for example the books of Beutler (2005) and Montenbruck and Gill (2000) for more extended treatments of this topic. However we will see later in this chapter that the simple orbit integration procedure of a Kepler orbit with a small perturbing acceleration can give us a good but simple understanding of the general effects of Earth radiation on the GPS satellite orbits.

Table 4.1– Keplerian orbital elements for PRN06

Semimajor axis $a\ [km]$	Eccentricity e	Inclination $i\,[\mathrm{deg}]$	RAAN $\Omega\,[\mathrm{deg}]$	Argument of perigee $\omega\,[\mathrm{deg}]$
26560.699	0.0062068	53.5060	155.9994	282.1291

In the next chapter, with the purpose of having a more precise computation of the effect, we will make use of the Bernese GPS Software, see Beutler et al. (2009), which can take into account almost all perturbations acting on the orbits, using very sophisticated integration tools and with the incorporation of real GPS measurements.

The example computed in this chapter refers to the GPS satellite PRN06, whose initial conditions of the equation of motion are given in Table 4.1, one of the GPS satellites that can be tracked by SLR stations. The information of the satellite is provided by Kelso (2009), for the day 154 of 2009. Five of the Keplerian elements are in the last table while the sixth Keplerian element, the perigee passing time, is assumed to be zero. The simulation is carried out for one year and the starting position of the Sun coincides with the Vernal Equinox.

Since in this chapter we only want to acquire a general understanding of the perturbation caused by Earth radiation on the GPS orbits, we have chosen to use the simplest Earth radiation and satellite models: the analytical Earth radiation model (constant albedo) combined with the cannon-ball or analytical box-wing TEST models. Looking at the results obtained in Chapter 3 we know that although there is a difference between the analytical Earth radiation model and our most realistic one (using CERES data), the general behaviour of the models is the same. However in the case of the satellite models, it is necessary to consider both the cannon-ball and box-wing models since the differences between them are large, see for example Figure 3.4, while the difference between the Block type or TEST satellite is small.

The study of the more complex Earth radiation and satellite models will be done in the next chapter, when we will study the effect of Earth radiation on real GPS orbits using the Bernese GPS Software.

4.1.2 Reference Systems

The equation of motion of the satellite (4.1) is valid only in an inertial reference system, therefore one uses a space fixed Earth centred one, where the Z axis points in the direction of the North Pole, the X axis is along the Vernal Equinox and the Y axis completes the right handed system, see Figure 4.1. This reference system is quasi inertial since the Earth rotates around the Sun and also the Sun rotates around the galaxy centre, but it can be assumed inertial for the study of our problem.

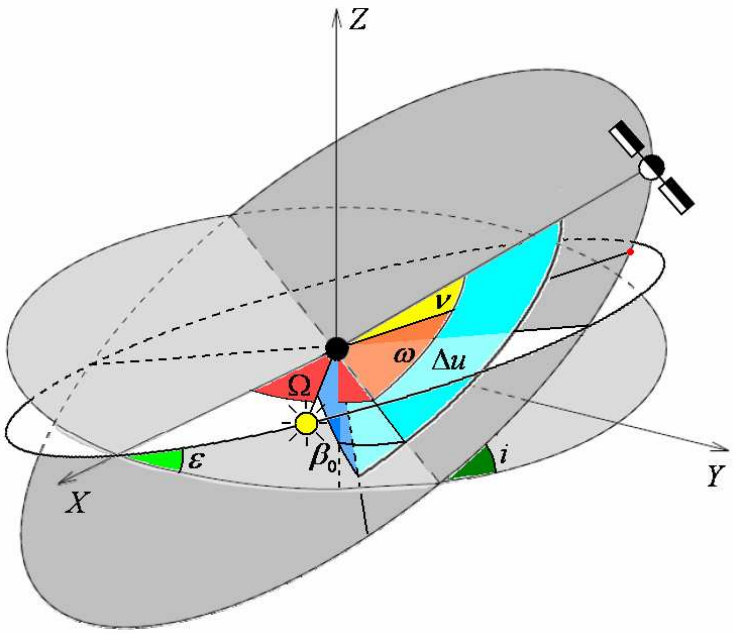

Figure 4.1 Space fixed Earth centred reference system

In Figure 4.1 three of the Keplerian orbital elements are explicitly shown for an arbitrary satellite: the right ascension of the ascending node (RAAN) Ω, the argument of perigee ω and the inclination i. The perigee passing time can be related to the true anomaly ν, while the semimajor axis a and eccentricity e which are related to the shape of the elliptical orbit are not shown. Moreover the argument of latitude of the satellite is computed as $u = \omega + \nu$.

We can also see in Figure 4.1 the position of the Sun in the space fixed Earth centred reference system, with β_0 the Sun elevation angle above the orbital plane of the satellite and Δu the argument of latitude of the satellite with respect to the argument of latitude of the Sun. Finally the obliquity of the ecliptic is given by $\varepsilon = 23.45°$.

The results of the orbit integration will be not shown in the space fixed Earth centred reference system but rather in a reference system moving with the satellite and with a specific orientation with respect to the satellite orbit, which is more convenient for the study of orbit perturbations. This reference system is constructed as follows:

Radial direction

$$\hat{r} = \vec{r} / |\vec{r}|, \tag{4.3}$$

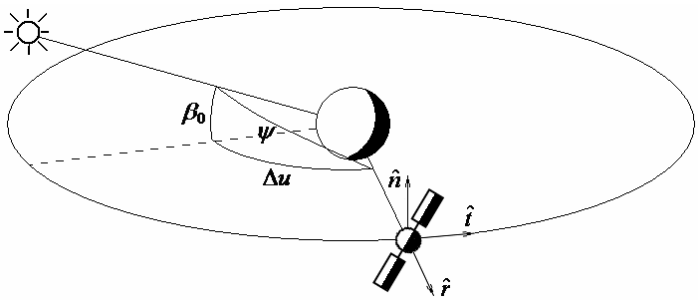

Figure 4.2 Orbital reference system

Cross track or normal direction

$$\hat{n} = \hat{r} \times \vec{v} / |\vec{v}|, \tag{4.4}$$

Along track or tangential direction

$$\hat{t} = \hat{n} \times \hat{r}. \tag{4.5}$$

Note that the along track direction coincides with the velocity direction for perfect circular orbits, while the cross track direction is always perpendicular to the orbital plane. This orbital reference system is shown in Figure 4.2, there we see again the angles β_0 and Δu which give the relative orientation of the satellite orbit with respect to the Sun. Note that the angle ψ between satellite, Earth and Sun, that we have used in the previous two chapters to describe the Earth radiation and satellite models can be calculated simply as

$$\cos\psi = \cos\beta_0 \cos\Delta u. \tag{4.6}$$

This simple relationship between the previous angles guided us to change slightly the initial conditions for the orbit integration process and instead of starting when the perigee passing time or the true anomaly are at zero, we start at $\Delta u = 0°$. This selection of initial conditions is important and will give us later a simple understanding of the problem. The orbit integration is carried out over one year, so the Sun completes one revolution around the satellite orbit, but the integration process is initialized every revolution such that for $\Delta u = 0°$ the position and velocity vectors of the perturbed orbit (numerically integrated) and the Keplerian orbit (analytically integrated) are exactly the same.

The computation of β_0 and Δu as a function of time can be done by assuming the orbits of satellite and Sun to be circular, then one finds the intersection of the two circles for a given set of orbital elements and for a specific time of the year. The explicit computation is not written here but for the interested reader, it is a recommended and interesting exercise of spherical trigonometry.

Figure 4.3 shows the sun elevation angle as function of the number of revolutions for the specific GPS orbit described in Table 4.1. Note that the curve is not a simple trigonometric function like sine or cosine, but of course it is periodic over one year. Furthermore when the maximum of the curve reaches high values one sees a triangular shape of it (Figure 4.3) and when the maximum reaches lower values the shape of the curve is smother (not shown).

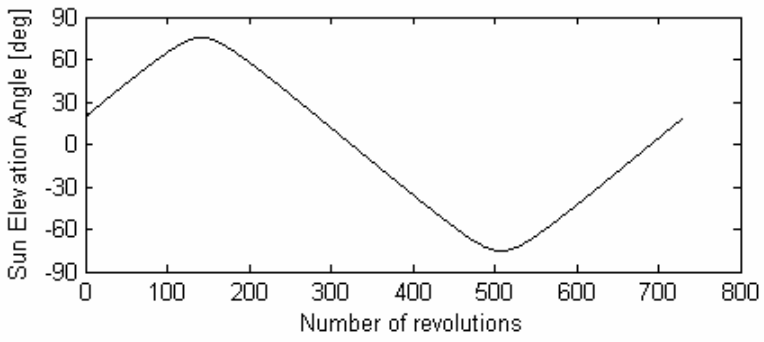

Figure 4.3 Sun elevation angle over one year

4.1.3 Recapitulation

Before proceeding with the results that we have in this chapter, let us summarize what we are capable to compute at this point of the Thesis:

- Irradiance using four different Earth radiation models (Chapter 2) of increasing complexity for a given satellite and Sun positions.
- Acceleration using three different satellite models (Chapter 3) of increasing complexity, for a given irradiance vector and relative position of satellite, Earth and Sun.
- Relative position of Sun and satellite for a simple GPS unperturbed orbit over one year, as described in this Introduction.

One can think of this list as program subroutines, the first two are available in the Appendix. The only computation missing now is a program that combines the Earth radiation and satellite models in a consistent way and computes the acceleration acting on the satellites for any given satellite and Sun positions (also provided in the Appendix). Note that for computing Figure 3.5(a) this last computation was already used. With these three relative small subroutines (around 400 lines in total) which are capable of computing the acceleration on satellites due to Earth radiation, it is expected that the person interested can implement and use them standalone or inside more sophisticated software packages.

Finally with respect to the structure of this chapter we will proceed as follows:

- The on-orbit acceleration acting on the example GPS satellite is computed for the simplest Earth radiation and satellite models.
- The perturbed orbit is computed by numerical integration for the selected Earth radiation and satellite models to study the general behaviour of the perturbation.
- A new reference orbit is constructed to get radial residuals in a GPS like orbit estimation process, in order to get an understanding of the effect of the perturbation on the radial direction.

These last steps will be done having in mind the Satellite Laser Ranging (SLR) technique that can measure very precisely satellite orbits especially in the radial direction. Furthermore as describe in the introduction of this thesis, currently a radial bias exists between SLR measurements of GPS orbits and the orbits computed by the International GNSS Service (IGS). Moreover the cause of this bias has been suggested by some studies to be related to the Earth radiation impacting the GPS satellites.

4.2 On-Orbit Acceleration

4.2.1 Per Revolution Acceleration

In Figure 4.4 the acceleration over one revolution is plotted for the cannon-ball and box-wing models, for two different Sun elevation angles, see also Figure 4.3. For angles $0 \le \Delta u < 90°$ and $270° < \Delta u \le 360°$ the satellite is above the illuminated part of the Earth so the acceleration comes from the effect of reflected visible and emitted infrared radiation, while for $90° < \Delta u < 270°$ the acceleration is mainly due to the emitted infrared radiation of the Earth.

Regarding the components of the acceleration, the radial one is what we already got in Chapter 3, but now for the box-wing model we have an interesting behaviour of the along track and cross track components, which will be further discussed in the following section.

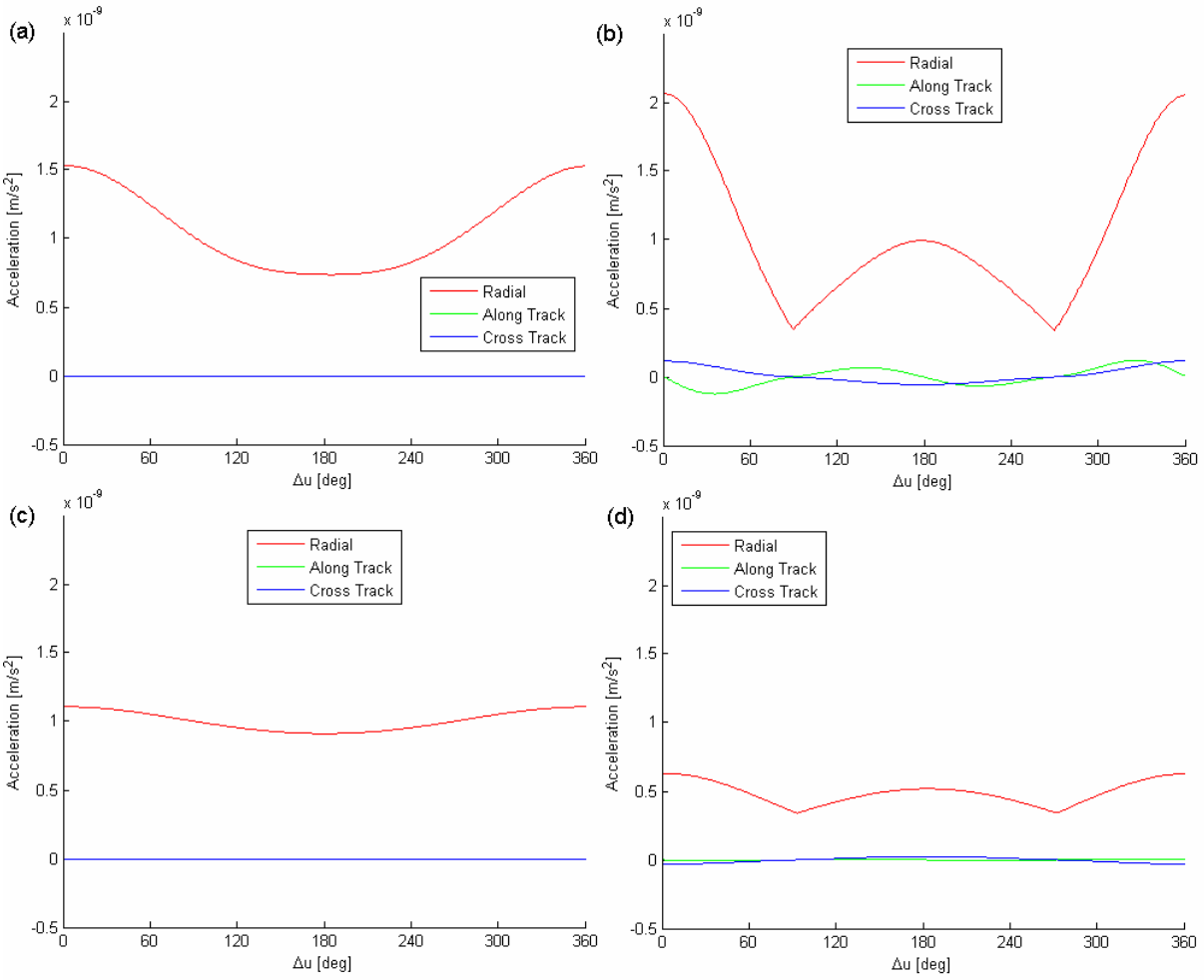

Figure 4.4 Acceleration over one revolution. Left: cannon-ball model. Right: box-wing model. Top $\beta_0 = 19.8°$. Bottom $\beta_0 = -74.8°$

4.2.2 Per Year Acceleration

The results of computing the acceleration for the cannon-ball and box-wing models over one year are shown in Figure 4.5, note the difference in magnitude between both models. On the other hand there is a big correlation of the accelerations for both models with respect to the Sun elevation angle, for example by comparing with Figure 4.3 one can see that for high Sun elevation angles the acceleration decreases and vice versa, also noticeable in Figure 4.4.

After plotting the acceleration over one revolution and over one year, we find a short periodic variation of the acceleration (Δu angle) and a long periodic variation (β_0 angle), therefore a very interesting way to plot the acceleration is as a function of these two angles. The results for the radial acceleration of the cannon-ball and box-wing models are shown in Figure 4.6 and the along track and cross track accelerations of the box-wing model are plotted in Figure 4.7. Note in these figures that the maximum Sun elevation angle is $\beta_0 = \pm 75°$. Furthermore the consistent behaviour of the accelerations in this system just show that we have found possibly the simplest set of variables to describe the acceleration acting on the satellites due to Earth radiation. Also note that these figures as a function of β_0 and Δu show all the details of the accelerations over one year and per revolution.

The radial accelerations of the cannon-ball and the box-wing model, have both the maximum at the daylight side of the Earth ($\beta_0 = 0°$ and $\Delta u = 0°$), while at the dark side of the Earth ($\beta_0 = 0°$ and $\Delta u = 180°$) we find a different behaviour of the satellite models, with a minimum for the cannon-ball model and a local maximum for the box-wing model. This difference of the models is a key factor that brings us closer to explain the characteristic pattern of the SLR – GPS radial residuals obtained by Urschl et al. (2008), see Figure 1.1.

The along track and cross track accelerations (Figure 4.7) have a clear behaviour depending also on the position of the Sun respect to the satellite. We see a twice per revolution perturbation of the along track components and a once per revolution perturbation for the cross track component, with a change of sign according to the Sun elevation angle sign for the latter one.

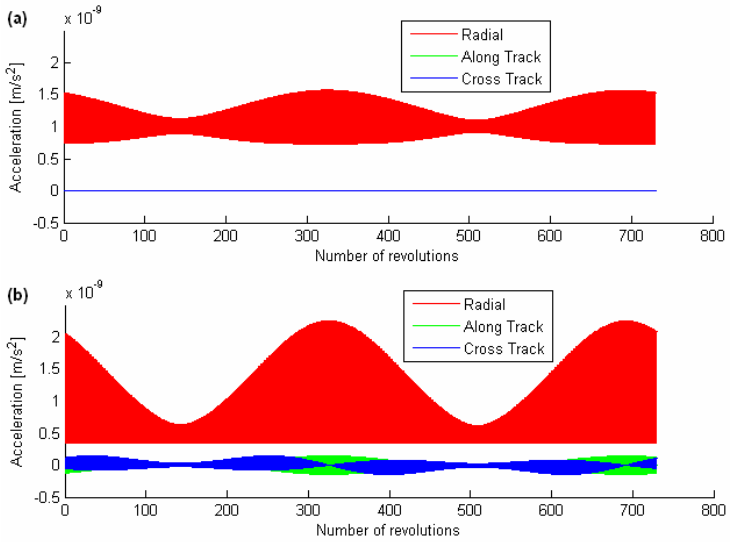

Figure 4.5 Acceleration as a function of number of revolutions for (a) cannon-ball and (b) box-wing models

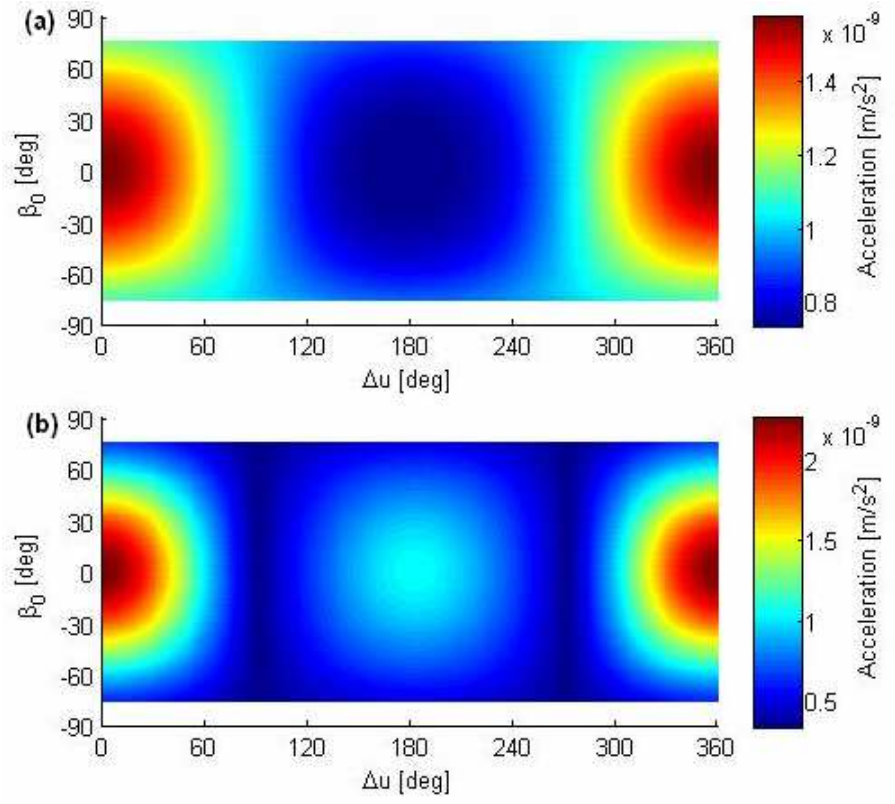

Figure 4.6 Radial acceleration as a function of β_0 and Δu for (a) cannon-ball and (b) box-wing models

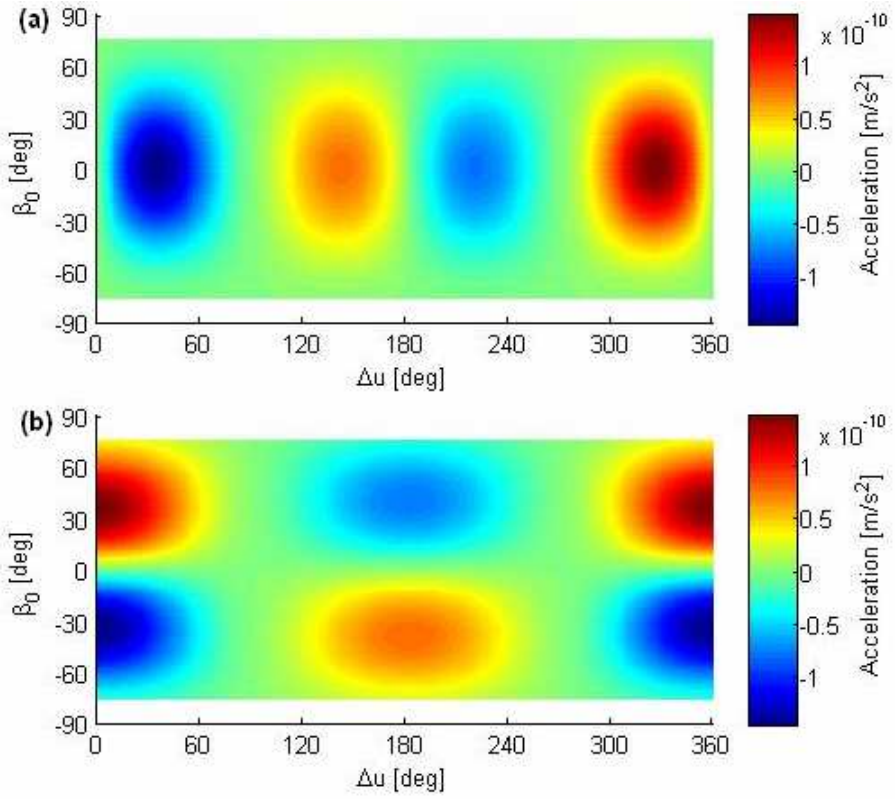

Figure 4.7 (a) Along track and (b) cross track acceleration as a function of β_0 and Δu for the box-wing model

4.3 Perturbation on Kepler Orbit

4.3.1 Per Revolution Perturbation

The perturbed orbit is numerically integrated as described in the introduction of this chapter, the results of the integration are plotted in Figure 4.8 in the form of residuals: perturbed orbit minus initial Kepler orbit. Note that for the orbit integration we use the initial conditions from the Kepler orbit, therefore the perturbation is zero for $\Delta u = 0°$. With respect to the magnitude of the effect, for one revolution we have a maximum of $0.1\,m$ in the radial component of the position and around $-0.5\,m$ in the along track component, while in the cross track we do not see a significant effect.

In contrast to Figure 4.4 we show here the effect for just one Sun elevation angle, however the effect on the position and velocity is similar as for the acceleration. The perturbation decreases as the sun elevation increases.

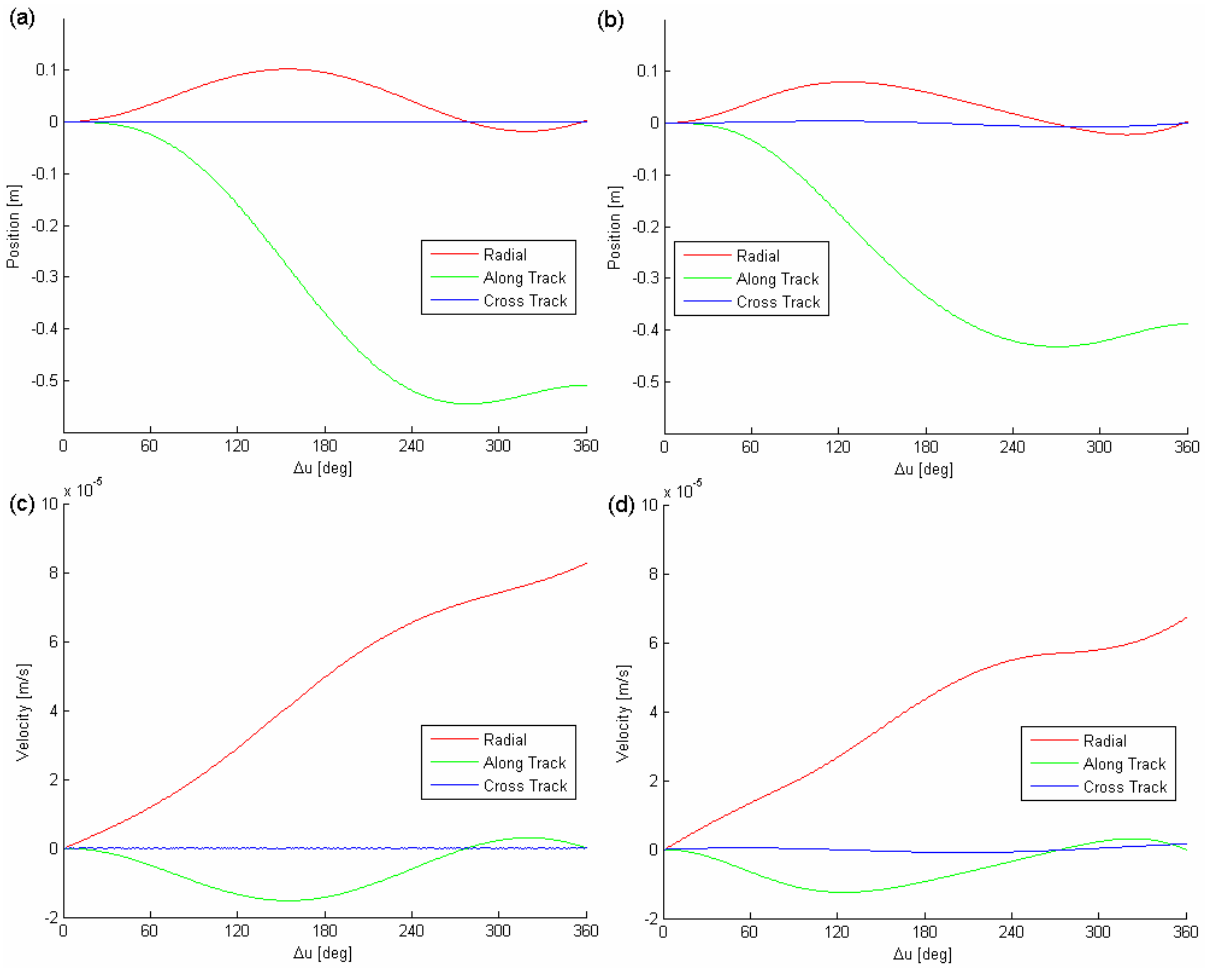

Figure 4.8 Orbit perturbation over one revolution for $\beta_0 = 19.8°$. Left: cannon-ball model. Right: box-wing model. Top: position. Bottom: velocity

Something very interesting to observe is that although the acceleration acting on the satellite is largest in the radial direction, the effect on the position is the largest in the along track direction over one revolution of the satellite. One can generally explain this behaviour through Kepler's Third Law:

$$n^2 a^3 = GM \tag{4.7}$$

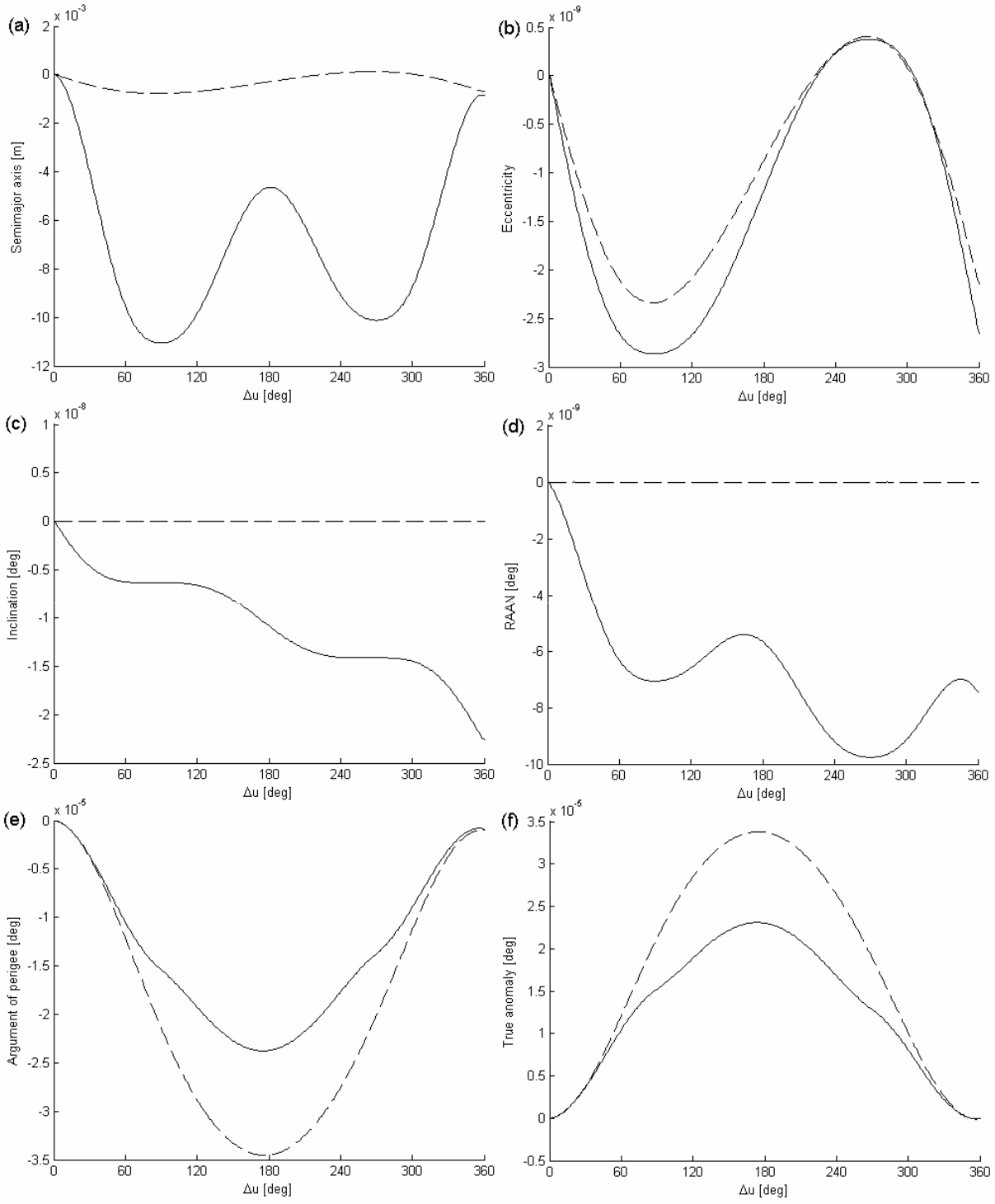

Figure 4.9 Perturbed Keplerian orbital elements over one revolution for $\beta_0 = 19.8°$.
Dashed line: cannon-ball model. Solid line: box-wing model

where $n = 2\pi/T$ is the mean motion of the satellite given in rad/s, with T the period of the orbit and a the semimajor axis of the orbit. One can also relate the mean motion to the velocity of the satellite (for circular orbits) by $v = na$, therefore a positive change in the radial direction (increase of a) implies a decrease of the mean motion and consequently of the velocity of the satellite in the along track direction, which will also decrease the position in the along track direction in an accumulative way as we can see in Figure 4.8. Consequently what we have is that a radial acceleration has a direct impact in the radial position but also an indirect one in the along track direction.

In Figure 4.9 we plot the Keplerian orbital element of the perturbed orbit minus the ones of the unperturbed orbit, there we can also see clear differences between the cannon-ball and box-wing models. For example the change of semimajor axis for the box-wing model is very different compared to the change for the cannon-ball model, not only in magnitude but also in the shape of the curve. For the other elements the differences are less pronounced, the inclination and right ascension of the ascending node in the case of the cannon-ball model remain zero since for this model there is no cross track accelerations.

The argument of perigee and the true anomaly seem to be totally opposite to each other but in fact the sum of them (in radians) multiplied by the semimajor axis gives the position change in the along track direction, which will be an important factor in the next section.

The results we have until now are interesting since we can see the effect of the Earth radiation on a typical GPS satellite orbit for two different satellite models. However they are of limited use because we want to study if the acceleration due to Earth radiation can or not be responsible for the observed radial bias derived from SLR measurements of GPS orbits. Consequently, in order to continue with the study of the GPS – SLR orbit anomaly and to get a general understanding of it, we have to construct a different unperturbed reference orbit.

4.3.2 Unperturbed Reference Orbit

As mentioned in the last paragraph, we will construct an unperturbed reference orbit, so we are able to simulate SLR measurements of GPS satellites and compare them to a realistic GPS reference orbit. The construction of an appropriate reference orbit is equivalent to the problem of finding a set of initial conditions for the perturbed orbit, since it is clear that at the beginning of the integration process the perturbed and the unperturbed orbit are not necessarily the same. Both process of finding the initial conditions of the perturbed orbit or, as in our case, an equivalent unperturbed reference orbit are not trivial.

In this chapter as we are mainly concern to have a general understanding of the effects of Earth radiation on GPS satellite orbits we adopt the approach of constructing an unperturbed reference orbit, something that will imply general but realistic assumptions on how the SLR and GPS measurements work. On the other hand in the next chapter, we will work with the Bernese GPS Software, which uses sophisticate tools to find appropriate initial conditions since the orbits of the satellites are estimated from force models and by fitting real GPS measurements from many ground stations around the world.

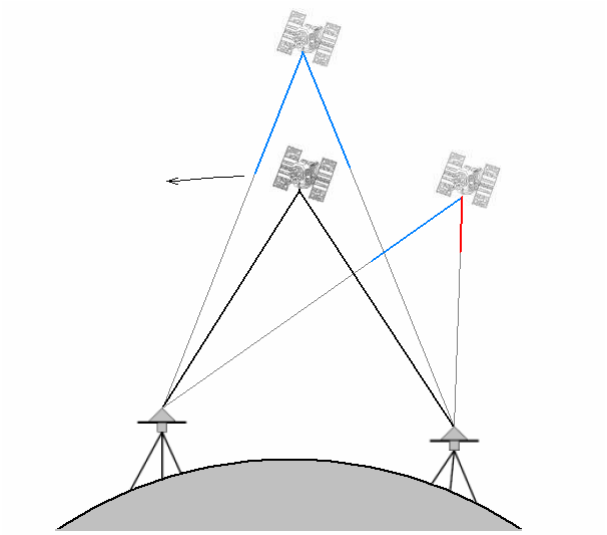

Figure 4.10 GPS single differences. Range difference: blue -> positive, red -> negative

The perturbed orbit, computed in the last section, contains the perturbation due to Earth radiation acting on the satellites, it is then considered as the ‘true’ orbit and can be related to the orbit that SLR would measure. With respect to the SLR measurements we just assume that they are mainly accurate in the radial direction since basically the system measures the time that a laser pulse takes between being transmitted, reflected at the satellite and received back at a ground station. We refer to Seeber (2003) for more information about SLR.

The unperturbed orbit once it is transformed into an adequate reference orbit can be assumed to be similar to the orbit derived from GPS measurements. Here one main assumption is that the along track position of the satellite can be measured to higher accuracy compared to the radial direction.

When single differences are formed from GPS measurements by differencing the observations of the same satellite acquired at both ends of a baseline formed by two receivers, see Hugentobler and Steigenberger (2008), it is possible to reduce or eliminate common errors like the one of the satellite clock. However by looking at Figure 4.10, one sees that an orbit error in the radial direction causes the same sign of range change for two ground stations and could be easily absorbed by the clock of the satellite that at some point has to be estimated. On the other hand, an error in the along track direction causes a different sign for the range change of the same stations and could not be simply absorbed by the satellite clock.

Also since the direction of motion of the satellite is basically the same as the along track direction, the geometry of the satellite with respect to the stations on the Earth changes fast in this direction, another reason to assume that the position in the along track direction should be well known.

The last two paragraphs lead to the next assumption that the mean motion of the satellite is very well determined. This is a key issue for the construction of the reference orbit since it implies that the mean motion of the perturbed orbit and the reference orbit should be the same. It also means that although the orbits derived from GPS measurements can be biased

in the radial direction, in the along track direction should not exists a bias or in general should be much smaller as the one of the radial direction.

Taking into account the arguments just given for the construction of an unperturbed reference orbit, we proceed to find the average Keplerian orbital elements of it as follows:

- The eccentricity, inclination, right ascension of the ascending node and argument of perigee are given just by the average of the same elements of the perturbed orbit over one revolution.
- The semimajor axis of the reference orbit is found by changing the semimajor axis of the reference orbit, such that this orbit and the perturbed one have the same average mean motion.
- The true anomaly is changed such that it coincides in average with the one of the perturbed orbit, doing that we can obtain orbit residuals mainly in the radial direction.

As it can be seen the change of semimajor axis corresponds to the assumption we made for GPS orbits while the change of true anomaly is to simulate SLR measurements available just in the radial direction. Specifically how the computation is done will be explain in the following.

Change of Semimajor Axis

To obtain how much we must change the semimajor axis of the reference orbit, we use the partial derivatives of Kepler's Third Law to get the effect a change of mean motion would have in the semimajor axis:

$$\Delta a = -\frac{2}{3} a_K \frac{\Delta n_{KP}}{n_K}. \tag{4.8}$$

In here no sub index is used for the reference orbit, while K is used for the unperturbed Kepler orbit and P for the perturbed one.

Then the change of mean motion Δn_{KP} between the perturbed and unperturbed orbits can be found by using the change of the argument of latitude Δu_{KP}, which as mentioned before multiplied in (radians) by the semimajor axis gives the change in the along track component of the position, see Figure 4.8. Then we fit a linear function depending on the time to Δu_{KP}, the slope of this line is then simply an average of Δn_{KP} given in radians per second. Note that this slope, according to Figure 4.8 is negative, giving as a consequence a positive change of the semimajor axis.

Change of True Anomaly

In order that the true anomaly of the reference orbit coincides in average to the one of the perturbed orbit, we compute it in the following way

$$\nu = \nu_P + \omega_P - \overline{\omega}_P \tag{4.9}$$

where $\overline{\omega}_p$ is the average argument of perigee of the perturbed orbit.

Note that the reference orbit is an unperturbed one and the corresponding Keplerian orbital elements change from one revolution to another. The residuals between the perturbed and the reference orbit are shown in Section 4.3.4.

4.3.3 $\Delta GM_{\oplus}$ Perturbed Orbit

Considering just the assumption that the mean motion of the perturbed and reference orbits should be the same, one can think of the effects on Kepler's Third Law for a specific (just in radial direction) acceleration. Proceeding as in (4.8) but for $\Delta n_{KP} = 0$ and $\Delta GM_{\oplus} \neq 0$ we find the semimajor axis of the perturbed orbit due to a change of $GM_{\oplus}$:

$$a_P = a_K + \frac{1}{3} a_K \frac{\Delta GM_{\oplus}}{GM_{\oplus}}. \tag{4.10}$$

Moreover $\Delta GM_{\oplus}$ can be found from the unperturbed equation of motion of the satellite by introducing a change of the acceleration $\Delta \ddot{r} = \left| \vec{f}_E \right|$ on it:

$$\Delta GM_{\oplus} = -r_K^2 \left| \vec{f}_E \right|. \tag{4.11}$$

Note that the change of the semimajor axis is always negative (for outwards acceleration) and therefore the semimajor axis of the perturbed orbit is smaller than the one of the unperturbed orbit. In other words we apply a radial acceleration to the satellite and the effect is a contraction of the orbit, something not intuitive and possible due to the way GPS measurements and orbit determination works. Furthermore we can compute radial residuals even easier than in the last section since the change of mean motion was set to be zero, then the $\Delta GM_{\oplus}$ perturbed orbit and the unperturbed Kepler orbit should coincide in the along track direction and can be directly compared, the results will be shown in the following pages.

Note that the new orbits just constructed here, the unperturbed reference orbit and the $\Delta GM_{\oplus}$ perturbed orbit, intend to give a general understanding of the effect of Earth radiation on GPS orbits and not necessarily fulfil the equation of motion or are totally physical correct. However the assumption made here to construct them, specially the invariance of the mean motion, will be partially confirmed in the next chapter.

4.3.4 Per Year Radial Residuals

The orbit residuals, specially the radial residuals, obtained between the perturbed orbit and the unperturbed reference orbit are presented in this section. Also in the figures the radial residuals between the $\Delta GM_{\oplus}$ perturbed orbit and the unperturbed Kepler orbit are included. Therefore we have two simple methods to compare SLR-like (albedo) with GPS-like (no albedo) orbits, obtaining a general understanding of the effect of Earth radiation on GPS satellites orbits. It is assumed that the SLR-like orbit is closer to a true orbit, while the GPS-like is an estimated orbit. The residuals should be understood as SLR minus GPS orbits.

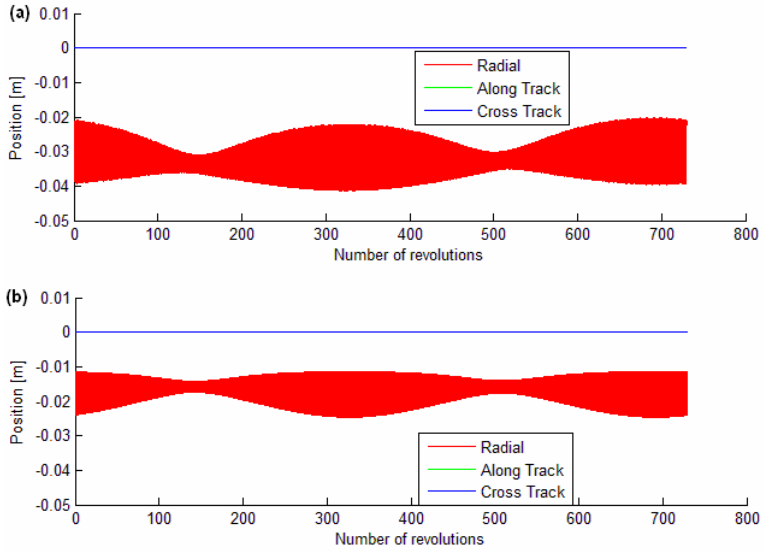

Figure 4.11 Orbit residuals for cannon-ball model as function of number of revolutions, using (a) reference and (b) $\Delta GM_{\oplus}$ orbits

As it can be seen in Figure 4.11 and Figure 4.12, by using both methods we obtained a negative shift of few centimetres in the radial residuals, this result coincides in sign and order of magnitude with the GPS – SLR orbit anomaly which is around $-5\,cm$. This result alone indicates that the Earth radiation is a key factor contributing to the bias between GPS and SLR orbits.

The radial residuals, both for the cannon-ball and the box-wing model, have a strong dependency with the Sun elevation angle (Figure 4.3), with the largest residuals for low Sun elevation angles and vice versa. In Figure 4.11 and Figure 4.12 we see some difference between the satellite models but we do not see an important difference between the two comparison methods used, however more important differences are noted when the residuals are plotted as function of the β_0 and Δu.

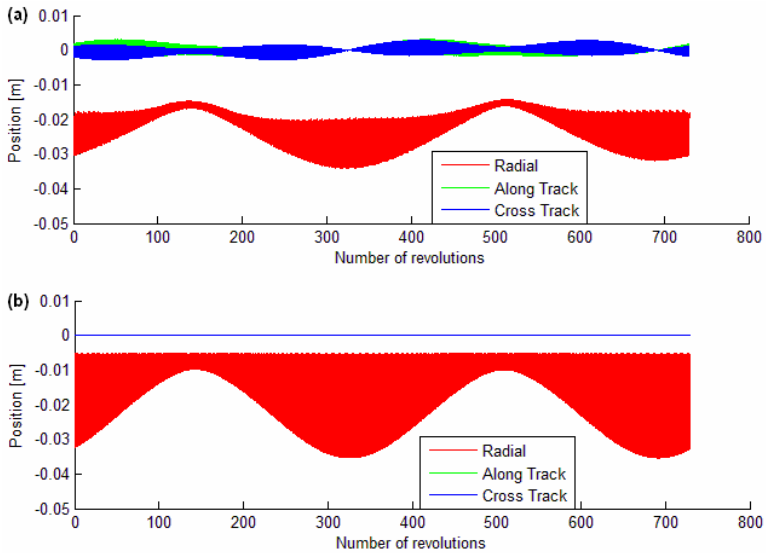

Figure 4.12 Orbit residuals for box-wing model as function of number of revolutions, using (a) reference and (b) $\Delta GM_{\oplus}$ orbits

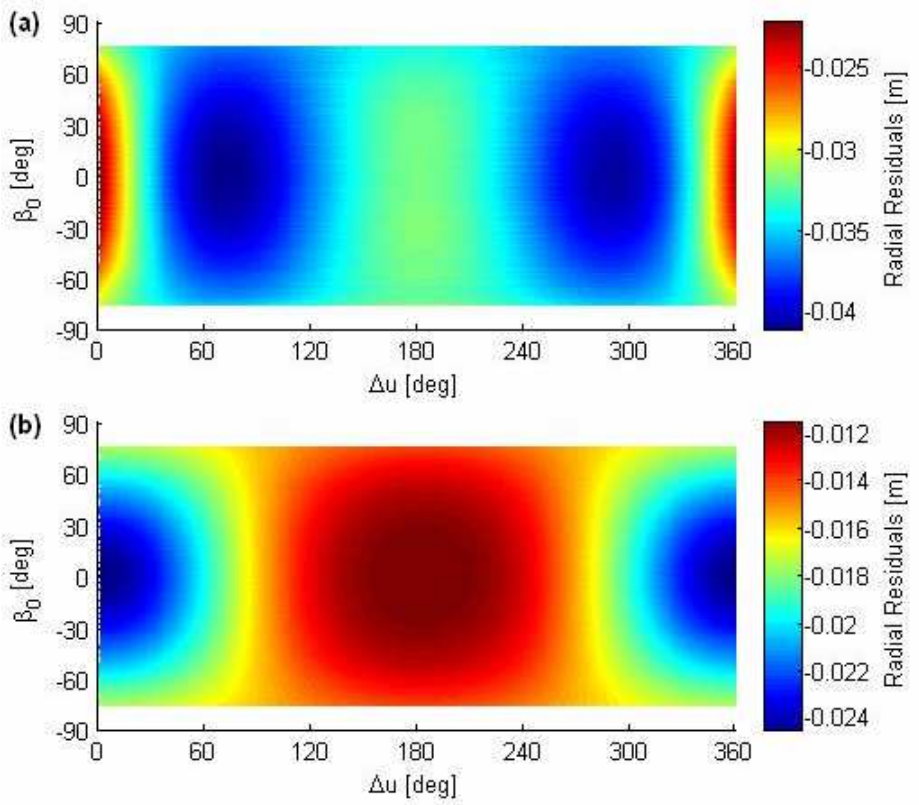

Figure 4.13 Radial residuals for cannon-ball model as a function of β_0 and Δu , using (a) reference and (b) $\Delta GM_{\oplus}$ orbits

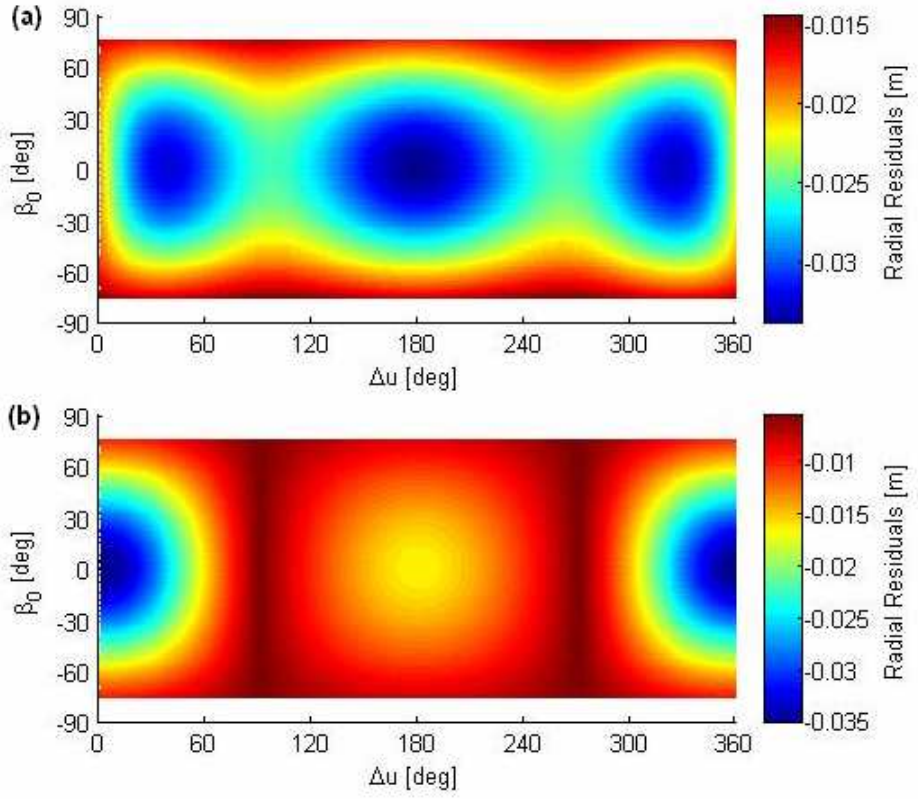

Figure 4.14 Radial residuals for box-wing model as a function of β_0 and Δu , using (a) reference and (b) $\Delta GM_{\oplus}$ orbits

Figure 4.12(a), as expected, is the only one where orbit residuals in the along track and cross track directions are obtained. Note that at least the cross track component is correlated with the acceleration in the same direction that was plotted in Figure 4.5(b).

The radial residuals are plotted as function of the β_0 and Δu in Figure 4.13 and Figure 4.14, where a clear dependency of the residuals with the relative position of the Sun can be seen. It is also evident that there is a strong once per year and once per revolution dependency of the residuals. Furthermore these figures remain basically the same independently on the chose of initial conditions of the Kepler orbit (Table 4.1) as along as they belong to GPS satellites.

First let us focus on the differences between the approaches used to compare the orbits. In general the residuals obtained by using the $\Delta GM_{\oplus}$ perturbed orbit are totally correlated to the acceleration plotted in Figure 4.6. On the other hand the residuals obtained by the unperturbed reference orbit are rather more complicated, these residuals are considered to be more correct around $\Delta u = 180°$ and less as the satellite is in the beginning or end of the orbit, since we used simple averages to get the Keplerian orbital elements of the reference orbit. Therefore what we see in Figure 4.13(a) and Figure 4.14(a) close to $\Delta u = 0°$ and $\Delta u = 360°$ is considered to be an effect on how the reference orbit was constructed, this is corrected in the next chapter with the Bernese GPS Software since it calculates the initial conditions of the perturbed orbit by least squares adjustment.

Now regarding the differences between the satellite models we find something similar to what was found in Section 4.2.2, that we see a similar behaviour of both models around $\Delta u = 0°$ and $\Delta u = 360°$ while the radial residuals around $\Delta u = 180°$ are completely different, having for the box-wing model an additional height reduction at the dark side of the Earth caused by the Earth infrared radiation acting on the solar panels.

Note that radial residuals obtained by using the box-wing model have great correspondence to Figure 1.1 where the SLR - GPS residuals obtained by Urschl et al. (2008) are shown, while when comparing with the results of the cannon-ball model, the curvature of the residuals have a different sign.

With the simple numerical orbit integration used in this chapter and the two methods for orbit comparison between SLR-like and GPS-like orbit, we have gained a good general understanding of our problem and have two main conclusions:

- The Earth radiation acting on GPS satellites can produce a negative radial shift in the same order of magnitude as the GPS – SLR orbit anomaly.
- The use of a box-wing satellite model is a key factor to explain the peculiar pattern observed in the residuals between SLR and GPS orbits.

5 Impact on Real GPS Orbits

5.1 Introduction

5.1.1 Bernese GPS Software

In the last three chapters we have developed different Earth radiation and GPS satellite models, that together produce a specific acceleration perturbing the orbits of these satellites, furthermore it has been demonstrated (using a simple example) that this acceleration can produce a peculiar pattern similar to the one observed in the residuals between SLR measurements and GPS orbits. All this was done using simple tools; the three main Matlab subroutines to compute the desired acceleration are provided in the Appendix of this Thesis.

In this chapter we will include the mentioned subroutines in one of the most sophisticated software to process GPS data, the Bernese GPS Software, see Dach et al. (2007) and Beutler (2009), with the purpose of studying the impact of Earth radiation on real GPS orbits, like the ones generated by CODE (Center for Orbit Determination in Europe). More specifically we use the same orbit estimation used by CODE, see Beutler et al. (1994) and Steigenberger et al. (2009).

Note that the Bernese GPS Software is a very complex program which contains many thousands of lines of code, therefore for more information about it we refer to Dach et al. (2007). Also the whole process for the estimation of GPS orbits, like the ones published by the IGS, is very complex so we refer to Beutler et al. (1994) and Schaer et al. (2009). Some generalities about the orbit estimation used in here are:

- GPS observations from 190 IGS stations around the world are used.
- The force models include the principal perturbations of the orbit. In order of magnitude the perturbations are: low terms of geopotential, attraction of Sun and Moon, solar radiation pressure, solid Earth and ocean tides and finally general relativity. In addition we include here the acceleration due to Earth radiation.
- The equation of motion (4.1), where $\vec{f}_E$ would include (in this case) all the perturbations mentioned above, is numerically integrated and fitted to the real GPS observations through a least squares adjustment.

More specifically, cleaned single difference files with fixed ambiguities from the CODE contribution to the IGS reprocessing, see Steigenberger et al. (2009), were used to determine daily GPS orbits for different albedo models estimating six orbital parameters and

five empirical solar radiation pressure parameters as well as one stochastic pulse in the middle of the arc. This is done using GPS observations for the year 2007

Additionally a reference orbit which does not include Earth radiation pressure will be computed. Also orbits are computed with and without an a priori solar radiation pressure model. The results will be given as residuals between the different orbits, in order to obtain the effect of the perturbation and to identify the key components for an adequate modelling of the Earth radiation acting on GPS satellites.

Once the new orbits are computed (for the selected models) they are compared using SLR measurements from several stations around the world. The comparison is done as follows: SLR measurements minus GPS orbits. The SLR measurements are only available for PRN05 and PRN06, since these GPS satellites are currently the only ones equipped with laser retro reflectors arrays (LRA), therefore the results will be presented only for these two satellites.

It must be also mentioned that the results presented here with the Bernese GPS Software are possible due to the tools already developed by the Institute of Astronomical and Physical Geodesy at the Technical University of Munich.

5.1.2 Selection of Models

Table 5.1 Selection of Earth radiation and satellite models

Test #	Abbreviation	Earth Radiation Model	Satellite Model
ALB-R	E0-S0-R	None	None
ALB-0	E0-S0	None	None
ALB-1	E1-S1	Analytical ($\alpha = 0.3$)	Cannon-Ball
ALB-2	E2-S1	Numerical ($\alpha = 0.3$)	Cannon-Ball
ALB-3	E2-S2	Numerical ($\alpha = 0.3$)	Box-Wing Analytical
ALB-4	E3-S2	Latitude dependent	Box-Wing Analytical
ALB-5	E4-S2	CERES data	Box-Wing Analytical
ALB-6	E4-S2-B	CERES data	Box-Wing Analytical (Block specific)
ALB-7	E4-S3-B	CERES data	Box-Wing Num. (Block specific)
ALB-8	E4-S3-BA	CERES data	Box-Wing Num. (Block specific + Antenna)
ALB-9	E4-S3-BA-R	CERES data	Box-Wing Num. (Block specific + Antenna) A priori ROCK model

The number of possible model combinations that can be tested at this point is not small, let us remember that we have four different Earth radiation models, three different satellite models, plus we can choose if we use the same simple optical properties for all satellites or if they are block specific and we can turn on or off the antenna trust. In total there is a maximum of $4 \times 3 \times 2 \times 2 = 48$ possibilities. It is clear that we do have to test all of them to identify the key factors that are essential for an adequate modelling of the Earth radiation acting on GPS satellites.

We have then selected different Earth radiation and satellite models by adding one level of complexity for each test, see Table 5.1. In total we thus have to perform only nine different tests. Differences between the results of successive tests then show the impact of the respective model update.

Additionally we have also computed orbits that include an a priori solar radiation pressure model, the ROCK model (R), see Fliegel et al. (1992) and Fliegel and Gallini (1996). This last test is given by ALB-9 with a corresponding reference orbit without Earth radiation pressure given by ALB-R.

5.2 On-Orbit Acceleration

The acceleration acting on the GPS satellites PRN05 and PRN06 is plotted in Figure 5.1 for eight selected models (Earth radiation and satellite models) and just for one specific orbit. Note that the Sun elevation angle (β_0) is different for both satellites and therefore the magnitude of the acceleration also differs, see also Figure 4.4. Furthermore the acceleration is given in radial, along track and cross track components as described in the previous chapter.

Already here in the plots of accelerations for the selected models, we can see the factors that contribute most to the acceleration. First of all note that the different Earth radiation models do not have a drastic effect on the acceleration, while the change of the curves comes mostly from the different satellite models. Adding the solar panels to the satellite model (E2-S2) changes the picture drastically as the satellite's cross section as seen from the Earth varies much during one satellite revolution. Moreover also by including block specific optical properties we see another change of the curves and finally if the acceleration due to antenna thrust is included, there is an additional radial shift of the acceleration. Note that the use of a numerical box-wing model compared to the analytical one mostly modifies the acceleration just around $\Delta u = 90°$ and $\Delta u = 270°$.

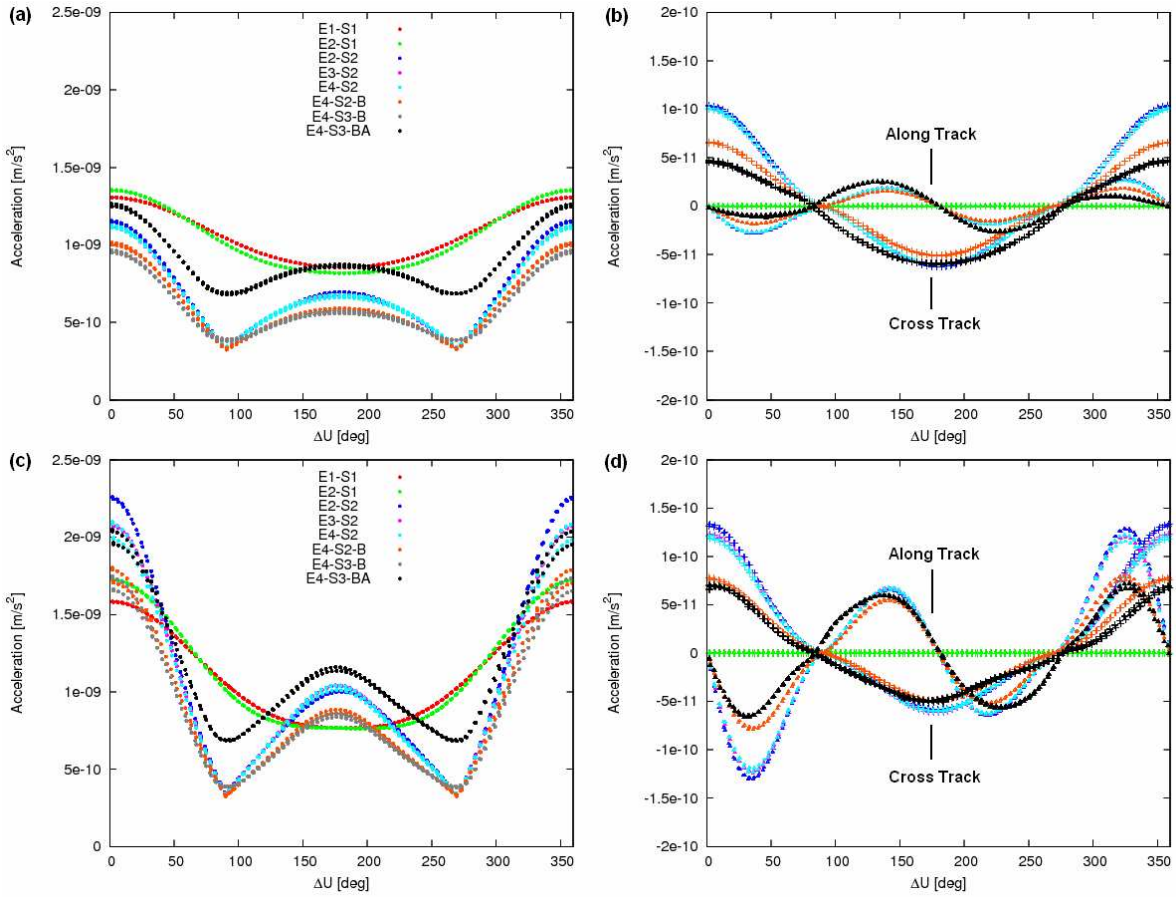

Figure 5.1 Example of on-orbit acceleration for the selected models. Top: PRN05 ($\beta_0 = 55.5°$). Bottom: PRN06 ($\beta_0 = 20.2°$). Right: radial acceleration. Left: Along track and cross track accelerations

5.3 Orbit Residuals

In this section we present the results from the computation of orbit residuals, more specifically we will present the results in three ways:

1) Difference of orbit with Earth radiation pressure (ALB-i) minus reference orbit without it (ALB-0). Results just for the most simple (ALB-1) and for the two most sophisticated models (ALB-8 and ALB-9) are presented.
2) Difference of orbit with Earth radiation pressure (ALB-i+1) minus previous orbit with Earth radiation pressure (ALB-i).
3) The same as 1), but the radial residuals are plotted as a function of β_0 and Δu .

The first way will give us an idea of the perturbation acting on the satellite and the magnitude of it. The second way will allow us to identify which of the Earth radiation or satellite models are critical for a correct but simple modelling of the Earth radiation acting on GPS satellites.

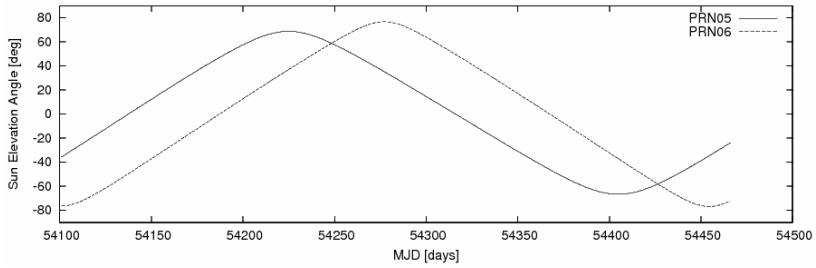

Figure 5.2 Sun elevation angle (β_0) for PRN05 and PRN06 for year 2007

And finally with the third way we will be able to see how the radial residuals behave over one revolution and over one year, see also Figure 4.13 and Figure 4.14.

Moreover, since the orbit residuals are plotted for the satellites PRN05 and PRN06, it is useful to plot the Sun elevation angle for both satellites over the complete year, see Figure 5.2. Note that there is a phase shift between the curves of Figure 5.2, this same shift can also be appreciated in Figure 5.3 to Figure 5.7.

The orbit residuals of three selected models (ALB-1, ALB-8, ALB-9) with respect to the reference orbit (ALB-0) are presented in Figure 5.3, Figure 5.4 and Figure 5.5. Note that for the three models there is always a radial shift of around $1-2\,cm$. Something that was already noted by Ziebart et al. (2007), that the Earth radiation pressure reduces the SLR-GPS anomaly by this amount. Also from last chapter we know the reason of this reduction of the orbit is that GPS measurements, being essentially angular measurements due to required clock synchronization, determine with high accuracy the mean motion of the satellite. Consequently as demonstrated in the last chapter a positive radial acceleration (equivalent to a reduction of GM) can reduce the semi major axis of the orbit and therefore the radial component of it.

Furthermore there is a big difference between the models, also visible in Figure 5.6 and Figure 5.7, coming mostly from the change of a cannon-ball to a box-wing model and also from the use of an a priori model for the solar radiation pressure. Also one can note that the radial residuals basically follow the Sun elevation angle curves, with bigger residuals for small values of Sun elevation angle, something that was already pointed out in the previous chapter.

Considering the along track and cross track components we find non negligible effects in the orbit differences, note that residuals for these components are in the same order of magnitude as the ones for the radial component. It is interesting that although the along track and cross track accelerations are around one order of magnitude smaller than the radial acceleration (Figure 5.1), the effect on the position of the satellite is of the same order of magnitude for the three components.

For completeness in Table 5.2 and Table 5.3 the differences between orbits shown in Figure 5.3 to Figure 5.7 are presented in a quantitative way. The mean and standard deviation were computed for the three components of the orbits differences over one year. These two tables allow us to have then also a qualitative instrument to distinguish which model components are more important.

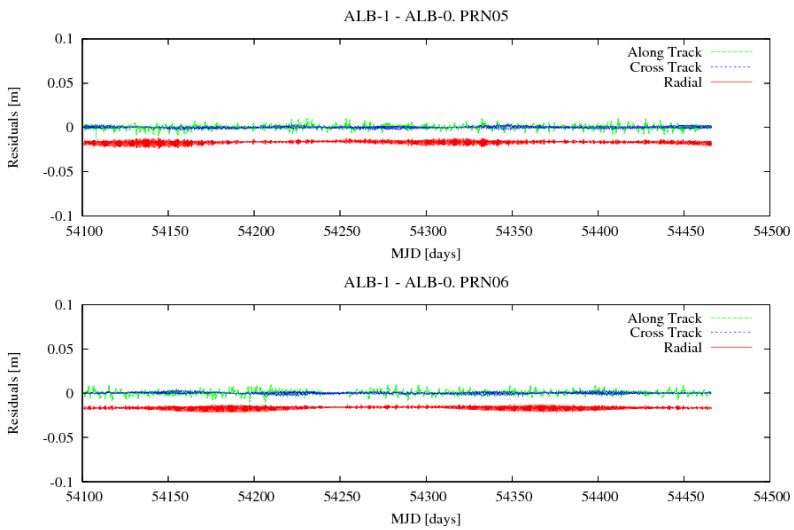

Figure 5.3 Orbit residuals ALB-1 – ALB-0 for PRN05 and PRN06

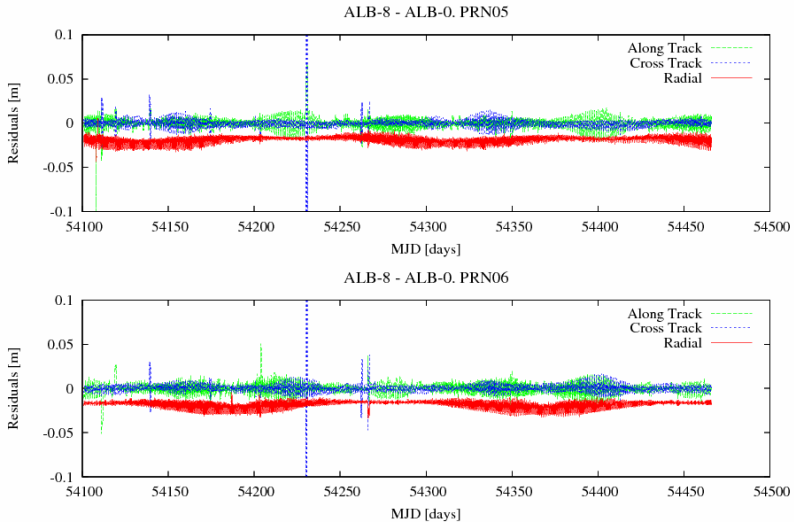

Figure 5.4 Orbit residuals ALB-8 – ALB-0 for PRN05 and PRN06

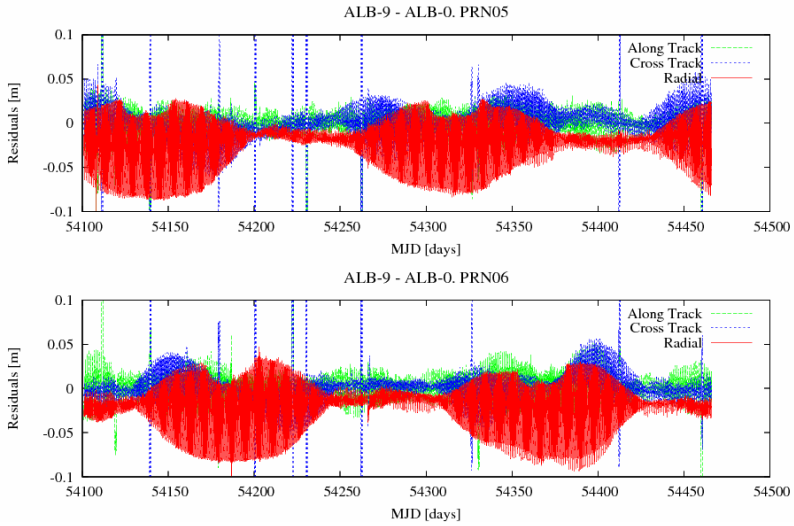

Figure 5.5 Orbit residuals ALB-9 – ALB-0 for PRN05 and PRN06

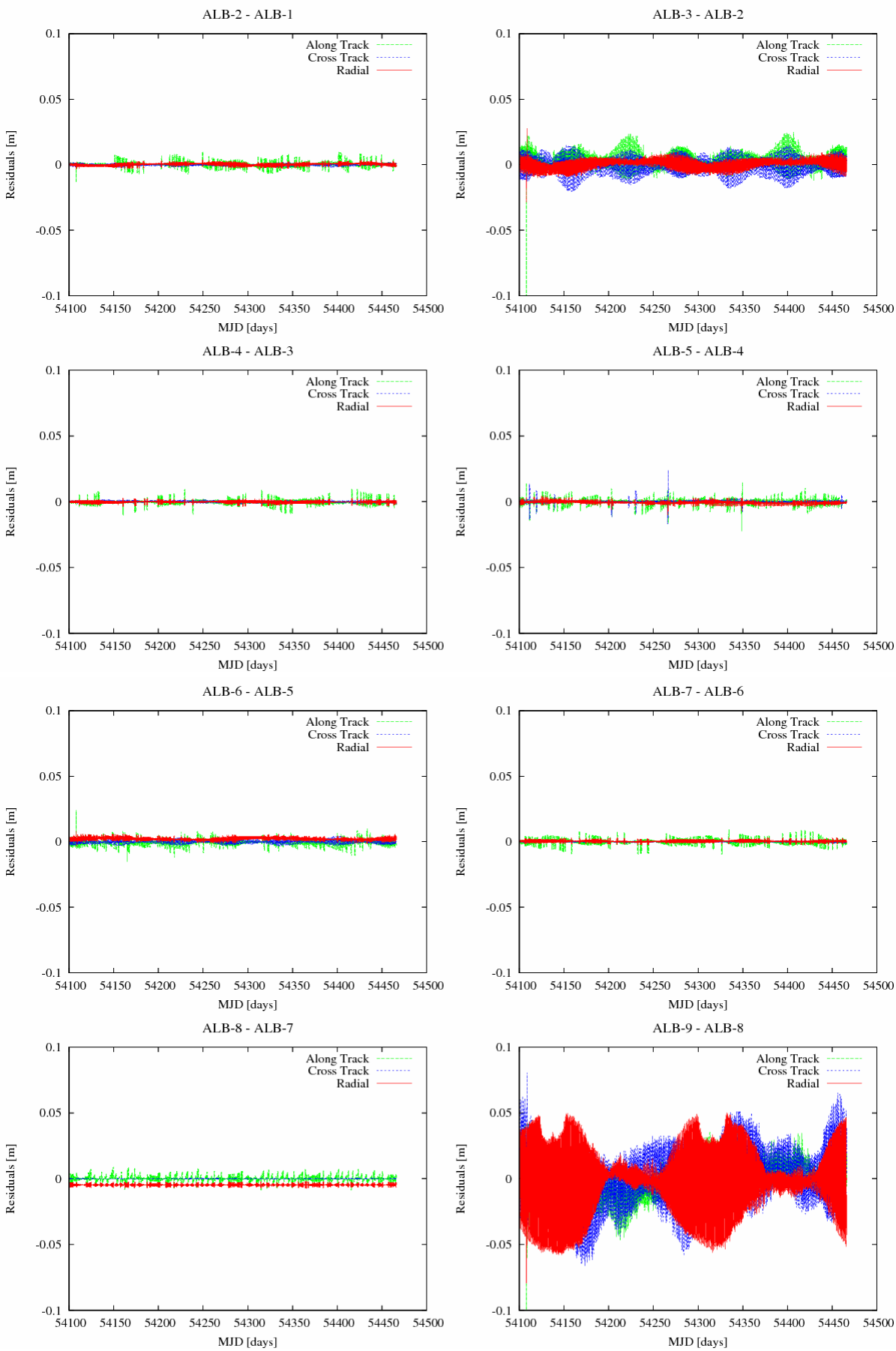

Figure 5.6 Orbit residuals between selected models for PRN05

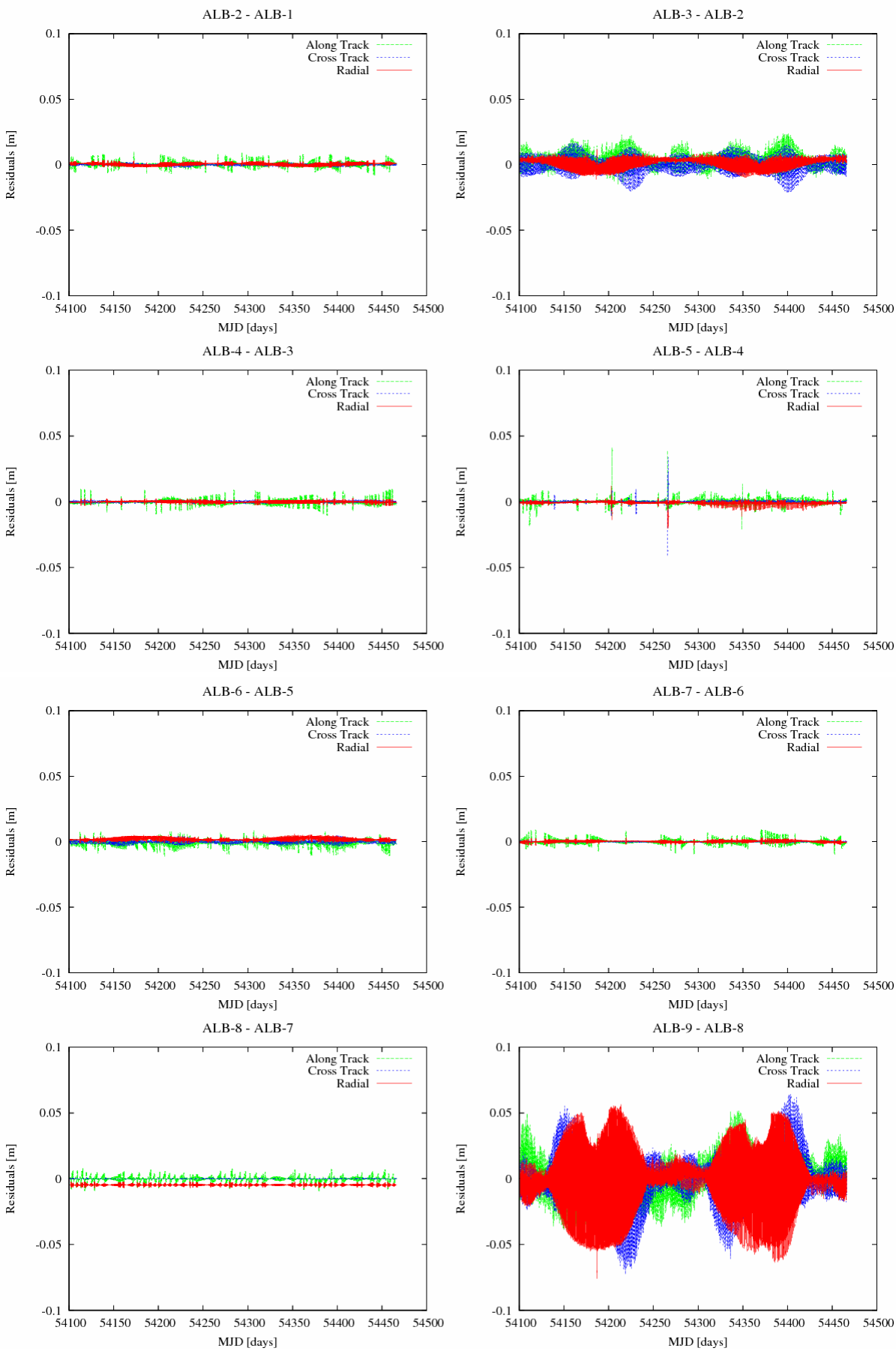

Figure 5.7 Orbit residuals between selected models for PRN06

Table 5.2 Orbit residuals between selected models for PRN05, mean +/- standard deviation

Models difference	Radial [m]	Along Track [m]	Cross Track [m]
ALB-1 – ALB-0	-0.0165 +/- 0.0017	0.0005 +/- 0.0023	0.0001 +/- 0.0010
ALB-8 – ALB-0	-0.0186 +/- 0.0036	-0.0001 +/- 0.0062	-0.0004 +/- 0.0074
ALB-9 – ALB-0	-0.0197 +/- 0.0222	-0.0028 +/- 0.0361	-0.0002 +/- 0.0419
ALB-2 – ALB-1	0.0003 +/- 0.0010	0.0004 +/- 0.0023	-0.0001 +/- 0.0006
ALB-3 – ALB-2	0.0005 +/- 0.0035	0.0037 +/- 0.0057	-0.0006 +/- 0.0056
ALB-4 – ALB-3	-0.0002 +/- 0.0008	-0.0003 +/- 0.0020	0.0000 +/- 0.0006
ALB-5 – ALB-4	-0.0007 +/- 0.0011	-0.0002 +/- 0.0025	0.0000 +/- 0.0012
ALB-6 – ALB-5	0.0022 +/- 0.0011	-0.0007 +/- 0.0025	0.0001 +/- 0.0012
ALB-7 – ALB-6	0.0004 +/- 0.0008	-0.0001 +/- 0.0023	0.0000 +/- 0.0003
ALB-8 – ALB-7	-0.0047 +/- 0.0008	0.0000 +/- 0.0022	0.0000 +/- 0.0002
ALB-9 – ALB-8	-0.0010 +/- 0.0205	-0.0005 +/- 0.0134	0.0002 +/- 0.0173

Table 5.3 Orbit residuals between selected models for PRN06, mean +/- standard deviation

Models difference	Radial [m]	Along Track [m]	Cross Track [m]
ALB-1 – ALB-0	-0.0164 +/- 0.0016	0.0006 +/- 0.0023	0.0002 +/- 0.0009
ALB-8 – ALB-0	-0.0179 +/- 0.0037	-0.0000 +/- 0.0056	0.0002 +/- 0.0075
ALB-9 – ALB-0	-0.0187 +/- 0.0223	-0.0016 +/- 0.0538	-0.0006 +/- 0.0310
ALB-2 – ALB-1	0.0004 +/- 0.0010	0.0005 +/- 0.0021	0.0000 +/- 0.0006
ALB-3 – ALB-2	0.0015 +/- 0.0036	0.0038 +/- 0.0055	-0.0000 +/- 0.0052
ALB-4 – ALB-3	-0.0001 +/- 0.0008	-0.0004 +/- 0.0022	0.0000 +/- 0.0006
ALB-5 – ALB-4	-0.0009 +/- 0.0012	-0.0000 +/- 0.0025	-0.0000 +/- 0.0012
ALB-6 – ALB-5	0.0020 +/- 0.0011	-0.0010 +/- 0.0024	-0.0000 +/- 0.0011
ALB-7 – ALB-6	0.0003 +/- 0.0008	0.0001 +/- 0.0020	0.0000 +/- 0.0003
ALB-8 – ALB-7	-0.0047 +/- 0.0007	-0.0001 +/- 0.0020	0.0000 +/- 0.0001
ALB-9 – ALB-8	-0.0008 +/- 0.0207	-0.0004 +/- 0.0144	-0.0008 +/- 0.0156

Regarding the differences between all models (Figure 5.3, Figure 5.6 and Figure 5.7) we can see that the first big change is obtained from ALB-1 – ALB-0, it means just by including a simple Earth radiation and satellite model in the orbit computation. Further on, also a very considerable effect it is obtained from ALB-3 – ALB-2, the change of cannon-ball to box-wing model. Note that the values computed in Table 5.2 and Table 5.3, show a large difference in the along track component between the cannon-ball and the box-wing models, also the standard deviation of the three components is much larger as compared to the effect of other model components

The results obtained by introducing an a priori solar radiation pressure (ALB-9 – ALB-8) present the biggest difference between models, something that was not at all expected. The large differences are also exhibited in the standard deviation computed in Table 5.2 and Table 5.3. The opinion of the author is that these results should be treated with precaution and if possible further studied. They are also mainly an indication that the modelling of solar radiation pressure stills plays a role in the orbits of GPS satellites and possible there is a problem in the ROCK model for Block II/IIA satellites, which as been already noted by Urschl et al. (2007).

As secondary effects we find that the differences between the Earth radiation models are small compared to other model components and it can be said that the improvement of the Earth radiation models does not have an important impact on the orbits. For example the use of the numerical model for constant albedo (ALB-2 – ALB-1), the latitude dependent model (ALB-4 – ALB-3) or the model with CERES data (ALB-5 – ALB-4) present similar differences between each other. This can be noted in Figure 5.6 and Figure 5.7 or in Table 5.2 and Table 5.3. The similar differences between the Earth radiation models is a simple consequence of the GPS satellite altitude since they are high enough such that varying surface albedo is averaged out over the visible illuminated surface area of the Earth.

The block specific optical properties of the satellite (ALB-6 – ALB-5) seem to be more important than the Earth radiation model at least for the radial component, see Table 5.2 and Table 5.3. And the acceleration due to antenna thrust (ALB-8 – ALB-7) as expected implies mostly a change in the radial component which can be seen in Figure 5.6 and Figure 5.7.

As simple conclusion of this section, we can divide the model components into three categories: critical, important and less important.

Critical:

- A box-wing satellite model.
- An Earth radiation model that includes emitted and reflected radiation.

Important:

- Block specific optical properties.
- Acceleration due to antenna thrust.

Less important:

- Type of Earth radiation model (reflectivity and emissivity data).
- Type of box-wing model (analytical or numerical).

From this last classification of the model components, we have that in general a good satellite model is very important, in particular the knowledge of the optical properties, dimensions and attitude of the satellite are factors that must be taken into account.

The results also show that the sophistication on the Earth radiation is less important. However from the results of Table 5.2 and Table 5.3 the model that included the complete CERES data still has a difference to the model with latitude dependency (ALB-5 – ALB-4). In the case that this model is not wish to be used the analytical Earth radiation model gives a reasonable and simple approximation of the previous one.

Finally a recommendation of the best but simplest satellite and Earth radiation model can be already given here:

- Earth radiation model with CERES data (E4 or ERM-CERES). Alternatively by introducing a small error the analytical model (E1 or ERM-A) can be used.
- Box-wing analytical model with block specific optical properties and with antenna thrust (S2-BA).

Now looking at the orbit residuals plotted as a function of β_0 and Δu (Figure 5.8 and Figure 5.9) note first of all that they are very similar to Figure 4.13(b) and Figure 4.14(b) of the last chapter. This means that the assumption made in the previous chapter, that the mean motion of the perturbed and unperturbed orbit is the same, should be in general correct.

Furthermore also note that in the case of the box-wing model (Figure 5.9) it resembles very much the SLR – GPS residuals presented in Figure 1.1, mostly the shape of the curves is very similar. However the variation from maximum to minimum in Figure 1.1 is around $5cm$, while for Figure 5.9 is just around $2mm$. Then it can not be concluded that the problem of explaining the pattern of SLR – GPS residuals is totally solved. From the results obtained here it just can be said that the Earth radiation can explain part of the SLR – GPS residuals, but the correlation between the two plots is evident.

The results computed by using the cannon-ball model (Figure 5.8) simply have an opposite sign as the SLR – GPS residuals at the night side of the Earth, as has been already mentioned in the previous chapter, therefore it is confirmed again that the use of a box-wing model is a key factor.

Regarding the results obtained by introducing an a priori solar radiation pressure model (Figure 5.10), although they should be interpreted with precaution, they are also very interesting. Note that a box-wing model was used in here but results are much similar to the one of a cannon-ball model, furthermore note that while for Figure 5.8 the total variation is around $2mm$, for Figure 5.10 the total variation is around $3.5\ cm$. And as mentioned before future studies should try to go deeper in this direction, but by now it outreaches the objectives of this thesis, since the solar radiation pressure acting on GPS satellites is not a simple topic and many works have been already written about it.

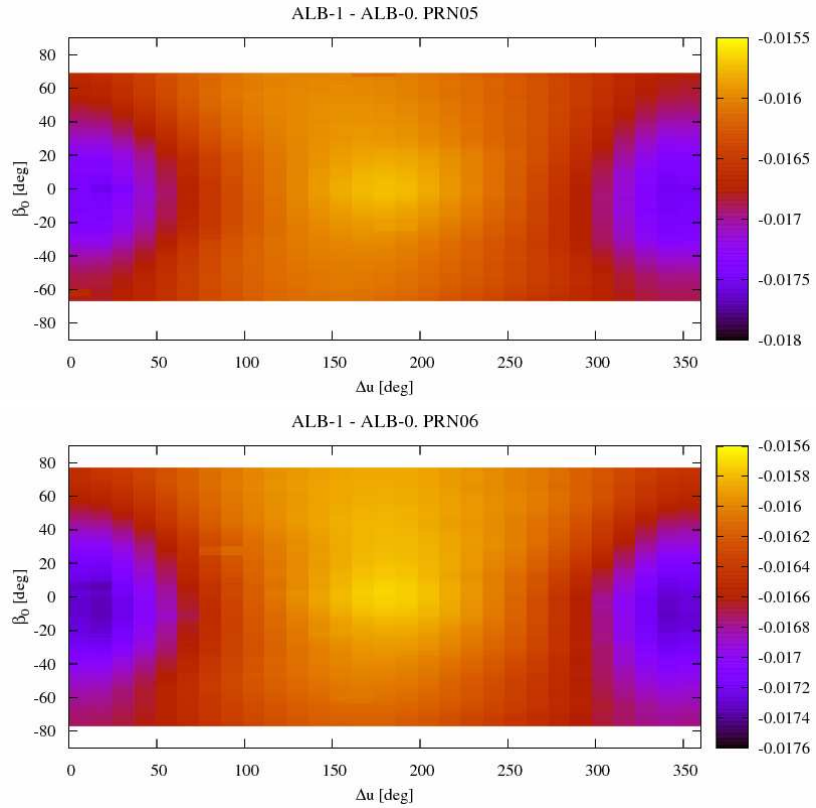

Figure 5.8 Radial residuals (in meters) ALB-1 – ALB-0 for PRN05 and PRN06 as a function of β_0 and Δu

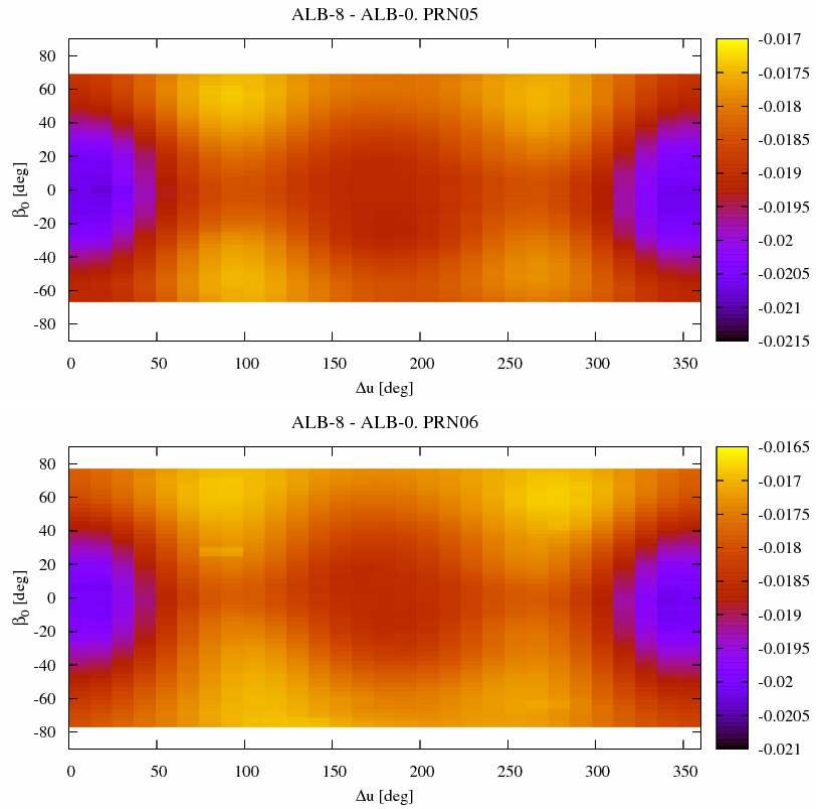

Figure 5.9 Radial residuals (in meters) ALB-8 – ALB-0 for PRN05 and PRN06 as a function of β_0 and Δu

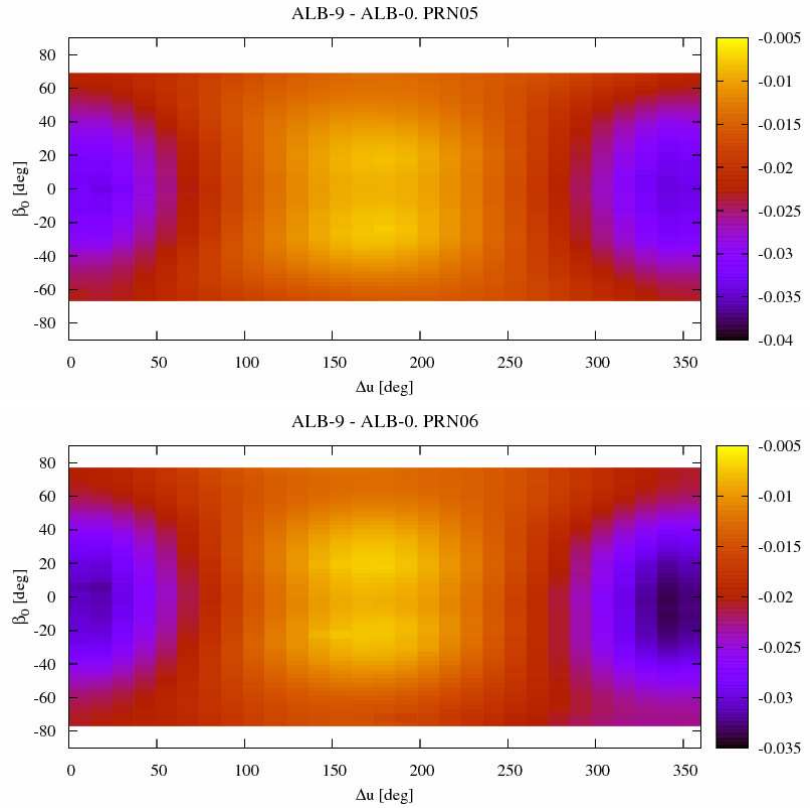

Figure 5.10 Radial residuals (in meters) ALB-9 – ALB-0 for PRN05 and PRN06 as a function of β_0 and Δu

5.4 SLR Validation

The orbits computed with the selected models (ALB-0 to ALB-9) can be compared with SLR measurements. The residuals between SLR measurements and GPS orbits are presented in Table 5.4 and Table 5.5. Additionally in this section a new orbit was computed (ALB-R) which does not include any acceleration due to Earth radiation but includes an a priori solar radiation pressure model.

Now in the SLR validation (Table 5.4 and Table 5.5) we can see that for models ALB-0 to ALB-8, where no a priori solar radiation pressure model is considered, we have a change of the mean that correspond to what was observed in Figure 5.3, Figure 5.6 and Figure 5.7 or in Table 5.2 and Table 5.3 when the difference between models were computed. For the standard deviation of the residuals we can not say anything since there is no significant change. Finally by putting our attention just on ALB-0, ALB-7 and ALB-8 we see that a reduction of $16.8\ mm$ and $16\ mm$ is obtained in the SLR – GPS bias for PRN05 and PRN06. For both satellites $4.7\ mm$ of this reduction is due to the thrust of the navigation antennas. Finally the SLR – GPS bias remains in $-6.8\ mm$ and $-10.1\ mm$ for the two GPS satellites.

Furthermore if the offset values of the laser retro reflectors arrays (LRA), reported by Davis and Trask (2007), are taken into account we would have a further reduction of the bias by $11\,mm$ for PRN05 and $13\,mm$ for PRN06. This would lead to a SLR – GPS bias of $4.2\,mm$ and $2.9\,mm$ for both satellites and to orbits with potentially sub-centimetre accuracy.

Table 5.4 SLR – GPS residuals for PRN05. Year 2007 with 2936 observations

Test #	Mean [m]	RMS [m]	Sigma [m]
ALB-R	-0.0324	0.0483	0.0358
ALB-0	-0.0236	0.0362	0.0275
ALB-1	-0.0080	0.0286	0.0275
ALB-2	-0.0092	0.0295	0.0281
ALB-3	-0.0099	0.0291	0.0273
ALB-4	-0.0098	0.0290	0.0273
ALB-5	-0.0092	0.0289	0.0274
ALB-6	-0.0112	0.0296	0.0274
ALB-7	-0.0115	0.0297	0.0274
ALB-8	-0.0068	0.0282	0.0274
ALB-9	-0.0151	0.0337	0.0302

Table 5.5 SLR – GPS residuals for PRN06. Year 2007 with 2418 observations

Test #	Mean [m]	RMS [m]	Sigma [m]
ALB-R	-0.0345	0.0502	0.0364
ALB-0	-0.0261	0.0416	0.0324
ALB-1	-0.0107	0.0342	0.0325
ALB-2	-0.0113	0.0348	0.0329
ALB-3	-0.0138	0.0349	0.0321
ALB-4	-0.0135	0.0349	0.0322
ALB-5	-0.0129	0.0348	0.0323
ALB-6	-0.0146	0.0355	0.0323
ALB-7	-0.0148	0.0355	0.0323
ALB-8	-0.0101	0.0338	0.0323
ALB-9	-0.0184	0.0402	0.0357

Regarding the orbits where an a priori solar radiation pressure model was used (ALB-R and ALB-9), note that the reduction of the bias is almost the same as the one mentioned before for ALB-0 and ALB-8, around $17.3\,mm$ for PRN05 and $16.1\,mm$ for PRN06. However note that a reduction of the standard deviation is also obtained in this case, which is much larger for PRN05 than for PRN06. This is an indication that a small reduction of the SLR – GPS residuals pattern (Figure 1.1) is obtained.

Again if the offsets for the laser retro reflectors arrays are introduced, we would have in this case orbits with a potential accuracy of $-4.1\,mm$ and $-5.4\,mm$ for both GPS satellites.

The comparison of ALB-R and ALB-0 is also very interesting, since one can see only the effect of the introduction of an a priori model for the solar radiation pressure in the computation of the orbit. Note that in general the orbits without the a priori model perform better (mean and standard deviation) in the SLR validation. This as mentioned in the previous section is an indication that more studies maybe needed for the modelling of solar radiation pressure or other non-conservative forces acting on GPS satellites. A similar effect has also been noted by Urschl et al. (2007).

Finally we present in Figure 5.11 the plots of residuals between the SLR measurements and the reference orbit ALB-R. We can see in this figure some characteristic pattern of the residuals, moreover the mean is clearly negative but the residuals have a dispersion of a few centimetres. We can also corroborate that the residuals used here are very similar to the ones previously obtained by Urschl et al. (2008) and presented in Figure 1.1.

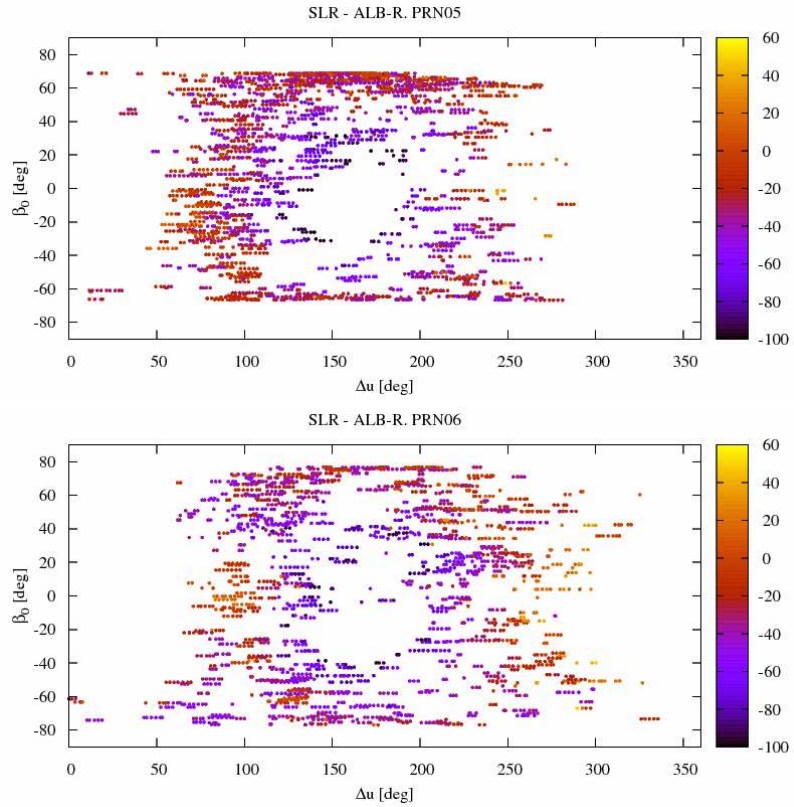

Figure 5.11 Radial residuals (in milimeters) SLR – ALB-R for PRN05 and PRN06 as a function of β_0 and Δu

6 Conclusions

In order to consider the perturbing acceleration due to Earth radiation pressure acting on GPS satellites, we needed two types of models: a Earth radiation model that computes the irradiance at the satellite position and a model of the satellite structure to interact with the radiation coming from the Earth.

In this thesis we have constructed four different diffuse Earth radiation models of increasing complexity. For a constant albedo of the Earth, we have an analytical but approximate model (valid only if the altitude of the satellite is much larger than the radius of the Earth) and a numerical one where no approximation is used. Furthermore using CERES data we have a numerical model with latitude dependent reflectivity and emissivity and a model where the complete CERES data is used (latitude and longitude dependent). The differences between the models are small since the GPS satellites are relative far from the Earth, see Figure 2.14 and Table 2.5. As the satellites see about 38% of the Earth's surface, the irradiance at the satellite position is a large average of the emitted or reflected radiation coming from the different surface elements of the Earth, which are visible to the satellite.

From the results obtained in the thesis it can be concluded that the analytical Earth radiation model with constant albedo is already a good approximation and if one wants to have a better model, the one that uses the complete CERES data can be recommended. Furthermore the assumption made for all models that the Earth behaves like a Lambertian sphere (diffuse reflection) should be in future studies proofed. In particular a next step should be to take into account the specular reflection (mirror like) to study the impact in the models. However the differences due to specular radiation are expected to be small, since some studies have suggested that this kind of reflection should have a small contribution (around 10%) in the irradiance that is received by a satellite, where the diffuse reflection is the most important component.

Regarding the satellite models, three models of increasing complexity were constructed: the cannon-ball model, the analytical box-wing model and the numerical box-wing model. The first one has average dimensions and optical properties, assuming the satellite to be a sphere. The analytical box-wing model includes the bus of the satellite and the solar panels, an analytical expression of the model could be found by assuming the irradiance coming from the Earth to be purely radial. The numerical box-wing model considers the irradiance from the full disc of the Earth; therefore the model is calculated in a numerical way. Also we have optical properties that are the same for all the GPS block types or are block specific. Finally the acceleration due to the antenna trust was also considered, since it is in the same order of magnitude as the acceleration due to Earth radiation.

The difference between the cannon-ball model and the box-wing models is found to be very important (Figure 3.4), because the relative position of the solar panels with respect to the

Earth changes drastically over one revolution, which is a simple consequence of the nominal satellite attitude. The difference between the analytical and the numerical box-wing models is found to be small (Figure 3.4), with the main difference for the case where the radiation coming from the full disc of the Earth can reach the front and back of the solar panels at the same time. Also it is found that the block specific optical properties and the acceleration due to antenna thrust are components of the satellite models that should be taken into account.

From the point of view of modelling, it can be said that while the Earth radiation models present small differences between each other, the inclusion of different components (or more details) in the satellite models is important. Therefore future efforts should focus more in the improving of the satellite models. For example the optical properties of the satellites in the infrared are practically unknown and this kind of radiation represents a big contribution in the radiation received by the satellites.

The acceleration acting on the satellite due to Earth radiation pressure was compared to the acceleration due to solar radiation pressure, see Figure 3.5. There we can find the answers to our second scientific question: *"Is this acceleration negligible or it is worth to include it in the current modelling of GPS orbits?"* The acceleration is not negligible, with an order of magnitude around $1.0\times10^{-9}\ m/s^2$ is similar to the effect due to the so-called Y-bias. Furthermore comparing the change of the acceleration due to the solar radiation pressure with the one due to Earth radiation pressure, one finds that there is a potential mismodeling of around 20% in the current a priori radiation models by no including the Earth radiation. Consequently the Earth radiation pressure is an effect that should be considered in the modelling of GPS orbits.

The combination of the Earth radiation and satellite models was done in Chapter 4, which allowed us to compute the acceleration acting on the satellites. The results were given in the radial, along track and cross track reference system and can be seen in Figure 4.6 and Figure 4.7, for the cannon-ball and the analytical box-wing model together with the analytical Earth radiation model for constant albedo. These results give a complete answer to the first scientific question: *"Which is the magnitude and behaviour of the acceleration due to Earth radiation pressure acting on GPS satellites?"* For the box-wing model (the more realistic one), the order of magnitude of the radial acceleration is around $1.0\times10^{-9}\ m/s^2$. Moreover the acceleration has a clear dependency on the relative position of satellite, Earth and Sun. Note that Figure 4.6(b) has the same shape of the SLR – GPS residuals obtained by Urschl et al. (2008), see Figure 1.1. The along track and cross track acceleration have an order of magnitude of around $1.0\times10^{-10}\ m/s^2$. The along track component presents a twice per revolution perturbation, while for the cross track direction it is once per revolution. Also these components have a clear dependency on the relative position of satellite, Earth and Sun.

By introducing this perturbing acceleration in the computation of a simple GPS orbit (Kepler orbit), the general effect of this perturbation could be studied. By doing that we found the answers to the third question. "*Is this perturbation in the orbit capable of producing a radial shift in the orbits and if it does why?"* Yes, the Earth radiation pressure can produce a negative radial shift of around $1-2\ cm$ in orbits of GPS satellites, which has been also noted by Ziebart et al. (2007). The cause of this radial shift comes from way the GPS measurements works, which are capable of achieving a higher accuracy for the along track position of the satellite than for the radial position. This has as consequence that the mean motion of the unperturbed and perturbed orbit should be the same. Therefore a positive radial acceleration implies an apparent negative change of GM, and by using Kepler's third

law we find a negative change of the semimajor axis of the orbit which is related to the radial position, see Figure 4.12.

The perturbing acceleration for selected combinations of Earth radiation and satellite models (Figure 5.1) was then included in the Bernese GPS Software. The analysis with this software was done using GPS observations from around 190 IGS stations around the world and for a complete year of data. The resulting GPS orbits were compared between each other and with SLR measurements. Also orbits with and without an a priori solar radiation pressure model were computed. By plotting the obtained radial residuals between the perturbed and the reference orbit as a function of the relative position of satellite, Earth and Sun, we find the answer to the fourth scientific question: "*Can this perturbation produce a similar pattern as the one observed between SLR measurements and GPS orbits (Figure 1.1)?"* Yes, the Earth radiation can produce a similar pattern as the one observed in Figure 1.1, see for example Figure 5.9. Since the SLR measurements are mainly available at night, the observed pattern would be then caused by the Earth infrared radiation acting on the solar panels. However the variation from maximum to minimum in Figure 1.1 is around $5\,cm$, while for Figure 5.9 is just around $2\,mm$. Also it is important to mention that the radial residuals when a cannon-ball model is used (Figure 5.8) have a minimum for $\Delta u = 0°$ instead of a maximum like Figure 5. This is another indication that the use of a box-wing model is a key factor.

The comparison of the orbits (using the selected models) with each other (Figure 5.6, Figure 5.7, Table 5.2 and Table 5.3) give us enough elements to answer the fifth question: *"Which are the key factors for an adequate but simple modelling of the effect of Earth radiation on GPS satellites?"* The key factors are:

- Earth radiation model with CERES data. Alternatively by introducing a small error the analytical model can be used.
- Box-wing analytical model with block specific optical properties and with antenna thrust.

The orbits computed with the Bernese GPS Software were compared with SLR measurements for the year 2007 using the same software. The results presented in Table 5.4 and Table 5.5 answer the last questions of this thesis: *"Is the GPS – SLR orbit anomaly reduced in a long term by including this acceleration on the computation of real GPS orbits?"* Yes it is reduced by around 16 mm, from which 5 mm are due to the antenna thrust. Furthermore if one includes the LRA offsets mentioned by Davis and Trask (2007), this would lead to a further reduction of the bias in the sub-centimeter region, which leads to potentially orbits of this accuracy

Additionally to the objectives of this thesis, it was found, like Urschl et al. (2007), that it is important if the orbits include or not an a priori solar radiation pressure model. Note in Table 5.4 and Table 5.5 that by no including an a priori model leads to better results than by including it, possibly and indication that the modelling of solar radiation pressure stills plays a role in the accuracy of the GPS orbits.

7 References

Barkstrom BR (1984) The Earth Radiation Budget Experiment. Bulletin of the American Meteorological Society 65(11): 1170-1185

Bar-Server Y, Kuang D (2004) Improved Solar-Radiation Pressure Models for GPS Satellites. NASA Tech Briefs (NPO-41395)

Beutler G (2005) Methods of Celestial Mechanics I & II. Springer, Germany

Beutler G, Brockmann E, Gurtner W, Hugentobler U, Mervart L, Rothacher M, Verdum A (1994) Extended orbit modelling techniques at the CODE processing center of the international GPS service for geodynamics (IGS): theory and initial results. Manuscripta Geodaetica 19: 367-386

Beutler G et al (2009) Bernese GPS Software Version 5.0. http://www.bernese.unibe.ch/. Accessed 7 Sep 2009

Bhanderi D, Bak T (2005) Modelling Earth Albedo for Satellites in Earth Orbit. AIAA Guidance, Navigation, and Control Proceedings

Bhanderi D (2007) Earth Albedo Toolbox v1.0. http://www.control.aau.dk/~danji//downloads/. Accessed 4 Aug 2009

Borderies N, Longaretti PY (1990) A new treatment of the albedo radiation pressure in the case of a uniform albedo and of a spherical satellite. Celestial Mechanics and Dynamical Astronomy 49: 69-98

Boyd R (1983) Radiometry and the Detection of Optical Radiation. John Wiley & Sons, USA

Dach R, Hugentobler U, Fridez P, Meindl M (2007) Bernese GPS Software, Version 5.0. Astronomical Institute, University of Bern

Davis MA, Trask AJ (2007) Insight into the GPS navigation product accuracy using the SLR measurements. Available at http://ilrs.gsfc.nasa.gov/docs/davisgpstray.pdf

Dow JM, Neilan RE, Gendt G (2005) The International GPS Service (IGS): Celebrating the 10th Anniversary and Looking to the Next Decade. Advances in Space Research 36(3): 320-326

Duha J, Afonso GB, Ferreira LDD (2006) Thermal re-emission effects on GPS satellites. Journal of Geodesy 80: 665-674

Fliegel H, Gallini T, Swift E (1992) Global Positioning System Radiation Force Model for Geodetic Applications. Journal of Geophysical Research 97(B1): 559-568

Fliegel H, Gallini T (1996) Solar Force Modelling of Block IIR Global Positioning System satellites. Journal of Spacecraft and Rockets 33(6): 863-866

Gruber T (2008) Lecture Notes on Orbit Mechanics 2. Technische Universität München

Güller R (2009) NAVSTAR-GPS Das Globale Positionierungssystem. http://www.gpswien.at/Artikel1.htm. Accessed 19 Aug 2009

Henninger J (1984) Solar Absorptance and Thermal Emittance of Some Common Spacecraft Thermal-Control Coatings. NASA Reference Publication 1121

Hugentobler U (2008) Lecture Notes on Orbit Mechanics 2. Technische Universität München

Hugentobler U, Steigenberger P (2008) Lecture Notes on Precise GNSS. Technische Universität München

Karttunen H, Kröger P, Oja H, Poutanen M, Donner KJ (1996) Fundamental Astronomy. 3rd edn. Springer, Germany

Kelso TS (2009) NORAD Two-Line Elements Sets. http://celestrak.com/NORAD/elements. Accessed 3 Jun 2009

Kiehl J, Trenberth K (1997) Earth's Annual Global Mean Energy Budget. Bulletin of the American Meteorological Society 78:197-208

Knocke PC, Ries JC, Tapley BD (1988) Earth radiation pressure effects on satellites. Proceedings of AIAA/AAS Astrodynamics Conference: 577-587

Kusterer J (2009) CERES Data and Information. http://eosweb.larc.nasa.gov/PRODOCS/ceres/table_ceres.html. Accessed 30 Sep 2009

Lindsey R (2008) Climate and Earth's Energy Budget. http://earthobservatory.nasa.gov/Features/EnergyBalance/. Accessed 7 Aug 2009

Martin C, Rubincam D (1996) Effects of Earth albedo on the LAGEOS I satellite. Journal of Geophysical Research 101(B2): 3215-3226

McPeters R (2009) Total Ozone Mapping Spectrometer. http://toms.gsfc.nasa.gov/. Accessed 6 Aug 2009

Misra P, Enge P (2001) Global Positioning System, Signals, Measurements and Performance. Ganga-Jamuna Press, USA

Montenbruck O, Gill E (2000) Satellite Orbits: Models, Methods and Applications. Springer, Germany

Pisacane V, Moore R (1994) Fundamentals of Space Systems. Oxford University Press, United Kingdom

Qiu J, Goode PR, Pallé E, Yurchyshyn V, Hickey J, Montañes Rodriguez P, Chu MC, Kolbe E, Brown CT, Koonin SE (2003) Earthshine and Earth's albedo: 1. Earthshine observations and measurements of the lunar phase function for accurate measurements of the Earth's Bond albedo. Journal of Geophysical Research 108(D22): 4709

Schaer S et al. (2009) CODE Analysis Strategy Summary. ftp://igscb.jpl.nasa.gov/pub/center/analysis/code.acn. Accessed 23 Sep 2009

Seeber G (2003) Satellite Geodesy. 2nd edn. Walter de Gruyter, Germany

Sibthorpe A (2006) Precision Non-Conservative Force Modelling For Low Earth Orbiting Spacecraft. PhD Thesis, University College London

Springer T, Beutler G, Rothacher M (1999) A new solar radiation pressure model for GPS. Advances in Space Research 23(4): 673-676

Steigenberger P, Hugentobler U, Lutz S, Dach R (2009) CODE contribution to the IGS reprocessing. Proceedings of High Performance Computing in Science and Engineering, Garching

Taylor F W (2005) Elementary Climate Physics. Oxford University Press, United Kingdom

Urschl C, Beutler G, Gurtner W, Hugentobler U, Schaer S (2007) Contribution of SLR tracking data to GNSS orbit determination. Advances in Space Research 39(10): 1515-1523

Urschl C, Beutler G, Gurtner W, Hugentobler U, Schaer S (2008) Calibrating GNSS orbits with SLR tracking data. Proceedings of the 15th International Workshop on Laser Ranging: 23-26

Urschl C, Gurtner W, Hugentobler U, Schaer S, Beutler G (2005) Validation of GNSS orbits using SLR observations. Advances in Space Research 36: 412-417

Wielicki BA, Barkstrom BR, Harrison EF, Lee III RB, Smith GL, Cooper JE (1996) Clouds and the Earth's Radiant Energy System (CERES): An Earth Observing System Experiment. Bulletin of the American Meteorological Society 77: 853-868

Ziebart M, Adhya S, Sibthorpe A, Cross P (2003) GPS Block IIR Non-Conservative Force Modelling: Computation and Implications. Proceedings of ION-GNSS-2003: 2671 – 2678

Ziebart M, Adhya S, Sibthorpe A, Edwards S, Cross P (2005) Combined radiation pressure and thermal modelling of complex satellites: Algorithms and on-orbit tests. Advances in Space Research 36: 424 – 430

Ziebart M, Cross P, Adhya S (2002) Modelling Photon Pressure: The Key To High-Precision GPS Satellite Orbits. GPS World 13(1): 43-50

Ziebart M, Edwards S, Adhya S, Sibthorpe A, Arrowsmith P, Cross P (2004) High Precision GPS IIR Orbit Prediction using Analytical Non-conservative Force Models. Proceedings of ION GNSS 2004: 1764-1770

Ziebart M, Sibthorpe A, Cross P (2007) Cracking the GPS – SLR Orbit Anomaly. Proceedings of ION-GNSS-2007: 2033-2038

8 Appendix

8.1 COMP_ERM Subroutine

```
function [PRG_OUT1,PRG_OUT2] = COMP_ERM(sun_vec,sat_vec,sat_abs,psi)

%
% COMP_ERM: EARTH RADIATION MODEL COMPUTATION
%
%   INFORMATION NEEDED BY THE PROGRAM:
%   S0:           Solar constant = 1367 W/m^2
%   RE:           Mean Radious of the Earth = 6371 km
%   ALBEDO:       Total Albedo of the Earth = 0.3
%   COEF_CERES:   Coefficients needed for latitude dependent reflectivity
%                 and emissivity, for a given year.
%   DOY:          Day of Year
%   REFL_CERES:   Reflectivity matrix from CERES data
%   EMIT_CERES:   Emissivity matrix from CERES data
%   ERM:          Earth Radiation Model (ERM-A = 1, ERM-N = 2, ERM-LAT = 3,
%                 ERM-CERES = 4)
%   SAT:          Satellite Model (cannon ball = 1,box-wing analytical = 2,
%                 box-wing numerical = 3)
%
%   INPUTS OF THE PROGRAM:
%   sun_vec:      Sun direction vector in ECEF coordinates
%   sat_vec:      Satellite direction vector in ECEF coordinates
%   sat_abs:      Magnitude of satellite position vector
%   psi:          Angle between satellite, Earth and Sun
%
%   OUPUTS OF THE PROGRAM:
%   Irradiance magnitude for SAT <= 2
%   Acceleration vector for SAT == 3


global S0;
global RE;
global ALBEDO;
global COEF_CERES;
global DOY;
global REFL_CERES;
global EMIT_CERES;
global ERM;
global SAT;

% Top of Atmosphere for CERES
TOA = RE + 30*1000;
```

```
% EARTH RADIATION ANALYTICAL MODEL ---------------------------------------
if ERM == 1

Fac_A = (pi*TOA^2)*S0/sat_abs^2;
if (psi >= 0) && (psi <= pi)
    Phase_VI = ((2*ALBEDO)/(3*pi^2))*((pi-psi).*cos(psi)+sin(psi));
    Phase_IR = (1-ALBEDO)/(4*pi);
else
    Phase_VI = NaN;
    Phase_IR = NaN;
end
IRR_SUM_VI = Fac_A*Phase_VI;
IRR_SUM_IR = Fac_A*Phase_IR;


% EARTH RADIATION NUMERICAL MODELS ----------------------------------------
elseif ERM >= 2

% Coefficients for latitude dependent model
if ERM == 3
    coeff = COEF_CERES;
    doy = DOY;
    ALB_coeff(1) = coeff(1,1) + coeff(1,2)*cos(2*pi*doy/365) +
coeff(1,3)*sin(2*pi*doy/365);
    ALB_coeff(2) = coeff(2,1) + coeff(2,2)*cos(2*pi*doy/365) +
coeff(2,3)*sin(2*pi*doy/365);
    ALB_coeff(3) = coeff(3,1) + coeff(3,2)*cos(2*pi*doy/365) +
coeff(3,3)*sin(2*pi*doy/365);
    EM_coeff(1) = coeff(4,1) + coeff(4,2)*cos(2*pi*doy/365) +
coeff(4,3)*sin(2*pi*doy/365);
    EM_coeff(2) = coeff(5,1) + coeff(5,2)*cos(2*pi*doy/365) +
coeff(5,3)*sin(2*pi*doy/365);
    EM_coeff(3) = coeff(6,1) + coeff(6,2)*cos(2*pi*doy/365) +
coeff(6,3)*sin(2*pi*doy/365);
end

% Compute body-fixed system from ECEF coordinates
if (SAT == 3)
    % Vector perpendicular to satellite and Sun vectors
    ort_vec = cross(sat_vec,sun_vec);
    ort_abs = sqrt(ort_vec(1)^2 + ort_vec(2)^2 + ort_vec(3)^2);
    ort_vec = ort_vec/ort_abs;

    % Completes system, positive in the direction of the Sun
    nrd_vec = cross(ort_vec,sat_vec);
    nrd_abs = sqrt(nrd_vec(1)^2 + nrd_vec(2)^2 + nrd_vec(3)^2);
    nrd_vec = nrd_vec/nrd_abs;
end

% Integration grid 2.5° x 2.5°
lat_int = (pi/180)*(-88.75:2.5:88.75);
lon_int = (pi/180)*(-178.75:2.5:178.75);
dif_ang = pi/72;

IRR_SUM_VI = 0;
IRR_SUM_IR = 0;
ACC_SUM_VI = [0,0,0];
ACC_SUM_IR = [0,0,0];
```

```
for z = 1:length(lat_int)
    for a = 1:length(lon_int)

        % Sphere normal vector and differential of area
        dif_area = (TOA^2)*cos(lat_int(z))*dif_ang^2;
        v_norm =
[cos(lat_int(z))*cos(lon_int(a)),cos(lat_int(z))*sin(lon_int(a)),sin(lat_in
t(z))];

        % Actual vector from surface element to satellite
        v_dist = sat_abs*sat_vec-TOA*v_norm;
        D2 = v_dist(1)^2 + v_dist(2)^2 + v_dist(3)^2;
        v_sat = v_dist/sqrt(D2);

        % Angle of incident Sun light
        cos_gamma = sum(sun_vec.*v_norm);

        % Angle of emitted or reflected radiation
        cos_theta = sum(v_sat.*v_norm);

        % Earth Radiation Numerical Models
        % ERM-N
        if ERM == 2
            refl_coef = ALBEDO;
            emit_coef = 1-ALBEDO;

        % ERM-LAT
        elseif ERM == 3
            refl_coef =
ALB_coeff(1)+ALB_coeff(2)*cos(lat_int(z))+ALB_coeff(3)*sin(lat_int(z));
            emit_coef =
EM_coeff(1)+EM_coeff(2)*cos(lat_int(z))+EM_coeff(3)*sin(lat_int(z));

        % ERM-CERES
        elseif ERM == 4
            refl_coef = REFL_CERES(z,a);
            emit_coef = EMIT_CERES(z,a);
        end

        % Reflected radiation over illuminated part of the Earth,
        % visible to the satellite
        if (cos_theta >= 0) && (cos_gamma >= 0) && (isfinite(refl_coef) ==
1)
            E_refl = (refl_coef/(pi*D2))*cos_theta*cos_gamma*S0*dif_area;
        else
            E_refl = 0;
        end


        % Emitted radiation over part of the Earth visible to the satellite
        if (cos_theta >= 0)  && (isfinite(emit_coef) == 1)
            E_emit = (emit_coef/(4*pi*D2))*cos_theta*S0*dif_area;
        else
            E_emit = 0;
        end

        % Magnitude of Irradiance vector
        IRR_SUM_VI = IRR_SUM_VI + E_refl;
        IRR_SUM_IR = IRR_SUM_IR + E_emit;
```

```
        % Box-Wing Numerical Model, body-fixed reference system
        if SAT == 3
            if cos_theta >= 0
                irr_vec =
[sum(v_sat.*sat_vec),sum(v_sat.*nrd_vec),sum(v_sat.*ort_vec)];

                [Arad_VI,Arad_IR] = COMP_SAT(E_refl,E_emit,psi,irr_vec);

                ACC_SUM_VI = ACC_SUM_VI + Arad_VI;
                ACC_SUM_IR = ACC_SUM_IR + Arad_IR;
            end
        end

    end
end

end


% PROGRAM OUTPUT ----------------------------------------------------------

if SAT <= 2
    PRG_OUT1 = IRR_SUM_VI;
    PRG_OUT2 = IRR_SUM_IR;
elseif SAT == 3
    PRG_OUT1 = ACC_SUM_VI;
    PRG_OUT2 = ACC_SUM_IR;
end
```

8.2 COMP_SAT Subroutine

```
function [ACC_SUM_VI,ACC_SUM_IR] = COMP_SAT(Eabs_VI,Eabs_IR,psi,irr_vec)

%
% COMP_SAT: GPS SATELLITE MODEL COMPUTATION
%
%   INFORMATION NEEDED BY THE PROGRAM:
%   CV:           Velocity of light in vacuum
%   SAT:          Satellite Model (cannon ball = 1,box-wing analytical = 2,
%                 box-wing numerical = 3)
%   GPS_AREA:     Area of satellite components
%   GPS_RF_:      Reflectivity of satellite components
%   GPS_SP_:      Specularity of satellite component
%                 Using (k=1 satellite bus, k=2 back of solar panels,
%                 k=3 front of solar panels)
%   GPS_BALL:     Other satellite constants needed: (k=1 mass, k=2 area to
%                 mass ratio, k=3 cannon-ball coefficient
%
%   INPUTS OF THE PROGRAM:
%   Eabs_VI:      Magnitude of irradiance vector (visible)
%   Eabs_IR:      Magnitude of irradiance vector (infrared)
%   psi:          Angle between satellite, Earth and Sun
%   irr_vec:      Irradiance direction vector in body-fixed coordinates
```

```
%
%   OUPUTS OF THE PROGRAM:
%   Acceleration vector

global CV;
global SAT
global GPS_AREA;
global GPS_RF_VI;
global GPS_SP_VI;
global GPS_RF_IR;
global GPS_SP_IR;
global GPS_BALL;


% ANALYTICAL SATELLITE MODEL COMPUTATION ---------------------------------
if SAT <= 2

% Cannon-Ball Model
if SAT == 1
    ACC_RAD_VI = (Eabs_VI/CV)*GPS_BALL(2)*GPS_BALL(3);
    ACC_RAD_IR = (Eabs_IR/CV)*GPS_BALL(2)*GPS_BALL(3);

    ACC_NRD_VI = 0;
    ACC_NRD_IR = 0;

    ACC_ORT_VI = 0;
    ACC_ORT_IR = 0;

% Box-Wing Model
elseif SAT == 2
    FAC_VI = (Eabs_VI/CV)*(1/GPS_BALL(1));
    FAC_IR = (Eabs_IR/CV)*(1/GPS_BALL(1));

    ACCRAD_BUS_VI = FAC_VI*GPS_AREA(1)*(1 + (2/3)*GPS_RF_VI(1) +
(1/3)*GPS_SP_VI(1)*GPS_RF_VI(1));
    ACCRAD_BUS_IR = FAC_IR*GPS_AREA(1)*(1 + (2/3)*GPS_RF_IR(1) +
(1/3)*GPS_SP_IR(1)*GPS_RF_IR(1));

    ACCNRD_BUS_VI = 0;
    ACCNRD_BUS_IR = 0;

    % Check for back and front side of Solar Panels
    if psi <= pi/2
        k = 2;
    elseif psi > pi/2
        k = 3;
    end

    ACCRAD_SOL_VI = FAC_VI*GPS_AREA(k)*abs(cos(psi))*(1 +
(2/3)*GPS_RF_VI(k)*(1-GPS_SP_VI(k))*abs(cos(psi)) +
GPS_SP_VI(k)*GPS_RF_VI(k)*cos(2*psi));
    ACCRAD_SOL_IR = FAC_IR*GPS_AREA(k)*abs(cos(psi))*(1 +
(2/3)*GPS_RF_IR(k)*(1-GPS_SP_IR(k))*abs(cos(psi)) +
GPS_SP_IR(k)*GPS_RF_IR(k)*cos(2*psi));

    ACCNRD_SOL_VI = FAC_VI*GPS_AREA(k)*cos(psi)*((2/3)*GPS_RF_VI(k)*(1-
GPS_SP_VI(k))*sin(psi) + GPS_SP_VI(k)*GPS_RF_VI(k)*abs(sin(2*psi)));
    ACCNRD_SOL_IR = FAC_IR*GPS_AREA(k)*cos(psi)*((2/3)*GPS_RF_IR(k)*(1-
GPS_SP_IR(k))*sin(psi) + GPS_SP_IR(k)*GPS_RF_IR(k)*abs(sin(2*psi)));
    ACC_RAD_VI = ACCRAD_BUS_VI + ACCRAD_SOL_VI;
```

```
    ACC_RAD_IR = ACCRAD_BUS_IR + ACCRAD_SOL_IR;

    ACC_NRD_VI = ACCNRD_BUS_VI + ACCNRD_SOL_VI;
    ACC_NRD_IR = ACCNRD_BUS_IR + ACCNRD_SOL_IR;

    ACC_ORT_VI = 0;
    ACC_ORT_IR = 0;

end


% NUMERICAL SATELLITE MODEL COMPUTATION ----------------------------------
elseif SAT == 3

% Check for satellite orientation, respect to radial radiation
if (psi >= 0) && (psi < pi/2)
    sol_psi = psi;
    k = 2;
elseif (psi >= pi/2) && (psi <= pi)
    sol_psi = psi-pi;
    k = 3;
end

% Check for satellite orientation, respect to actual direction of radiation
if abs(irr_vec(2)) > cos(sol_psi)
    if (psi >= 0) && (psi < pi/2)
        if irr_vec(2) > 0
            k = 2;
        elseif irr_vec(2) < 0
            k = 3;
            sol_psi = sol_psi-pi;
        end
     elseif (psi >= pi/2) && (psi <= pi)
        if irr_vec(2) > 0
            k = 2;
            sol_psi = pi + sol_psi;
        elseif irr_vec(2) < 0
            k = 3;
        end
    end
end

% Normal and tangent vectors for satellite bus
bus_nrm = [1,0,0];
if (irr_vec(1) == bus_nrm(1)) && (irr_vec(2) == bus_nrm(2)) && (irr_vec(3)
== bus_nrm(3))
    bus_tan = [0,0,0];
else
    bus_ort = cross(irr_vec,bus_nrm);
    abs_bus_ort = sqrt(bus_ort(1)^2+bus_ort(2)^2+bus_ort(3)^2);
    bus_ort = bus_ort/abs_bus_ort;

    bus_tan = cross(bus_nrm,bus_ort);
    abs_bus_tan = sqrt(bus_tan(1)^2+bus_tan(2)^2+bus_tan(3)^2);
    bus_tan = bus_tan/abs_bus_tan;
end
bus_ang = acos(sum(irr_vec.*bus_nrm));

% Normal and tangent vectors for Solar Panels
sol_nrm = [cos(sol_psi),sin(sol_psi),0];
```

```
if (irr_vec(1) == sol_nrm(1)) && (irr_vec(2) == sol_nrm(2)) && (irr_vec(3)
== sol_nrm(3))
    sol_tan = [0,0,0];
else
    sol_ort = cross(irr_vec,sol_nrm);
    abs_sol_ort = sqrt(sol_ort(1)^2+sol_ort(2)^2+sol_ort(3)^2);
    sol_ort = sol_ort/abs_sol_ort;

    sol_tan = cross(sol_nrm,sol_ort);
    abs_sol_tan = sqrt(sol_tan(1)^2+sol_tan(2)^2+sol_tan(3)^2);
    sol_tan = sol_tan/abs_sol_tan;
end
sol_ang = acos(sum(irr_vec.*sol_nrm));

% Final computation of accelerations
fac_bus_VI = (GPS_AREA(1)/GPS_BALL(1))*(Eabs_VI/CV)*cos(bus_ang);
fac_bus_IR = (GPS_AREA(1)/GPS_BALL(1))*(Eabs_IR/CV)*cos(bus_ang);

fac_sol_VI = (GPS_AREA(k)/GPS_BALL(1))*(Eabs_VI/CV)*cos(sol_ang);
fac_sol_IR = (GPS_AREA(k)/GPS_BALL(1))*(Eabs_IR/CV)*cos(sol_ang);

acc_bus_nrm_VI = fac_bus_VI*((1+GPS_SP_VI(1)*GPS_RF_VI(1))*cos(bus_ang) +
(2/3)*GPS_RF_VI(1)*(1-GPS_SP_VI(1)));
acc_bus_nrm_IR = fac_bus_IR*((1+GPS_SP_IR(1)*GPS_RF_IR(1))*cos(bus_ang) +
(2/3)*GPS_RF_IR(1)*(1-GPS_SP_IR(1)));

acc_bus_tan_VI = fac_bus_VI*(1-GPS_SP_VI(1)*GPS_RF_VI(1))*sin(bus_ang);
acc_bus_tan_IR = fac_bus_IR*(1-GPS_SP_IR(1)*GPS_RF_IR(1))*sin(bus_ang);

acc_sol_nrm_VI = fac_sol_VI*((1+GPS_SP_VI(k)*GPS_RF_VI(k))*cos(sol_ang) +
(2/3)*GPS_RF_VI(k)*(1-GPS_SP_VI(k)));
acc_sol_nrm_IR = fac_sol_IR*((1+GPS_SP_IR(k)*GPS_RF_IR(k))*cos(sol_ang) +
(2/3)*GPS_RF_IR(k)*(1-GPS_SP_IR(k)));

acc_sol_tan_VI = fac_sol_VI*(1-GPS_SP_VI(k)*GPS_RF_VI(k))*sin(sol_ang);
acc_sol_tan_IR = fac_sol_IR*(1-GPS_SP_IR(k)*GPS_RF_IR(k))*sin(sol_ang);

ACC_RAD_VI = acc_bus_nrm_VI*bus_nrm(1) + acc_bus_tan_VI*bus_tan(1) +
acc_sol_nrm_VI*sol_nrm(1) + acc_sol_tan_VI*sol_tan(1);
ACC_RAD_IR = acc_bus_nrm_IR*bus_nrm(1) + acc_bus_tan_IR*bus_tan(1) +
acc_sol_nrm_IR*sol_nrm(1) + acc_sol_tan_IR*sol_tan(1);

ACC_NRD_VI = acc_bus_nrm_VI*bus_nrm(2) + acc_bus_tan_VI*bus_tan(2) +
acc_sol_nrm_VI*sol_nrm(2) + acc_sol_tan_VI*sol_tan(2);
ACC_NRD_IR = acc_bus_nrm_IR*bus_nrm(2) + acc_bus_tan_IR*bus_tan(2) +
acc_sol_nrm_IR*sol_nrm(2) + acc_sol_tan_IR*sol_tan(2);

ACC_ORT_VI = acc_bus_nrm_VI*bus_nrm(3) + acc_bus_tan_VI*bus_tan(3) +
acc_sol_nrm_VI*sol_nrm(3) + acc_sol_tan_VI*sol_tan(3);
ACC_ORT_IR = acc_bus_nrm_IR*bus_nrm(3) + acc_bus_tan_IR*bus_tan(3) +
acc_sol_nrm_IR*sol_nrm(3) + acc_sol_tan_IR*sol_tan(3);

end


% PROGRAM OUTPUT ------------------------------------------------------

ACC_SUM_VI = [ACC_RAD_VI, ACC_NRD_VI, ACC_ORT_VI];
ACC_SUM_IR = [ACC_RAD_IR, ACC_NRD_IR, ACC_ORT_IR];
```

8.3 COMP_ACC Subroutine

```
function [ACC_VI,ACC_IR,Arad_VI,Arad_IR] = COMP_ACC(sat_spf,sun_spf,t)
%
% COMP_ACC: COMPUTATION OF ACCELERATION ACTING ON SATELLITE
%
%   INFORMATION NEEDED BY THE PROGRAM:
%   WE:           Earth rotation rate = 2*pi/86164
%   ERM:          Earth Radiation Model (ERM-A = 1, ERM-N = 2, ERM-LAT = 3,
%                 ERM-CERES = 4)
%   SAT:          Satellite Model (cannon ball = 1, box-wing analytical =
2,
%                 box-wing numerical = 3)
%
%   INPUTS OF THE PROGRAM:
%   sat_spf:      Satellite vector in Space fixed Earth centred coordinates
%   sun_spf:      Sun vector in Space fixed Earth centred coordinates
%   t:            Time in seconds (used for simple conversion into Earth
%                 fixed Earth centred coordinates)
%
%   OUPUTS OF THE PROGRAM:
%   ACC_:         Acceleration vector in Space fixed Earth centred
%                 coordinates
%   Arad_:        Acceleration vector in body-fixed coordinates

global WE;
global ERM;
global SAT;


% VECTORS AND ANGLES FOR MODELS ------------------------------------------

% Geocenter distance to satellite
sat_abs = sqrt(sat_spf(1)^2 + sat_spf(2)^2 + sat_spf(3)^2);

% Normalized satellite position vector, space-fixed
sat_spf = [sat_spf(1)/sat_abs, sat_spf(2)/sat_abs, sat_spf(3)/sat_abs];
sun_spf = [sun_spf(1), sun_spf(2), sun_spf(3) ];

% Angle between satellite, Earth and Sun
psi = acos(sum(sun_spf.*sat_spf));

% Vector perpendicular to sun and satellite direction, space-fixed
ort_vec = cross(sat_spf,sun_spf);
ort_abs = sqrt(ort_vec(1)^2 + ort_vec(2)^2 + ort_vec(3)^2);
ort_vec = [ort_vec(1)/ort_abs, ort_vec(2)/ort_abs, ort_vec(3)/ort_abs;];

% Vector in the plane satellite-sun, space-fixed
nrd_vec = cross(ort_vec,sat_spf);
nrd_abs =  sqrt(nrd_vec(1)^2 + nrd_vec(2)^2 + nrd_vec(3)^2);
nrd_vec = [nrd_vec(1)/nrd_abs, nrd_vec(2)/nrd_abs, nrd_vec(3)/nrd_abs;];

%Sun and satellite vector in Earth fixed coordinates
sat_erf = [0,0,0];
sat_erf(1) = sat_spf(1)*cos(WE*t) + sat_spf(2)*sin(WE*t);
sat_erf(2) = -sat_spf(1)*sin(WE*t) + sat_spf(2)*cos(WE*t);
sat_erf(3) = sat_spf(3);
```

```
sun_erf = [0,0,0];
sun_erf(1) = sun_spf(1)*cos(WE*t) + sun_spf(2)*sin(WE*t);
sun_erf(2) = -sun_spf(1)*sin(WE*t) + sun_spf(2)*cos(WE*t);
sun_erf(3) = sun_spf(3);


% ALBEDO MODEL COMPUTATION ------------------------------------------------

if (ERM == 1) && (SAT == 3)
    SAT = 2;
end

if SAT <= 2
    [Eabs_VI,Eabs_IR] = COMP_ERM(sun_erf,sat_erf,sat_abs,psi);
elseif SAT == 3
    [Arad_VI,Arad_IR] = COMP_ERM(sun_erf,sat_erf,sat_abs,psi);
end

if SAT <= 2
    [Arad_VI,Arad_IR] = COMP_SAT(Eabs_VI,Eabs_IR,psi);
end


% TOTAL ACCELERATION ------------------------------------------------------

ACC_VI = [0,0,0];
ACC_VI(1) = Arad_VI(1)*sat_spf(1) + Arad_VI(2)*nrd_vec(1) +
Arad_VI(3)*ort_vec(1);
ACC_VI(2) = Arad_VI(1)*sat_spf(2) + Arad_VI(2)*nrd_vec(2) +
Arad_VI(3)*ort_vec(2);
ACC_VI(3) = Arad_VI(1)*sat_spf(3) + Arad_VI(2)*nrd_vec(3) +
Arad_VI(3)*ort_vec(3);

ACC_IR = [0,0,0];
ACC_IR(1) = Arad_IR(1)*sat_spf(1) + Arad_IR(2)*nrd_vec(1) +
Arad_IR(3)*ort_vec(1);
ACC_IR(2) = Arad_IR(1)*sat_spf(2) + Arad_IR(2)*nrd_vec(2) +
Arad_IR(3)*ort_vec(2);
ACC_IR(3) = Arad_IR(1)*sat_spf(3) + Arad_IR(2)*nrd_vec(3) +
Arad_IR(3)*ort_vec(3);
```